

Journal of Print and Media Technology Research

Scientific contributions

Discrete model of the inking apparatus
of offset printing machine

Eldar A. Aliyev and Mehri H. Khanbabaeva

167

Static- and dynamic-wetting measurements
on 3-aminopropyltriethoxysilane-functionalized
float glass surfaces as a method for indicating
adhesion forces

*Sarah Patejdl, Ulrich Jung, Christopher Knoth
and Patrick Görrn*

177

TaxoCatalog: expert system for semantically
personalizing paper-based product catalogs
in omni-channel context
using background knowledge

Heiko Angermann

197

Global trends in the study of projection
mapping technology using bibliometric analysis

*Intan Permata Sari, Agus Juhana
and Nurhidayatulloh Nurhidayatulloh*

219

ISSN 2414-6250



9 772414 625001

Editor-in-Chief

Published by **iarigai**
www.iarigai.org

Gorazd Golob (Ljubljana)

The International Association of Research
Organizations for the Information, Media
and Graphic Arts Industries

Journal of Print and Media Technology Research

A PEER-REVIEWED QUARTERLY

PUBLISHED BY

The International Association of Research Organizations
for the Information, Media and Graphic Arts Industries
Magdalenenstrasse 2, D-64288 Darmstadt, Germany
<http://www.iarigai.org>
journal@iarigai.org

EDITORIAL BOARD

EDITOR-IN-CHIEF

Gorazd Golob (Ljubljana, Slovenia)

EDITORS

Anne Blayo (Grenoble, France)
Timothy C. Claypole (Swansea, UK)
Edgar Dörsam (Darmstadt, Germany)
Nils Enlund (Helsinki, Finland)
Patrick Arthur C. Gane (Helsinki, Finland)
Mladen Lovreček (Zagreb, Croatia)
Scott Williams (Rochester, USA)

ASSOCIATE EDITOR

Markéta Držková (Pardubice, Czech Republic)

SCIENTIFIC ADVISORY BOARD

Ian Baitz (Toronto, Canada)
Irena Bates (Zagreb, Croatia)
Davide Deganello (Swansea, UK)
Jay Amrish Desai (Nagpur, India)
Elena Fedorovskaya (Rochester, USA)
Diana Gregor Svetec (Ljubljana, Slovenia)
Jon Yngve Hardeberg (Gjøvik, Norway)
Gunter Hübner (Stuttgart, Germany)
Dejana Javoršek (Ljubljana, Slovenia)
Igor Karlovits (Ljubljana, Slovenia)
Helmut Kipphan (Schwetzingen, Germany)
Yuri Kuznetsov (St. Petersburg, Russian Federation)
Magnus Lestelius (Karlstad, Sweden)
Igor Majnarić (Zagreb, Croatia)
Thomas Mejtoft (Umeå, Sweden)
Erzsébet Novotny (Budapest, Hungary)
Alexandra Pekarovicova (Michigan, USA)
Anastasios Politis (Athens, Greece)
Cathy Ridgway (Egerkingen, Switzerland)
Wolfgang Schmidt (Munich, Germany)
Tomáš Syrový (Pardubice, Czech Republic)
Li Yang (Stockholm, Sweden)
Werner Zapka (Stockholm, Sweden)

A mission statement

To meet the need for a high quality scientific publishing platform in its field, the International Association of Research Organizations for the Information, Media and Graphic Arts Industries is publishing a quarterly peer-reviewed research journal.

The journal is fostering multidisciplinary research and scholarly discussion on scientific and technical issues in the field of graphic arts and media communication, thereby advancing scientific research, knowledge creation, and industry development. Its aim is to be the leading international scientific journal in the field, offering publishing opportunities and serving as a forum for knowledge exchange between all those interested in contributing to or learning from research in this field.

By regularly publishing peer-reviewed, high quality research articles, position papers, surveys, and case studies as well as review articles and topical communications, the journal is promoting original research, international collaboration, and the exchange of ideas and know-how. It also provides a multidisciplinary discussion on research issues within the field and on the effects of new scientific and technical developments on society, industry, and the individual. Thus, it intends to serve the entire research community as well as the global graphic arts and media industry.

The journal is covering fundamental and applied aspects of at least, but not limited to, the following topics:

Printing technology and related processes

- ⊕ Conventional and special printing
- ⊕ Packaging
- ⊕ Fuel cells and other printed functionality
- ⊕ Printing on biomaterials
- ⊕ Textile and fabric printing
- ⊕ Printed decorations
- ⊕ Materials science
- ⊕ Process control

Premedia technology and processes

- ⊕ Colour reproduction and colour management
- ⊕ Image and reproduction quality
- ⊕ Image carriers (physical and virtual)
- ⊕ Workflow and management

Emerging media and future trends

- ⊕ Media industry developments
- ⊕ Developing media communications value systems
- ⊕ Online and mobile media development
- ⊕ Cross-media publishing

Social impact

- ⊕ Media in a sustainable society
- ⊕ Environmental issues and sustainability
- ⊕ Consumer perception and media use
- ⊕ Social trends and their impact on media

Submissions to the Journal

Submissions are invited at any time and, if meeting the criteria for publication, will be rapidly submitted to peer-review and carefully evaluated, selected and edited. Once accepted and edited, the papers will be published as soon as possible.

✉ Contact the Editorial office: journal@iarigai.org

Journal of Print and Media Technology Research

4-2023

December 2023



The information published in this journal is obtained from sources believed to be reliable and the sole responsibility on the contents of the published papers lies with their authors. The publishers can accept no legal liability for the contents of the papers, nor for any information contained therein, nor for conclusions drawn by any party from it.

Journal of Print and Media Technology Research is listed in:

Emerging Sources Citation Index

Scopus

DOAJ – Directory of Open Access Journals

Index Copernicus International

NSD – Norwegian Register for Scientific Journals, Series and Publishers

Contents

A letter from the Editor <i>Gorazd Golob</i>	165
---	-----

Scientific contributions

Discrete model of the inking apparatus of offset printing machine <i>Eldar A. Aliyev and Mehri H. Khanbabaeva</i>	167
Static- and dynamic-wetting measurements on 3-aminopropyltriethoxysilane-functionalized float glass surfaces as a method for indicating adhesion forces <i>Sarah Patejdl, Ulrich Jung, Christopher Knoth and Patrick Görrn</i>	177
TaxoCatalog: expert system for semantically personalizing paper-based product catalogs in omni-channel context using background knowledge <i>Heiko Angermann</i>	197
Global trends in the study of projection mapping technology using bibliometric analysis <i>Intan Permata Sari, Agus Juhana and Nurhidayatulloh Nurhidayatulloh</i>	219

Topicalities

Edited by Markéta Držková

News & more	233
Bookshelf	235
Events	241



A letter from the Editor

Gorazd Golob

Editor-in-Chief

E-mail: gorazd.golob@jpmtr.org

journal@iarigai.org

With the present December issue of the Journal, a period of nine years of my editorial work is concluded. At the end of 2014 Nils Enlund as the Editor-in-Chief and Mladen Lovreček, the Executive Editor at the time decided for changes and by the Board of *iarigai*, I was appointed as Editor-in-Chief, together with Markéta Držková as Associate Editor. It was a challenge to continue the successful kick-off in 2012 when the first issue was published and regular publishing of papers from the print and media research field on a high scientific level began. The transition process was an interesting and exciting experience for all of us. In the past nine years, the publishing model was changed for several times, from a subscription and *iarigai*-membership-based model to an open-access Journal, listed in ESCI, Scopus, and DOAJ databases. However, the goals were set and should be positioned even higher, to have a publication on a level comparable to the level typically assessed through the Impact Factor, for the key journal in our research field(s).

Four papers are currently published. Thematically the first one covers mathematical modelling of the inking apparatus of an offset printing press. The measurements of surface characteristics of float glass surfaces for indicating adhesion forces is a topic of the second paper. The following paper is on an expert system for the semantical personalizing of paper-based product catalogs. The Scientific contributions section is concluded with an analysis of global trends in the study of projection mapping technology by using the data of published papers, and their citations applied by the researchers who are publishing in the same research field.

In the Topicalities, edited by Markéta Držková (marketa.drzkova@jpmtr.org) an overview of standards and technical notes on color science and lightning, issued by CIE in the last year is shown in the section News & more. There is also available an overview of Fogra research projects and the information on the recent drupa Global Trends report. In the Bookshelf section, an overview of books published in the last year is available, from the fields of augmented reality, creativity, printing and packaging technologies, textile technology, dyes and colorants, biopolymers, additive manufacturing, and history.

Traditionally three interesting academic dissertations from the field are presented. Xirui Peng defended his thesis on 3D/4D printing using digital light processing and direct ink writing at Georgia Institute of Technology, USA. A thesis on text comprehension across print and audio was defended by Anisha Singh at the University of Maryland, USA. The third presented thesis on electrically driven hydrogel-based soft actuators was defended by Jeong-Yun Sun at the Seoul National University, Korea.

In the overview of the Events announced for the beginning of 2024, symposia, conferences, workshops, tradeshow, and other events around the globe are listed. The pandemic issues in the past are only a bad memory now, so all activities are open to the public, and online attendance is only an option in some cases.

Now it is time to thank all the editors, reviewers, authors, readers, and other experts and users of the Journal of Print and Media Technology Research. Without their confidence and trust, their help and support, and their expertise and knowledge, it would not be possible to publish this quarterly, without significant delays, corrections, and excuses. I would also like to thank the Board and members of *iarigai* for their financial, technical, moral, and friendly support through the years. The list of all of them would be a long one, so expressing all the names is omitted in this letter.

The new Editor-in-Chief of the Journal, Dr. Daniel Bohn (danielbohn@jpmtr.org), has been already elected, and we are expecting new steps in the further development, and setting of new high goals for the Journal. On this occasion, I would like to express my best wishes and a lot of success to him and the editorial team.

Ljubljana, December 2023

JPMTR-2314
DOI 10.14622/JPMTR-2314
UDC 681.6-053.67|53.07

Research paper | 183
Received: 2023-10-14
Accepted: 2023-11-26

Discrete model of the inking apparatus of offset printing machine

Eldar A. Aliyev and Mehri H. Khanbabaeva

Azerbaijan Technical University,
H. Javid Ave. 25, Baku, Azerbaijan, AZ1073

elab57@mail.ru
mxanbabayeva@mail.ru

Abstract

Nowadays offset printing method is actively used in modern printing houses for printing graphic arts products, and makes it possible to obtain large print runs of high-quality full-color images. Offset printing technology allows to automate a large number of processes and due to this get a low cost of production, and equipment utilization rate. The purpose of this research is to create a scientific basis for structural and mathematical modeling of the inking apparatus of an offset printing machine. To achieve this goal, a discrete model of the ink apparatus was built as a control object associated with the movement and ink flow of the printing process, and the research results were summarized in the form of a mathematical model. Also, a methodology for the distribution of ink layers in the inking apparatus was developed. The inking apparatus is considered a dynamic system formed by a set of rollers and cylinders. The discrete model is based on the actual movement pattern of ink layers, considered as a directed graph. The sections of the trajectory of the ink layer movement are considered as arcs of the graph, and the contact points of rollers are considered as nodes of the graph, which correspond to the thickness of the ink layer for certain nodes and discrete moments of time. The necessary mathematical basis for computer modeling of an inking apparatus of complex structure has been created. The process of dividing the ink layer was described using difference equations. For computer implementation, based on the Gauss method of numerical solution of the systems of linear algebraic equations, software has been developed using the Visual Basic program, which allows to determine the divisions and thickness of the ink layer on the surfaces of the elements of the inking system. The discrete model with the help of difference equations describes the discrete process of division of the ink layer taking into account the time of displacement of the layer on the surfaces of rollers and cylinders. The result of modeling is cyclic processes of ink layer division, generalized in the form of dynamic characteristics. The extension of the proposed methodology to the inking apparatus of complex structure makes it possible to apply this methodology to the study of the inking apparatus of different designs.

Keywords: mathematical model, ink layer, difference equation, dynamic characteristic

1. Introduction

Analysis of the most common printing methods shows that the offset planographic printing method has the highest rate of development compared to other printing methods. This is due to the technical and economic advantages of the method and its better pictorial (rendering) capabilities. According to findings by Heidi Toliver-Nigro (2006), offset printing is the most common commercial printing method. This type of printing can nowadays reproduce almost any original while achieving high-quality printing performance. The increasing role of control intensively develops the automation of the functions of the printing press in the printing process. Automation increases the iden-

tity of circulation prints, contributes to the reduction of paper waste, and increases the equipment utilization rate. The basis for solving the problem of complex automation is the study of dynamic properties of the printing process as an object of automatic control and the generalization of the results of the study in the form of a mathematical model.

The works of many scientists have revealed various approaches to the mathematical description of inking apparatus. The overwhelming number of studies of the printing process is devoted to the study of the mechanism of layer-by-layer ink partitioning between contact surfaces. A large number of ink transfer modeling equations have been developed (Dai, et al., 2008; Zhao,

2011; Wu, Wu and Wang, 2011; Panichkin and Varepo, 2014; Aliyev, 2019; Verkhola, Panovuk and Huk, 2019; Verkhola, et al., 2022). Similarly, in order to determine the conditions for obtaining high-quality prints, a large number of methods for mathematical description of the printing process have been developed. One of the directions in the development of these methods is the mathematical study of the movement of ink and dampening solution in inking and dampening units. Using the specified constants, as well as taking into account the existing structure and design parameters of these devices it is possible to build their formal mathematical description.

The inking apparatus of offset printing machines is the most important technological unit, whose dynamic and static properties significantly affect printing quality. The inking unit forms a layer of ink of the required thickness for its subsequent transfer to the printing plate. For this purpose, the ink is fed by a ductor cylinder (ink fountain roller) from the ink fountain, rolled out by rollers, and rolled by rollers on the printing plate. To improve ink mixing in the ink box, a passive activator located parallel to the axis of the ductor cylinder is proposed, which is presented in the research paper by Litunov, Timoschenko and Gusak (2014).

A mathematical model of ink flow in the area between the squeegee (ink blade) and the ductor cylinder is presented, based on the model of non-viscous fluid flow. This model allows a visual assessment of the ink flow. However, this paper does not provide any information about the ink flow behavior in the contact zones of rollers and cylinders and separation in the contact zones of the elements of the ink-printing system. In some works (Liu, Lu and Bai, 2012; Liu, Li and Lu, 2016), the ink transfer model was modified based on the Reynolds equation under the condition of taking into account the retention of ink in the roller gaps. As a result of modeling, the thicknesses of the ink layer in the contact zones of the rollers are established. However, there is no information about the separation of the ink layer in the contact zones of the printing apparatus (print unit) cylinders. Zhao (2011) investigated the inconsistency of different structures and parameters of the inking system of modern offset printing press. The surfaces of ink rollers and cylinders were discretized by computer simulation, based on which a mathematical model of constant time in the periodic and continuous ink supply system was created. However, when creating a mathematical model, the issues of separating the ink layer in the contact areas of the elements of the ink printing system were not considered. The study by Yan, Hui, and Ling (2009) considered the inking system in offset printing as a complex undirected graph and constructed a network diagram. The researchers claim that by creating a dynamic two-dimensional array to record

changes in ink thickness on an ink roller, the process of ink transfer during printing can be reliably and intuitively reproduced. However, the use of an undirected graph to determine the distribution of ink on an ink roller does not allow determining the actual pattern of movement of ink layers during discrete modeling of the ink apparatus. In the paper by Panichkin and Varepo (2014), ink flow between rotating cylinders and subsequent ink film breakdown were simulated using finite difference methods. The possibility of creating local areas of ink separation from the paper surface when leaving the print interaction zone is shown. However, in this work, when numerically calculating the movement of free boundaries, there is no information about the discrete modeling of the inking apparatus. In many works, the computer modeling method was used to study the inking system in offset printing (Dai, et al., 2008; Wu, Wu and Wang, 2011; Varepo, et al., 2018; Verkhola, Panovuk and Huk, 2019). Programs have been developed to simulate the flow of ink between cylinders. However, in these works, there is no information about the dynamic characteristics of the discrete model of the inking apparatus. Scientific publications (Aliyev, 2017; Aliyev, Khalilov and Ismailova, 2022) theoretically investigate ink transfer to the printing plate, taking into account the roughness of the surface of the printing plate. However, these works do not consider the modeling of the inking apparatus. The article by Aliyev (2019) considered the issues of modeling the inking apparatus of an offset printing machine. The model is built and the methodology for calculating the distribution of ink layers in the ink apparatus is developed. The regularity of the distribution of ink is established by calculating maximum and minimum layer thicknesses. However, the paper does not consider the regularity of ink distribution using discrete modeling of the ink apparatus. In a study by Verkhola, et al. (2022), a mathematical model of an offset inking and printing system was developed that describes the operating modes of all its components. The necessity of determining reliable values of ink-splitting coefficients in the contact zones of rollers and cylinders is substantiated. It is established that computer technologies allow for determining the amount of ink accumulated in the inking and printing system during printing, as well as the thickness and volume of ink on the surface of the prints. However, when creating a mathematical model, the dynamic characteristics of the inking apparatus are not considered.

The analysis of publications shows that there is no information about the discrete modeling of the ink apparatus in the process of ink transportation from the ink feeder to the plate cylinder in these works. Also based on the analysis of published scientific works, we can make the following conclusion about the state of the problem of mathematical modeling of the printing process:

- Traditional methods of mathematical analysis and theoretical mechanics cannot cover the study of complex and diverse dynamic phenomena of motion and interaction of the main material flows in offset printing. These methods also do not provide a complete mathematical description of the printing process as an object of automation. Therefore, it is desirable to develop mathematical methods of research based on software and hardware means of inking apparatus operation and their future model-oriented design.

The purpose of this work is to create a scientific basis for structural and mathematical modeling of the inking apparatus of offset printing machine. To achieve this goal, the following tasks were set:

- Construction of a discrete model of the inking apparatus as a control object related to the movement and flow of the ink in the printing process;
- Development of a methodology for the distribution of ink layers in the inking apparatus.

2. Materials and methods

2.1 Construction of a discrete model of the inking apparatus of an offset printing machine

The discrete model of the inking apparatus is based on the motion scheme of ink layers, i.e., in fact, the inking apparatus scheme, is considered as a directed graph. In this case, sections of the motion path of the ink layer are considered as branches of the graph, and the contact points of inks on the rollers are considered as nodes of the graph that correspond to the variables under consideration, i.e. thickness of the ink layer $h_i(n)$ for certain nodes i and discrete time instants n .

For each branch of the graph, two characteristics are introduced: 1) gear ratio β_i or $(1 - \beta_i)$; 2) bias factor α_i or $(1 - \alpha_i)$. Gear ratio β_i characterizes the proportion of the flow of ink transmitted in the forward direction after dividing the flow in the contact node; similarly gear ratio $(1 - \beta_i)$ characterizes the remaining fraction of the flow transmitted in the reverse direction. Bias factor α_i characterizes part of the ink path along the periphery of the roller between the contact nodes when the flow moves in the forward direction; bias factor $(1 - \alpha_i)$ characterizes, accordingly, the remaining part of the path when the flow moves in the opposite direction. In the work of Aliyev (2019) it is shown that in stationary mode, the amount of ink g_i , passing through each contact node in one printing cycle is equal to the amount of ink g_0 , which is supplied to the inking apparatus on average per printing cycle and the amount

of ink transferred to the impression, i.e. $g_0 = \delta_0 \gamma_0 = \dots = \beta_{(i-1)} h_{(i-1)} - (1 - \beta_i) h_i = \beta_i h_i - (1 - \beta_{(i+1)}) h_{(i+1)} = \dots = \sigma h$, where δ_0 is the pulse amplitude, γ_0 is the duty cycle, σ is the fill factor, h is the thickness of the ink layer on the impression. Consider a roller containing two nodes (Figure 1a). The outer layers of ink present between nodes, respectively, denote films of thickness f_{i-1} and f_i . The equations of the thickness of the layers of ink in the nodes of power and flow for the n -th turn will be:

$$h_{i-1} = (1 - \beta_i)E^{-(1-\alpha_i)}h_i + f_{i-1} \tag{1}$$

$$h_i = \beta_{i-1}E^{-\alpha_i}h_{i-1} + f_i$$

where E is the offset operator (Korn and Korn, 1978), which is used to determine the transition of the ink layer from one node to another node. Excluding h_{i-1} , we get the equation of the roller, characterizing the thickness of the ink layer in the consumable node:

$$h_i = b_i E^{-1} h_i + \beta_{i-1} E^{-\alpha_i} f_{i-1} + f_i \tag{2}$$

where $b_i = \beta_i(1 - \beta_i)$.

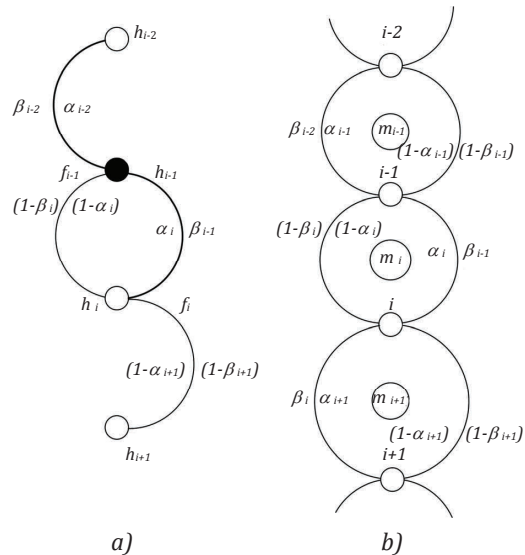


Figure 1: A discrete model of the ink apparatus; (a) – roller, (b) – baseline

Equation [2] is the basic equation of the ink roller, because it characterizes the dynamics of the ink layer, taking into account the division of the inner layer h_i at nodes and of contact receipts in these nodes from and to the outer layers f_{i-1} and f_i , respectively.

The case of considering the formation of the ongoing ink layer by a single node multiplicative operator E^{-1} and gear ratio combination b_i is insufficient if, in a real system, rollers have different rotation speeds. In this case, the calculated sampling period is chosen equal to the smallest of all the offset intervals: $\Delta t_p = (\Delta t_i)_{\min}$.

All other offset intervals are expressed (rounded) by an integer number of calculated offset intervals. Consider the baseline of the ink apparatus, shown in Figure 1b. In the center of the closed trajectory of the ink flow along the surface of the roller (cylinder), an image of the auxiliary graph is given, characterizing the direction of the flow (clockwise or counterclockwise), the number is indicated m_i , showing how many calculated sampling periods correspond to the time of one turn of the roller, i.e. $m_i = \tau_i / \Delta t_p$, where $\tau_i = \pi d_i / V_f$ (d_i – roller diameter, V_f – ink flow rate). Given the number m_i of sampling periods, the given displacement coefficients are expressed for the forward and reverse directions, respectively: $r_i = \alpha_i m_i$, $(m_i - r_i) = (1 - \alpha_i) m_i$. The time (interval) of the displacement of the ink flow on the surface of the roller is expressed in terms of the displacement coefficient and the time of the full turn of the roller: $\Delta t_i = r_i \tau_i$. For some discrete moment of time $n = t / \Delta t_p$, thickness of the ink layer in the i -th contact node is formed by summing the two components (Figure 1b): 1) the thickness of the ink layer h_{i-1} , coming from $(i-1)$ -th node in the i -th node in the direction of forward flow with a gear ratio β_i and negative bias (delay) $r_i = \alpha_i m_i$; 2) the ink layer thickness h_{i+1} coming from $(i+1)$ -th node in the direction of return flow with a gear ratio $(1 - \beta_{i+1})$ and negative bias $(1 - \alpha_{i+1}) m_{i+1}$.

Based on this, we write the equation of the contact node using the notation of the offset operator E :

$$h_i = \beta_{i-1} E^{-r_i} h_{i-1} - (1 - \beta_{i+1}) E^{-(m_{i+1} - r_{i+1})} h_{i+1} \quad [3]$$

We represent Equation [3] in the form of a linear difference order equation r_i :

$$h_i E^{r_i} \equiv \beta_{i-1} h_{i-1} + (1 - \beta_{i+1}) E^{r_{i+1} + r_i - m_{i+1}} h_{i+1} \quad [4]$$

It means that $r_i > (r_{i+1} - m_{i+1})$; otherwise, the equation is of order $(r_{i+1} - m_{i+1})$.

Solution of the difference equation of order r reduces in principle to solving a system r of first order difference equations. This way, we bring Equation [4] to a system of first order equations by introducing $h_i^{(r)} = E h_i^{(r-1)}$ as new variables so that $E h_i = h_i^{(1)}$:

$$E h_i^{(1)} = h_i^{(2)} \quad [5]$$

...

$$E h_i^{(r-2)} = h_i^{(r-1)}$$

$$E h_i^{(r-1)} = \beta_{i-1} h_{i-1} + (1 - \beta_{i+1}) E^{r_{i+1} + r_i - m_{i+1}}$$

In a similar way, difference equations of the form presented in Equation [4] and equivalent systems of difference equations of the first order of the form in Equation [5] for nodes as parts of a complex ink appa-

ratus, which can be given the serial numbers, can be written $1, 2, \dots, i, \dots, k, k+1, k+2$, where k is the total number of rollers in the baseline, and the indices $k+1, k+2$ relate to plate and offset cylinders. General system of linear difference equations of the first order for all $k+2$ baseline nodes can be written in matrix form, which is parallel to the first-order linear difference equation:

$$EH = AH + F(n) \quad [6]$$

where $H \equiv \{h_1, h_2, h_2^{(1)}, \dots\}$, $F(n) \equiv \{h_0(n), \dots\}$ are vectors (column matrices), and $A = [a_{ij}]$ square matrix of order S . The order of the matrix is determined by the total number $k+2$ nodes of the baseline, combined with the sum of the numbers of additional variables for individual nodes:

$$s = k + 2 + \sum_{i=1}^z (r_i - 1) \quad [7]$$

where z is the number of individual nodes.

Matrix elements $[a_{ij}]$ are nonzero only for nodes directly connected by transmission lines (branches of the graph). For variables $h_i^{(r_i-1)}$, connected only by the offset operator E , matrix elements are equal to unity. The solution of matrix Equation [6] with zero initial conditions is the vector

$$H = \sum_{n=0}^{m-1} A^{m-n-1} F(n) \quad [8]$$

The powers of the matrix A needed to solve Equation [8] can be calculated by Cayley-Hamilton's theorem (Korn and Korn, 1978). For matrix order $s > 4$ finding a solution is associated with laborious calculations, and therefore it is advisable to use digital computers.

2.2 Discrete model of the inking apparatus of complex structure

Consider a discrete model as applied to the inking apparatus of complex structure (Figure 2). As the initial we take the thickness of the ink layer $h_k = \text{const}$ on the surface of the duct cylinder. The transmission coefficients are assumed equal for all nodes, i.e. $\beta_i = \beta = 0.5$. In addition to the transfer coefficient, the ink flow transmitted to the plate cylinder is determined by the fill factor of the form by the printing elements. The interval of discreteness will take 1/4 of the time of turn of the form cylinder. The given displacement factors $r_i = \alpha_i m_i$ and coefficients m_i are expressed as rounded integers.

Applying the described methodology sequentially to all nodes of the inking apparatus as for the main (1, 2, 3, 4, 5, 6a, 7a, 8, 9), so for branches (2'; 6b; 7b; 4c, 5c, 6c, 7c), we compose the system of Equations [9].

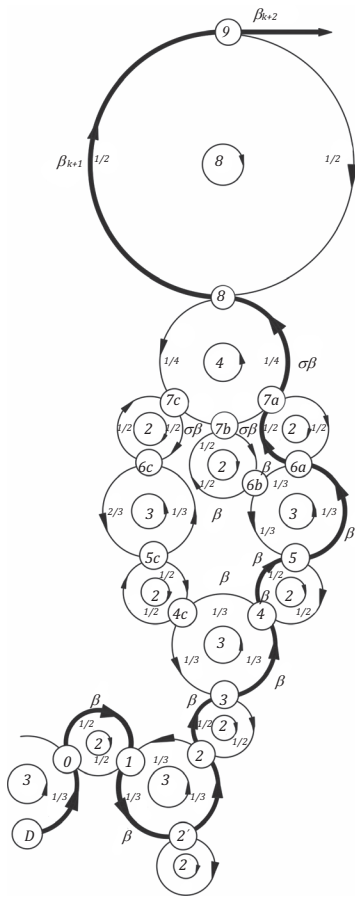


Figure 2: A discrete model of the inking apparatus of complex structure

$$\begin{aligned}
 \gamma h_0 &= E^{-1} \gamma h_D + (1 - \beta) E^{-1} \gamma h_1 & [9] \\
 \gamma h_1 &= \beta E^{-1} \gamma h_0 + (1 - \beta) E^{-1} h_2 \\
 h'_2 &= \beta E^{-1} \gamma h_1 + (1 - \beta) E^{-2} h'_2 \\
 h_2 &= \beta E^{-1} h_{2'} + (1 - \beta) E^{-1} h_3 \\
 h_3 &= \beta E^{-1} h_2 + (1 - \beta) E^{-1} h_{4c} \\
 h_4 &= \beta E^{-1} h_3 + (1 - \beta) E^{-1} h_5 \\
 h_5 &= \beta E^{-1} h_4 + (1 - \beta) E^{-1} h_{6b} \\
 h_{6a} &= \beta E^{-1} h_5 + (1 - \sigma \beta) E^{-1} h_{7a} \\
 h_{7a} &= \beta E^{-1} h_{6a} + \sigma \beta E^{-1} h_{7b} \\
 h_{6b} &= \beta E^{-1} h_{6a} + (1 - \sigma \beta) E^{-1} h_{7b} \\
 h_{7b} &= \beta E^{-1} h_{6b} + \sigma \beta E^{-1} h_{7c} \\
 h_{4c} &= \beta E^{-1} h_4 + (1 - \beta) E^{-1} h_{5c} \\
 h_{5c} &= \beta E^{-1} h_{4c} + (1 - \beta) E^{-1} h_{6c} \\
 h_{6c} &= \beta E^{-1} h_{5c} + (1 - \sigma \beta) E^{-1} h_{7c} \\
 h_{7c} &= \beta E^{-1} h_{6c} + (1 - \beta) E^{-1} h_8 \\
 h_8 &= \sigma \beta E^{-1} h_{7a} + (1 - \beta_{k+2}) E^{-1} h_9 \\
 h_9 &= \beta E^{-1} h_8
 \end{aligned}$$

$$\begin{aligned}
 E \gamma h_0 &= \gamma h_D + (1 - \beta) \gamma h_1 & [10] \\
 E \gamma h_1 &= \beta \gamma h_0 + (1 - \beta) h_2 \\
 E h'_2 &= h_{2'}^{(1)} \\
 E h_2 &= \beta h_{2'} + (1 - \beta) h_3 \\
 E h_3 &= \beta h_2 + (1 - \beta) h_{4c} \\
 E h_4 &= \beta h_3 + (1 - \beta) h_5 \\
 E h_5 &= \beta h_4 + (1 - \beta) h_{6b} \\
 E h_{6a} &= h_{6a}^{(1)} \\
 E h_{7a} &= h_{7a}^{(1)} \\
 E h_{6b} &= \beta h_{6a} + (1 - \sigma \beta) h_{7b} \\
 E h_{7b} &= h_{7b}^{(1)} \\
 E h_{4c} &= \beta h_4 + (1 - \beta) h_{5c} \\
 E h_{5c} &= \beta h_{4c} + (1 - \beta) h_{6c} \\
 E h_{6c} &= \beta h_{5c} + (1 - \sigma \beta) h_{7c} \\
 E h_{7c} &= \beta h_{6c} + (1 - \beta) h_8 \\
 E h_8 &= h_8^{(1)} \\
 E h_9 &= h_9^{(1)} \\
 E h_{2'}^{(1)} &= \beta E \gamma h_1 + (1 - \beta) h'_2 \\
 E h_{7b}^{(1)} &= \beta E h_{6b} + \sigma \beta h_{7c} \\
 E h_{6a}^{(1)} &= \beta E h_5 + (1 - \sigma \beta) h_{7a} \\
 E h_{7a}^{(1)} &= h_{7a}^{(2)} \\
 E h_{7a}^{(2)} &= \beta E h_{6a}^{(1)} + \sigma \beta h_{7b} \\
 E h_8^{(1)} &= h_8^{(2)} \\
 E h_8^{(2)} &= h_8^{(3)} \\
 E h_8^{(3)} &= \sigma \beta E h_{7a}^{(2)} + (1 - \beta_{k+2}) h_9 \\
 E h_9^{(1)} &= h_9^{(2)} \\
 E h_9^{(2)} &= h_9^{(3)} \\
 E h_9^{(3)} &= \beta h_8
 \end{aligned}$$

In the system of Equations [9] γ is the duty cycle, which is equivalent to pulsed power supply with period τ_0 .

By introducing additional variables, we then obtain the system of first-order Equations [10].

2.3 Digital modeling of the inking apparatus

The task of modeling is to obtain the thickness of the layers in the contact zones depending on the displacement interval. The description of the process of dividing the ink layer using difference equations creates the necessary mathematical basis for digital modeling of

the inking apparatus. Digital modeling is understood as such an organization of the computational process in a computer, which, in a certain sense, is similar to the process of dividing the ink layer in the inking apparatus. For computer implementation, software has been developed using the Visual Basic program, which, using macros, integrating with office programs, easily provides reproduction of graphic images of research results. The software is developed on the basis of the Gauss method for the numerical solution of systems of linear algebraic equations.

3. Results and discussion

Dynamic characteristics of the inking apparatus obtained as a result of digital modeling, i.e. the separation of the ink layer in the contact zones depending on the offset interval is shown in Figures 3 and 4. Figure 3a shows the beginning of the process (up to 2 rotations of the form cylinder), Figure 3b the continuation of the process (from 2 to 10 rotations of the form cylinder), and Figure 3c is a graphical representation of the process as a whole (from 2 to 20 rotations of the form cylinder) with continuous power supply. Figure 4a shows the beginning of the process (up to 2 rotations of the form cylinder), and Figure 4b the continuation of the process (from 2 to 20 rotations of the form cylinder) with pulsed power supply.

In continuous feeding (Figure 3), when the plate cylinder rotates up to 0.25 rotations, the thickness of the ink layer h_0 on the surface of the ductor cylinder, which contains the zero node of the baseline of the inking apparatus (Figure 2), reaches from 0 to 8 μm . This value remains stable up to 0.5 rotations of the plate cylinder. In the subsequent rotation of the plate cylinder up to 20 rotations, h_0 reaches up to 13 μm and the formation of the thickness of the ink layer on the surface of the ductor cylinder is stabilized. At 0.25 rotations of rotation of the plate cylinder, the formation of an ink layer h_1 begins on the surface of the first shaft, containing nodes 0 and 1 of the baseline. The layer thickness increases from 0 to 4 μm , which corresponds to 0.5 h_0 . This value remains stable from 0.5 to 0.75 rotations of the plate cylinder. In further rotation of the plate cylinder up to 20 rotations, h_1 reaches up to 10.5 μm and the formation of the thickness of the ink layer on the surface of the first roller stabilizes.

As can be seen from the graph (Figure 3), the process of the beginning of the formation and gradual increase in the thickness of the ink layer from h_2 to h_6 on the surfaces of subsequent rollers, containing nodes 2, 3, 4, 5, 6a, of the baseline (Figure 2), occurs sequentially every 0.25 rotations of the plate cylinder and ends at 1.75 rotations of the plate cylinder. When the plate cyl-

inder rotates from two rotations, the formation and gradual increase in the thickness of the ink layer h_7 occurs on the surface of the seventh shaft, which contains nodes 6a and 7a of the baseline (Figure 2). When the rotation of the plate cylinder reaches 20 rotations, the thickness of the ink layer h_7 reaches from 0 to 2 μm . At the same time, the process of stabilizing the formation of the thickness of the ink layer on the surfaces of all rollers also occurs.

With pulsed power supply (Figure 4), at 0.25 rotations of the plate cylinder, the thickness of the ink layer h_0 on the surface of the ductor cylinder of the inking apparatus, which contains the zero node of the baseline (Figure 2), reaches up to 8 μm . This value decreases to 0.25 μm when the plate cylinder rotates up to 2 rotations. In subsequent rotation of the plate cylinder up to 10 rotations, h_0 decreases to 0.07 μm . At 0.25 rotations of the plate cylinder, the formation of an ink layer h_1 begins on the surface of the first shaft, containing nodes 0 and 1 of the baseline. In this case, the thickness of the ink layer h_1 increases from 0 to 4 μm , which corresponds to 0.5 h_0 . This value decreases from 0.5 to 2 cylinder rotations to 0.38 μm and remains stable up to 2 cylinder rotations. With further rotation of the plate cylinder up to 10 rotations, h_1 decreases to 0.07 μm .

As can be seen from the graph (Figure 4), the process of the beginning of the formation and gradual increase in the thickness of the ink layers h_2 to h_6 on the surfaces of subsequent rollers occurs sequentially, starting at 0.75 rotations of the plate cylinder, every 0.25 rotations of the plate cylinder and ending at 1.75 rotations of the plate cylinder. When the plate cylinder rotates up to 2 rotations, there is a gradual decrease in the thickness of the ink layer from h_2 to h_6 on the surfaces of the rollers containing nodes 2, 3, 4, 5, 6a, of the baseline (Figure 2). Also, the formation and increase in the thickness of the ink layer h_7 occurs on the surface of the seventh shaft, which contains nodes 6a and 7a of the baseline (Figure 2). When the plate cylinder rotates up to 5 rotations, the thickness of the ink layer h_7 reaches from 0 to 0.06 μm and decreases to 0.05 μm from 5 to 10 rotations of the plate cylinder. Also, with 10 rotations of the plate cylinder, the process of stabilizing the formation of the thickness of the ink layers on the surfaces of all rollers occurs.

Dynamic characteristics are approximated with high accuracy by an exponential function, which can be written in a logarithmic form. Introducing the notation

$$\theta = \frac{t}{T_0}, \theta_0 = \frac{\tau}{T_0}, x_i = \frac{h_i}{h_i^0} \quad [11]$$

we represent the approximating function in two forms

$$x_i(\theta) = 1 - e^{\theta_0 - \theta}; \quad \ln(1 - x_i) = \theta_0 - \theta \quad [12]$$

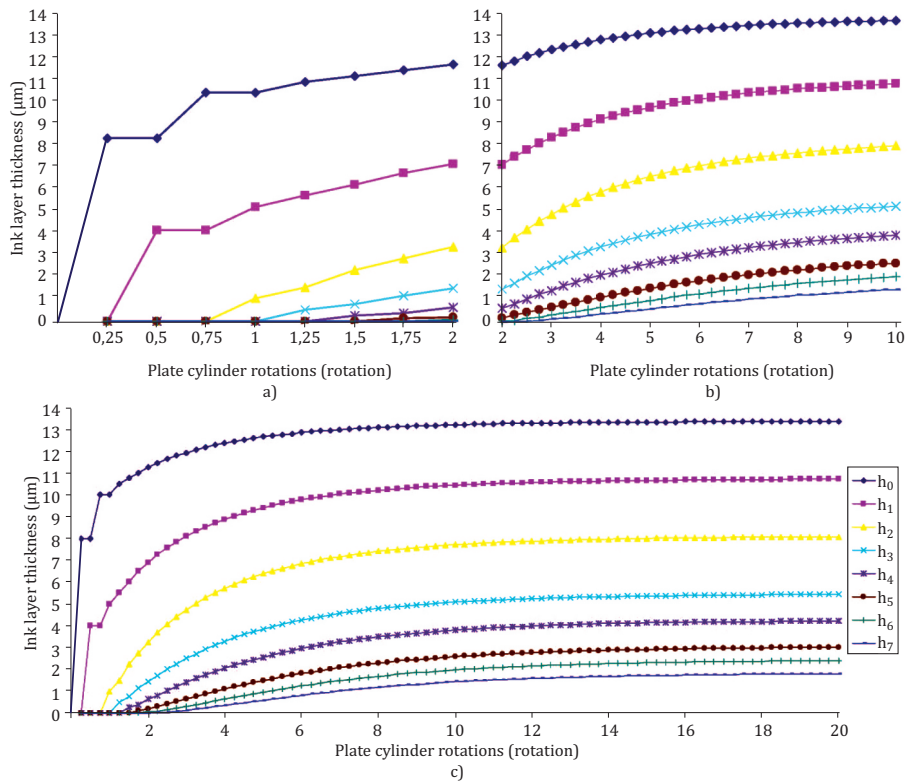


Figure 3: Dynamic characteristics of the inking apparatus at continuous power at the speed of the plate cylinder: (a) the beginning of the process; (b) continuation of the process; (c) a graphic representation of the process as a whole

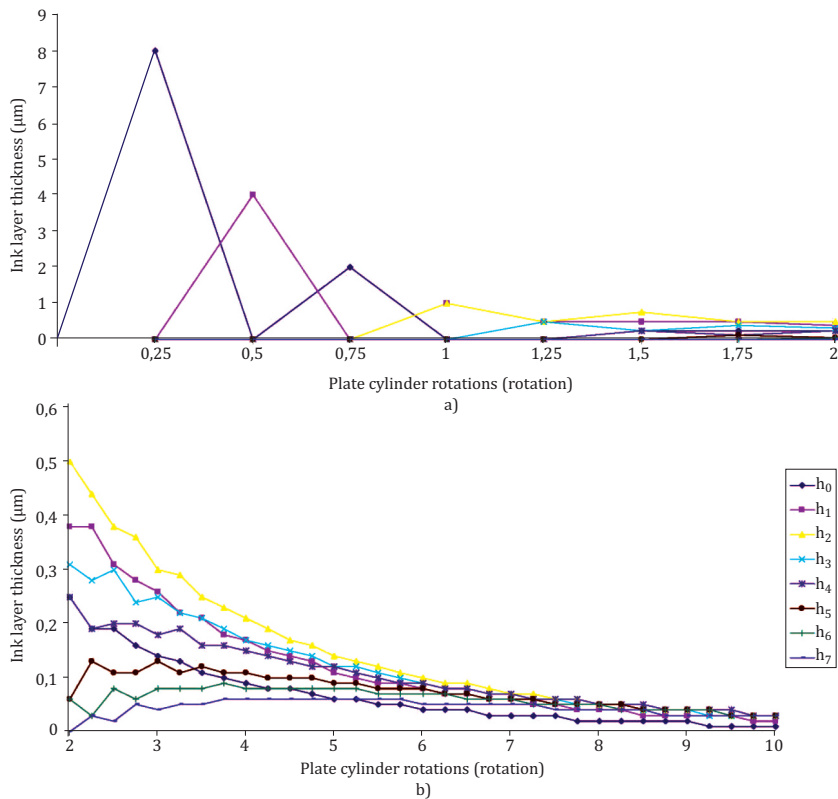


Figure 4: Dynamic characteristics of the inking apparatus at pulse power supply, with a rotation of the plate cylinder: (a) the beginning of the process; (b) continuation of the process

The exponential form directly follows from the simulation results. The logarithmic form gives a more accurate approximation, since it is expressed by a linear dependence.

An important property of the generalized output dynamic characteristic is that it does not depend on the number of rollers of the ink apparatus k , as well as on the transfer coefficient of ink to paper β_p . At the same time, the parameter of this characteristic is delay θ_0 , coefficient dependent: $\theta_0 = 0.2(1 + 2\sigma)$. With increasing σ relative delay θ_0 increases and the characteristic shifts to the right along the abscissa.

Concretization of generalized output and internal dynamic characteristics is performed using dependencies $T_0 = T_0(k, \sigma, \beta_p)$, $h_0 = h_0(k, \sigma, \beta_p)$ and $\theta_0 = \theta_0(\sigma) = \theta_0(k, i)$, which are obtained on the basis of the results of digital modeling.

The dependence of the time constant T_0 on the number of rolls k at various values of σ (0; 0.5; 1) and β_p (0; 0.5; 1) is shown in Figure 5. The dependence approaches linear if we determine $\ln T_0$.

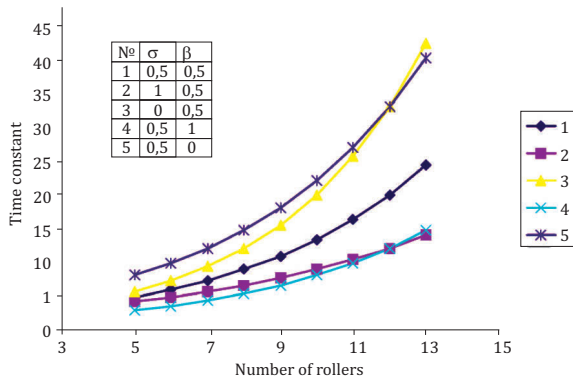


Figure 5: The dependence of the time constant T_0 on the number of rollers k in inking apparatus

Based on the data of digital modeling, an empirical formula can be proposed

$$\ln T_0 = 1.5 - \beta_p + 0.25(1 - 0.4\sigma)(k - 2) \quad [13]$$

allowing to determine T_0 at given values k, σ, β_p .

The generalized internal dynamic response at $\sigma = 0$ reflects the dynamics of the inner layers of the ink apparatus and also depends on the parameter θ_0 , which in this case can characterize either a delay or a lead. At a certain number of the inner layers i_0 characteristic goes through zero $\theta_0 = 0$. At $k \geq i > i_0$ there is a delay $\theta_0 > 0$; at $1 < i < i_0$ it is a lead $\theta_0 < 0$. For each number of rollers k in the ink apparatus there will be a value i_0 , which increases with increasing k .

4. Conclusions

To investigate the process of ink transfer and distribution occurring in the ink-printing system of an offset machine in the printing process, a discrete model of the ink apparatus related to the movement and ink flow of the ink apparatus is constructed. A method for determining the distribution of ink layers in the ink apparatus, using computer technology, is developed. For the basis of the discrete model of the ink apparatus, the scheme of movement of ink layers, which corresponds to the actual scheme of the ink apparatus, is taken. This scheme was considered as a directed graph. Sections of the trajectory of the ink layer were considered as arcs of the graph. In this case, the contact points of the rollers were taken as nodes of the graph, which correspond to the thickness of the ink layer $h_i(n)$ for certain nodes i and discrete time points n . To characterize the fraction of the ink flow transmitted in the forward direction after dividing the flow in the contact node and also the remaining fraction of the flow transmitted in the opposite direction for each branch, the transfer coefficient β_i or $(1 - \beta_i)$, respectively, is introduced into the graph. To characterize the part of the ink path along the periphery of the roller between the contact nodes when the flow is in the forward direction and the remaining part of the path when the flow is in the reverse direction, a displacement factor α_i or $(1 - \alpha_i)$ is introduced for each branch of the graph, respectively. The discrete model by means of difference equations describes the discrete process of ink layer partitioning considering the layer displacement time along the rollers surface. The proposed methodology for the distribution of ink layers can be extended to ink apparatus of complex structure having branched ink streams. In this case, the thickness of the ink layer $h_k = \text{const}$ on the surface of the ductor cylinder is taken as the initial one. Transmission coefficients are assumed equal for all nodes, $\beta_i = \beta = 0.5$. The discreteness interval is taken to be 1/4 of the rotation time of the plate cylinder. The given displacement coefficients $r_i = \alpha_i m_i$ and coefficients m_i are expressed as rounded integers. Dynamic characteristics of the inking apparatus, i.e. separation of the ink layer in the contact zones depending on the displacement interval is considered with continuous and pulsed power. It has been established that in continuous feeding, when the plate cylinder rotates from 0.25 to 2 rotations, every 0.25 rotations, there is a consistent formation and gradual increase in the thickness of the ink layer on the surfaces of all the shafts of the ink apparatus along the baseline. When the rotation of the plate cylinder reaches 20 rotations, the process of stabilizing the formation of the thickness of the ink layer on the surfaces of all rollers along the baseline occurs. With pulsed power, when the plate cylinder rotates from 0.25 to 1.75 rotations, every 0.25 rotations there is a sequential formation and gradual increase

in the thickness of the ink layers on the surfaces of all baseline shafts, with the exception of the seventh shaft. When the rotation of the plate cylinder reaches two rotations, a gradual decrease in the thickness of the ink layer on the surfaces of these rollers begins. From this moment, the thickness of the ink layer forms and increases on the surface of the seventh shaft up to 5 rotations and gradually decreases, starting from 5 rotations of the plate cylinder. When the rotation of the plate cylinder reaches 10 rotations, the formation of the thickness of the ink layers on the surfaces of all rollers along the baseline is stabilized. The considered

discrete model of the inking apparatus is a refinement and development of the previously considered single-capacity model, which increases the reliability of the final result. The proposed method makes it possible to determine the thickness of the ink layer on the print and the amount of ink required to print an edition, taking into account the amount of ink accumulating in the inking system during the printing process. To obtain reliable information about the size of the ink layer on a print during printing, it is necessary to develop an appropriate technique. To test this technique, experimental studies are required.

References

- Aliyev, E., 2017. Influence microgeometry offset printing plates for transfer ink from the printing form on dekel. In: *Proceedings of the Second International Symposium of Mechanism and Machine Science (ISMMS-2017)*. Baku, Azerbaijan, 11–14 September 2017. Baku, Azerbaijan: AzClFToMM-Azerbaijan Technical University, pp. 201–202.
- Aliyev, E.A., 2019. Modeling of the inking apparatus of the sheet printing machine. *Journal Européen des Systèmes Automatisés*, 52(6), pp. 551–557. <https://doi.org/10.18280/jesa.520602>.
- Aliyev, A., Khalilov, I. and Ismailova, S., 2022. Indirect ink transfer for offset printing, taking into account the roughness of the offset printing plate surface. *Machine Science*, 11(2), pp. 71–79. <https://doi.org/10.61413/ZTQB7024>.
- Dai, Q., Wang, C., Huang, Y. and Wang, L., 2008. Computer simulation on dynamic response of offset inking system. In: *2008 International Conference on Computer Science and Software Engineering*. Wuhan, China, 12–14 December 2008. IEEE, pp. 377–380. <https://doi.org/10.1109/CSSE.2008.553>.
- Korn, G. and Korn, T., 1978. *Spravochnik po matematike: dlya nauchnykh rabotnikov i inzhenerov*. Moskva: Nauka, pp. 401, 668–675. (In English: *Handbook of mathematics: for scientists and engineers*).
- Litunov, S.N., Timoschenko, O.A. and Gusak, E.N., 2014. Modelirovaniye techeniya kraski v krasochnom apparate pechatnoy mashiny s passivnym aktivatorom. *Omskiy nauchnyy vestnik*, 127(1) pp. 215–219. (In English: Modeling of ink flow in the inking apparatus of a printing machine with a passive activator. *Omsk Scientific Bulletin*).
- Liu, L.L., Lu, F. and Bai, J.Y. 2012. Simulation of inking system based on elasto-hydrodynamic lubrication. *Applied Mechanics and Materials*, 121–126, pp. 2883–2886. <https://doi.org/10.4028/www.scientific.net/AMM.121-126.2883>.
- Liu, L.L., Li, K. and Lu, F., 2016. Dynamic simulation modeling of inking system based on elasto-hydrodynamic lubrication. *International Journal of Heat and Technology*, 34(1), pp. 124–128. <https://doi.org/10.18280/ijht.340118>.
- Panichkin, A.V. and Varepo, L.G., 2014. The numerical calculation of the a viscous incompressible fluid transfer onto porous surface between rotating cylinders. In: E.K. Polychroniadis, A.Y. Oral and M. Ozer, eds. *International Multidisciplinary Microscopy Congress: Proceedings of InterM*. Antalya, Turkey, 10–13 October 2013. Springer, pp. 79–83. https://doi.org/10.1007/978-3-319-04639-6_11.
- Toliver-Nigro, H., 2006. *Tekhnologii pechaty*. Translated from English by N. Romanova. Moskva: Print-media centr. (In English: *Printing technologies/Designer's printing companion*).
- Varepo, L.G., Trapeznikova, O.V., Panichkin, A.V., Roey, B.A. and Kulikov, G.B., 2018. Software for quantitative estimation of coefficients of ink transfer on the printed substrate in offset printing. *Journal of Physics: Conference Series*, 998: 012041. <https://doi.org/10.1088/1742-6596/998/1/012041>.
- Verkhola, M., Panovuk, U. and Huk, I., 2019. Modeling and analysis of ink distribution in the ink printing system of the sequential-parallel structure. *ECONTECHMOD: An International Quarterly Journal on Economics of Technology and Modelling Processes*, 8(2), pp. 45–50.
- Verkhola, M., Panovyk, U., Kalytka, M. and Babysh, O., 2022. Modeling and analysis of the ink splitting factors influence on ink filling in offset printing. *Journal of Print and Media Technology Research*, 10(4), pp. 215–229. <https://doi.org/10.14622/JPMTR-2113>.
- Wu, Q.M., Wu, J.M. and Wang, R., 2011. Study for dynamic property of the inking system of offset press based on Matlab. *Applied Mechanics and Materials*, 121–126, pp. 392–396. <https://doi.org/10.4028/www.scientific.net/amm.121-126.392>.
- Yan, Z., Hui, R. and Ling, H., 2009. Dynamic simulation of offset printing inking system based on undirected graph. In: *ACC 2009: ETP/IITA World Congress in Applied Computing, Computer Science, and Computer Engineering*. Sanya, China, 8–9 August 2009. Engineering Technology Press.
- Zhao, M.L., 2011. The dynamic property analysis of ink system in offset press. *Advanced Materials Research*, 199–200, pp. 132–136. <https://doi.org/10.4028/www.scientific.net/AMRddd.199-200.132>.



JPMTR-2312
DOI 10.14622/JPMTR-2312
UDC 539.6-033.5:519.8|53.08

Original scientific paper | 184
Received: 2023-09-14
Accepted: 2023-11-14

Static- and dynamic-wetting measurements on 3-aminopropyltriethoxysilane-functionalized float glass surfaces as a method for indicating adhesion forces

Sarah Patejdl, Ulrich Jung, Christopher Knoth and Patrick Görrn

Bergische Universität Wuppertal,
Gaußstraße 20, 42119 Wuppertal, Germany

patejdl@uni-wuppertal.de
ujung@uni-wuppertal.de

Abstract

Earlier research demonstrated the dependence of 3-aminopropyltriethoxysilane (APTES) wetting properties on cleaning, functionalization, and post-treatment processes on oxide surfaces, e.g., glass surfaces or Si wafer surfaces, but not on float glass surfaces. Also, oxide glass surfaces were functionalized by different silanes and were applied with ultraviolet (UV) radiation-curable inks or adhesives. The resulting adhesion forces differed depending on the silane and the UV-curable ink or adhesive used. The chemical diversity of silanes leads to different surface energy on glass surfaces and was used to gain further insights into a correlation between wetting properties and the resulting adhesion forces. This work investigates the suitability of dynamic contact angle measurement (DCA) for indicating adhesion forces via contact angle hysteresis and the resulting drop age. Two types of test fluids (diiodomethane and water) are applied on hydrophilic float glass surfaces (air side and tin side) and on a hydrophobic PE foil surface. The functionalization of glass substrates is realised by reproducible vapour and solution deposition of APTES, which results in different wetting properties of float glass surfaces. The investigations are complemented by static contact angle measurements of different test fluids, and the appropriate surface energies are evaluated via the Owens, Wendt, Rabel, and Kaelble method. The polar and non-polar surfaces are clearly differentiable by contact angle hysteresis and drop age. The DCA results of the hydrophilic float glass surfaces and the hydrophobic PE foil surface confirm the suitability of using the DCA parameters hysteresis and drop age for indicating adhesion forces on functionalized float glass surfaces. The hysteresis and drop age of assumed completely APTES-functionalized float glass surfaces confirm the suitability of the DCA measurement for indicating adhesion forces, too. The test fluid diiodomethane is suitable for indicating adhesion forces on the air side of the float glass, and the test fluid water is suitable for indicating adhesion forces on the tin side of the float glass. With the increased water contact angle, the hysteresis and drop age increased using the polar test fluid water. This does not support the polarity theory of de Bruyne. By using the non-polar test fluid diiodomethane, the hysteresis and drop age decrease with increasing contact angle and also do not support the adhesion theory of de Bruyne. The research results show a way of indicating the adhesion forces of different functionalized float glass surfaces, by using only one silane, and serves as a pre-step for better understanding of e.g. UV-ink adhesion forces dependent on glass surface wetting properties.

Keywords: dynamic contact angle, hysteresis, drop age, 3-aminopropyltriethoxysilane, adhesion

1. Introduction and background

Among trialkoxyorganosilanes, 3-aminopropyltriethoxysilane (APTES) is one of the best-known and most commonly widely used trialkoxyorganosilane for chemical and physical modification of oxide surfaces, e.g., microscope slides and Si-wafer surfaces, and is used as a coupling agent to promote adhesion between inorganic and organic substrates (Plueddemann, 1991;

Mittal and O'kane, 1976). According to Plueddemann (1970, p. 185) and Wolf (2022, p. 4) the APTES molecule follows the general formula of organosilanes $(X)_3Si(CH_2)_3Y$; while X marks the alkoxy group, e.g., methoxy or ethoxy group (OCH_3 , OC_2H_5), Y marks the organofunctional group, e.g., amino, vinyl, mercapto, etc., and CH_2 marks the alkylene bridge (called spacer or linker), typically a propylene chain. APTES has three hydrolyzable ethoxy groups and one organofunctional amino

group (NH₂) per molecule. The bonding of inorganic to organic substrates is based on reversible hydrolysis and condensation processes and described by various authors like Osterholtz and Pohl (1992), Altmann and Pfeiffer (2003), Chauhan, et al. (2008), Da Silva, Öchsner and Adams (2011, pp. 239–243), Kim, Holinga and Somorjai (2011), Yadav, et al. (2014), Deetz and Faller (2015) and Koç, Sert Çok and Gizli (2020); the influencing parameters are listed by Issa and Luyt (2019). The aim is to attach the condensation process resulting siloxane bonds covalently to the silanol groups (Si-OH) of the SiO₂ surface or neighbour molecules via hydrogen bonding or electrostatic interactions to a polysiloxane network. There are different ways for APTES to build several surface and layer structures like covalent attachment, horizontal polymerization through adjacent APTES molecules and multilayers resulting from the trifunctionality of APTES molecule, which leads to vertical polymerization described by Fadeev and McCarthy (1999), Asenath Smith and Chen (2008), Pasternack, Rivillon Amy and Chabal (2008), Acres, et al. (2012) and Yadav, et al. (2014). The investigated adhesion forces of ultraviolet (UV) polymer films with fixed weight or concentration of APTES and other organosilanes in the ink formulation or adhesion forces of UV polymer films on APTES- and other organosilane-functionalized glass substrates were investigated by Zhang, et al. (2013) and Wang, et al. (2021). Especially the investigations of Wang showed off the different wetting behaviour of functionalized glass surface based on the chemical diversity of the used silanes. Additionally, the wetting behaviour of APTES-functionalized glass surfaces depends on the applied functionalization method. The two widely used deposition methods are the solution-based method and the vapour-based method described by Metwalli, et al. (2006) and Liang, et al. (2014). The most commonly applied solutions for functionalization are ethanol/water solutions (95:5), recommended by Arkles, et al. (2014) or toluene solutions described by Arslan, et al. (2006), Fiorilli, et al. (2008), Pasternack, Rivillon Amy and Chabal (2008), Kim, Holinga and Somorjai (2011), and with 0.2 % to 2.0 % volume fraction silane concentration described by Argekar, Kirley and Schaefer (2013), but mostly only applied for Si wafers or microscope slides. For the vapour-based method, homemade apparatus, (room temperature) chemical vapour deposition ((RT-) CVD) and molecular layer deposition (MLD) are used, described by Zhang, et al. (2010) and Canané (2019).

The APTES functionalization in the vapour phase is preferred because of the smaller and sparser particles (diameter $\Phi < 30$ nm) and more uniform monolayer on the Si wafer surface in comparison with the solution-based deposition method, which makes controlled polymerization difficult and shows low reproducibility and disordered layers on a substrate as described by

Van Der Voort and Vansant (1996), Fiorilli, et al. (2008), Liang, et al. (2014), and Munief, et al. (2018). Under “optimal” controlled conditions, the silanes assemble on the surface in a high-quality uniform self-assembled monolayer (SAM) mentioned by Silberzan, et al. (1991) and Van Der Voort and Vansant (1996). Nevertheless, the functionalization results depend also, e.g., on the used glass substrate and applied cleaning method, silane concentration, conditioning, storage, and hydration of the surface, duration of functionalization, and curing conditions (e.g., duration, temperature, cooling) and lead to difficult control of silane structures and layers described by Van Der Voort and Vansant (1996), Siqueira Petri, et al. (1999), Altmann and Pfeiffer (2003), Metwalli, et al. (2006), Matinlinna, Zhu, Lerum and Chen (2012), and Lung and Tsoi (2018). The diversity of existent investigations of functionalized surfaces under different applied cleaning- and functionalization methods and post-treatments complicates the comparison of functionalization results. Investigations in functionalized float glass surfaces could not be found. The float glass used in this research is a flat glass product manufactured by the typical Pilkington process described in Pilkington (1969) and has an atmosphere side, also called air side (AS), and a bath side, also called tin side (TS), which shows different surface properties, especially different surface wetting properties depending on applied cleaning method as investigated by Lazauskas and Grigaliūnas (2012). With the possibility of generating different wetting properties on hydrophilic leveled float glass surfaces with only one silane, further insights into the adhesion behaviour of e.g., UV-inks dependent on the different wetting properties are allowed. This work investigates the APTES functionalization of hydrophilic polar alkaline cleaned float glass surfaces in the vapour and solution phases with the help of static and dynamic contact angle measurements and evaluates surface energy. Additionally, a hydrophobic non-polar polyethylene (PE) foil surface was investigated. The polar and non-polar surfaces are clearly differentiable by the water contact angle, surface energy, contact angle hysteresis, and drop age and show off the suitability of dynamic contact angle (DCA) measurements for indicating adhesion forces on surfaces. The applied APTES functionalization methods lead to reproducible and different wetting properties of the air and tin sides of the float glass and lead to clear, differentiable contact angle hysteresis and drop age when taking the glass side and the test fluid used into account. Appendix gives a summarized overview of measured static contact angles (SCAs), corresponding surface energies (SEs) and DCA parameters drop age and hysteresis in Tables A1 to A5. The investigations show the suitability of DCA measurement for indicating adhesive forces resulting from the applied vapour- and solution-based functionalization processes with APTES, depending on the float glass sides.

2. Materials and methods

2.1 Materials

Table 1 lists all solid materials and fluids used in this research for sample preparation and measurement.

Table 1: Materials and fluids used

Substrates	<ul style="list-style-type: none"> • Float glass, clear, seamed edge, 126 mm × 50 mm × 2 mm • PE adhesion foil without adhesive, transparent, thickness D: 0.06 mm, IFOHA
Cleaning agents	<ul style="list-style-type: none"> • Laboratory dishwasher cleaner, Neodisher Labo GK, Dr. Weigert • Ethanol, ≥ 99.8 %, denatured, CAS-no.: 64-17-5 • Water, Aqua Dest., CAS-no.: 7732-18-5, Wittig Umweltchemie
Functionalization agents	<ul style="list-style-type: none"> • 3-aminopropyltriethoxysilane, 98.0 %, CAS-no.: 919-30-2, Thermo Scientific™ • Acetic acid, 100.0 %, Ph. Eur., pure, CAS-no.: 64-19-7 • Ethanol, ≥ 99.8 %, denatured, CAS-no.: 64-17-5 • Double-distilled water, Aqua Bidest • Silica gel orange, size 2–5 mm, CAS-no.: 1327-36-2, Carl Roth
Static contact angle and dynamic contact angle test-liquids	<ul style="list-style-type: none"> • Water, Aqua Dest., Wittig Umweltchemie • Diiodomethane, 99.0 %, stab., CAS-no.: 75-11-6, Alfa Aesar • Benzyl alcohol, 99.0 %, CAS-no.: 100-51-6, Alfa Aesar • Glycerol, 99.0 %, CAS-no.: 56-81-5, Alfa Aesar

2.2 Cleaning method

The float glass used was cleaned in a 60 °C mildly alkaline cleaning bath (4 g/l laboratory dishwasher cleaner (LDC), pH: 11.3–11.4) in distilled water in a stainless steel container (353 mm × 325 mm × 65 mm) with a matching lid for 1 h on a hot plate (\approx 40 °C) followed by distilled water rinsing of the float glass samples in a mini-dishwashing machine (MD 37004, Medion) using program P2 (wash: 50 °C, rinse: 65 °C, dry: 1h) to remove coarse organic and inorganic contaminants, to get the float glass surfaces hydrophilic with water

contact angles (WCAs \approx 1° after 10 s) and to provide a basis for comparing the wetting behaviour of APTES-functionalized float glass surfaces. The used cleaning method is called the “enhanced cleaning method”, abbreviated EM. The cleaned float glass was stored for one week at room temperature in dust-free sample boxes before starting with the functionalization process.

2.3 Functionalization methodologies

The wetting behaviour of the cleaned float glass surfaces was changed by using two functionalization methods. The APTES functionalization was carried out via the vapour phase (M1) and via the solution phase (M2) in the style of Wang, et al. (2021) with different variants like duration of functionalization and silane concentration.

2.3.1 APTES functionalization via vapour phase

For the APTES functionalization in the vapour phase, the APTES listed in Table 1 was used. One to two days before APTES functionalization, the silica gel was activated in the drying oven for 2 h at 120 °C, cooled down, and stored in a little glass container. On functionalization day, 130 g of the activated silica gel was filled in the crystallizer bowl (outer diameter Φ_o : 80 mm, height H : 45 mm, volume V : 150 ml) and placed on the bottom of the desiccator (DN200, Duran). Afterwards, the APTES is pipetted into the eight silane reservoirs (V : 60 μ l each, Φ_o : 10 mm, inner diameter Φ_i : 6 mm, H : 6.7 mm) of the polytetrafluoroethylene (PTFE) functionalization ring (Φ_o : 115 mm, Φ_i : 90 mm, H : 5 mm) and placed around the crystallizer bowl with the silica gel in it.

The porcelain perforated plate was positioned in the desiccator, and two sample holders (polyoxymethylene) with 16 float glass samples were placed on the perforated plate. Near them, the thermo-hygrometer (TP157-3, ThermoPro) was placed and the desiccator was closed. Afterwards, the desiccator was placed onto the hot plate (40 °C) of the magnetic stirrer (RSM 10HS, Phoenix Instruments), and the vacuum pump (AS29, Wiltec) was connected to the desiccator tap. By starting the vacuum pump the valve of the desiccator tap had to be open. The vacuum pump was running for about 2 min, and resulting in an under pressure of 0.08 MPa inside the desiccator. After 2 min, the valve of the desiccator tap was closed, and the vacuum pump could be stopped. The vacuum procedure was repeated every hour because of the short vacuum holding of the desiccator (< 60 min). During the functionalization process, the inside temperature increased to 21.5 °C and relative humidity decreased to 16 %. After functionalization (duration: 2 h, 4 h and 8 h), each of the float

glass samples was cleaned with a cleanroom cloth surrounded plastic squeegee with ≈ 3 ml of ethanol three times with two repetitions. Afterwards, the functionalized batch was rinsed clean in the mini-dishwashing machine and conditioned at room temperature for three days in dust-free sample boxes. Within four days, the SCA and DCA measurements were carried out.

2.3.2 APTES functionalization via solution phase

For APTES functionalization in the solution phase, all the listed functionalization agents were used (Table 1). The APTES solution consists of a mass fraction of 95 % ethanol ($570 \text{ g} \pm 1 \text{ g}$) and a 5 % mass fraction of double-distilled water ($30 \text{ g} \pm 0.1 \text{ g}$) to reach a volume of ≈ 800 ml. Thereby, the double-distilled water was added drop by drop to the ethanol with the disposable pipette (V : 30 ml) and was mixed using the PTFE magnetic stirring rod ($L \times \Phi$: 35 mm \times 9 mm) in a laboratory bottle (V : 1000 ml) with closed screw cap for 20 min at 100 rounds per min (rpm); 5 min before the time was up, 12 g / 48 g of APTES (2 % / 8 % mass fraction of the ethanol/water solution) was weighed in. After weighing, the APTES was added drop by drop to the ethanol / water solution and mixed for another 20 min.

After the time was up, the APTES was pre-hydrolyzed and could be adjusted to a pH of 5.0 with acetic acid. The silane solution was decanted from the laboratory bottle into the crystallizer bowl (Φ_0 : 140 mm, H : 65 mm, V : 900 ml) with the magnetic stirring rod and was covered with a polyvinylidene fluoride (PVDF) plate with a small gap for the electrode of the pH-measurement device (HI98103, Hanna Instruments) held by a tripod. The electrode was dipped ≈ 10 mm in the silane solution and needed ≈ 2 min to show a constant pH. Acetic acid was added step by step with a disposable syringe (V : 10 ml) into the silane solution till a pH of 5.0 ± 0.1 was reached. All the time, the silane solution was mixed at 100 rpm.

Two hours after the end of mixing the APTES into the ethanol / water solution, the PVDF sample holder was placed in the silane solution-filled crystallizer bowl, followed by the placing of float glass samples in the sample holder with an acid-proof tweezers. The crystallizer bowl was covered by the PVDF plate, and the float glass functionalized for 1 h in the silane solution.

After functionalization, the cleaning procedure of Chapter 2.3.1 was carried out and afterwards the samples were stored in the drying oven (UN30 Plus, Memmert) for 1 h at 80 °C, and then finally clearly rinsed in the mini-dishwashing machine, and conditioned at room temperature in dust-free sample boxes for 3 days. Within four days, the SCA and DCA measurements were carried out.

2.4 Instruments

A contact angle measuring device (OCA 50, Dataphysics) was used to measure SCAs with the sessile drop method and DCAs with the sessile drop method and tilting plate with test fluids according to DIN EN ISO 19403-7 and DIN EN ISO 19403-6 (Deutsche Institut für Normung, 2020; 2023) to get quantitative data about the static and dynamic wetting behaviour of cleaned and APTES-functionalized float glass surfaces as well as the PE foil surface.

An AFM measurement device (Innova AFM, Bruker) was used to measure the R_q -roughness in two types of cleaned float glass surfaces. The float glass was first cleaned with the alkaline cleaning process described in Chapter 2.2 and in the following cleaning step, the alkaline cleaned float glass was cleaned in an acetone and ethanol ultrasonic cleaning bath for 5 min. After both cleaning procedures, the R_q -roughness was randomly evaluated of $10 \mu\text{m} \times 10 \mu\text{m}$ sections in tapping mode.

2.5 Static contact angle methodology

For the SCA measurement, the liquid drops of the test fluids water, diiodomethane, benzyl alcohol, and glycerol were used (Table 1). The adjusted contact angle measuring parameters and equipment used are listed in Table 2.

Table 2: Adjustments and equipment for static contact angle measurement using device OCA 50 of Dataphysics

Syringe	Disposable, V : 1 ml
Dosing needle	Φ_0 : 0.91 mm, Φ_1 : 0.58 mm, L : 38.1 mm
Dosing volume	2 μl
Dosing rate	0.10 $\mu\text{l/s}$
Method	Sessile drop
Brightness	Grey value between 170 and 200 in an area of ≈ 30 px over the positioned baseline; in the case of PE foil, adjustment to maximum.
Measurement table	Standard table for (functionalized) float glass, intake plate for planar fixing of PE foil
Live window size	1100 \times 730 px
Frame rate	22.39 frames per second
Contour fitting	Ellipse-fitting method

The liquid drops were placed with a disposable syringe and dosing needle on the EM-cleaned APTES-functionalized float glass surfaces and the PE foil surface. All measurements were done in a dark environment to avoid reflections in the liquid drop placed on the substrate surface. The dosed liquid drops were slowly picked up by the table used, and the applied liq-

uid drops lied for 10 s on the substrate surface to reach an approximate three-phase equilibrium. The application procedure was recorded by video and started by exceeding the optical trigger line that was placed near the drop curvature. The data fit of the first complete and sharply contoured lying drop on the surface, 3 frames after drop application, was used as the starting point for the evaluation of contact angle data over time. The mean contact angles (CAMs) were evaluated after frame 224 (approx. 10 s). For each test fluid, 20 CAMs on both glass sides and on the PE foil surface were carried out and evaluated. The following interpretations refer exclusively to the median of the SCA measurements.

2.6 Dynamic contact angle methodology

For the DCA measurement, the test liquids diiodomethane and water (Table 1), and adjustments and equipment given in Table 3 were used.

Table 3: Adjustments and equipment for dynamic contact angle measurement using device OCA 50 of Dataphysics

Syringe	Disposable, V: 1 ml
Dosing needle	Φ_0 : 1.83 mm, Φ_1 : 1.37 mm, L: 38.1 mm
Dosing volume	Diiodomethane: 4 μ l; water: 20 μ l
Dosing rate	0.10 μ l/s
Method	Sessile drop
Brightness	Grey value between 170 and 200 in an area of \approx 30 px over the positioned baseline; in the case of PE foil, adjustment to the maximum.
Measurement table	Standard table for (functionalized-) float glass, intake plate with membrane vacuum pump of Dataphysics for planar fixing of PE foil
Live window size	1600 px \times 730 px
Frame rate	10.00 frames per second
Electronic tilting device	Relative velocity of 0.5°/s (0.10°/step)
Contour fitting	Polynomial-fitting method

The test fluids were placed with a disposable syringe on the EM-cleaned APTES-functionalized float glass surfaces and the PE foil surface. The table was taped to the float glass sample format to create the best possible vacuum. The float glass sample was placed in the centre of the intake plate to arrange the camera and the sample in a T-shape position. The dosed liquid drop of each test liquid was slowly picked up with a standard table or the running intake plate after the drop dosing ended and lied for 10 s on the substrate surface. The video recording started shortly before picking up the dosed drop. After the drop was lying on the surface, a timer run up to 10 s and then the tilting was immediately manually started. The tilting was stopped manually when the liquid drop had rolled out of the live window. From the last tilting table data of 0.00°, the frames were counted up, and the corresponding advancing and receding contact angles were shown in diagrams of DCA measurements over frame time (100 frames \approx 10 s). On both float glass sides (cleaned and functionalized ones) and on the PE foil surface, 5 DCAs were captured with test fluids diiodomethane and water and evaluated.

3. Results of evaluated SCA measurements and SE

In the following sections, the measured SCAs on the float glass surfaces are evaluated and exemplarily shown in appropriate boxplot and table. The SCA results of the PE foil and the APTES-functionalized float glass surfaces (M1/M2) are displayed in tables. Additionally, the SEs of investigated surfaces are evaluated with the Owens, Wendt, Rabel, and Kaelble (OWRK) method (Owens and Wendt, 1969; Rabel, 1971; Kaelble, 1970).

3.1 The SCA results of EM-cleaned hydrophilic float glass surfaces

Evaluated SCAs of EM-cleaned float glass surfaces are listed in Table 4 and shown in Figure 1. The WCA results, evaluated at frame 35 (circle-fitted), of three

Table 4: Contact angles: median, min. and max. and deviation of 20 SCA measurements of the test fluids used on the AS and TS of the EM-cleaned float glass surfaces; an ellipse fitted WCA of \approx 1° after 10 s is assumed

SCA [°]	Water	Diiodomethane	Benzyl alcohol	Glycerol
AS	1.0	45.2	28.9	18.9
Min./Max.	–	44.1/46.7	27.0/29.6	17.6/20.3
Deviation	–	\pm 1.3	\pm 1.3	\pm 1.4
TS	1.0	42.1	22.1	20.8
Min./Max.	–	39.3/44.4	20.5/23.4	18.0/23.4
Deviation	–	\pm 2.6	\pm 1.5	\pm 2.7

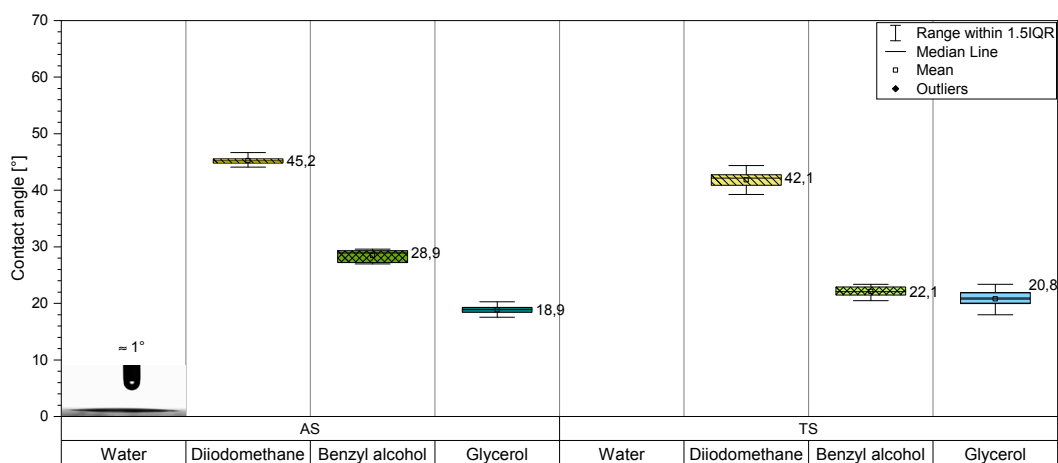


Figure 1: Solid contact angles of the EM-cleaned float glass surfaces with the test fluids used on the air side (AS) and the tin side (TS)

samples of EM-cleaned and one week at room temperature conditioned float glass were tested for normality with the Shapiro-Wilk test. One (GL_1) of the three samples showed normal distribution on both sides of the glass, with GL_1_1 DF (10), statistics: 0.927; $p = 0.423$ and GL_1_2, DF (10); statistics: 0.962; $p = 0.811$. This data series was tested for significance with the paired sample t -test and showed no significant difference between the glass sides (Table 5) and confirmed the result of Patejdl, Jung and Freieck (2022) with no significant difference between the wetting properties of the AS and TS after the alkaline cleaning procedure.

An ellipse-fitted WCA median of 1° was assumed after 10 s. The evaluated surface energies of the AS and TS complied with the leveling with SEs of 51.8 mJ/m^2 and 52.12 mJ/m^2 , respectively.

3.2 The SCA results of the hydrophobic PE foil surface

The SCA data of the PE foil surface (Table 6) show clearly the hydrophobic, non-polar wetting behaviour of the surface with a WCA median of 101.8° in comparison with the WCA data of hydrophilic EM-cleaned float glass surfaces (Table 6 vs Table 4). The SE of the PE foil surface was 30.9 mJ/m^2 , and much lower than the SEs of the EM-cleaned float glass surfaces, which were about 52.0 mJ/m^2 .

Further, the PE foil surface was more homogeneous, which can be seen in the deviations of CAM data in comparison with the EM-cleaned float glass surfaces (Table 6 vs Table 4). The PE foil surface is suitable as a benchmark for the homogeneity of surfaces.

Table 5: Significance tested by paired sample t -test on data series GL_1 AS to TS of the EM-cleaned float glass samples

Samples EM, DF(10)	t -statistic	Prob. > t	$p \leq .05$	$p \leq .01$	$p \leq .001$	Mean	SD	SEM	Median
GL_1_1	-2.106	0.064	-	-	-	5.128	0.987	0.312	5.366
GL_1_2			-	-	-	5.715	0.646	0.204	5.794

Table 6: Contact angles: median, min. and max. and deviation of SCA measurements of the test fluids used on the PE foil surface

SCA [°]	Water	Diiodomethane	Benzyl alcohol	Glycerol
PE foil	101.8	56.2	45.6	88.9
Min./Max.	100.6/102.3	55.6/57.0	44.5/46.0	86.9/89.7
Deviation	± 0.9	± 0.7	± 0.8	± 1.4



3.3 The SCA results of the M1 APTES-functionalized float glass surfaces in vapour phase

The EM-cleaned float glass was APTES-functionalized in the vapour phase by varying the functionalization duration (2 h, 4 h, 8 h). The comparison of the median WCA shows no increase in hydrophobicity with longer functionalisation times. Further, the WCA median of the AS and TS differed clearly in comparison to the EM-cleaned float glass surfaces. Exemplarily, these differences are shown in the Table 7 of the M1 (8 h) functionalized float glass surfaces. WCAs were evaluated on the AS between 35° and 41° and on the TS between 22° and 37° over functionalization durations of 2 h, 4 h and 8 h. The SEs were between 54.9 mJ/m² of M1 (2 h) and 55.2 mJ/m² of M1 (8 h) on the AS and on the TS between 55.6 mJ/m² of M1 (8 h) and 60.9 mJ/m² of M1 (2 h) and increased in comparison with the SEs of the EM-cleaned float glass surfaces.

3.4 SCA results of the M2 APTES-functionalized float glass surfaces in solution phase

The EM-cleaned float glass was APTES-functionalized in the solution phase with 2 % and 8 % silane concentrations in ethanol/water solution. The WCA median

of 2 % silane functionalized AS was 50° and on the TS 47.5° (Table 8). The WCA median of 8 % silane concentration showed despite of higher silane concentration, decreasing WCA median of 36.5° on the AS and 34.9° on the TS (Table 9). In contrast to APTES-functionalized float glass surfaces in vapour phase, the WCA median on the AS and TS of APTES-functionalized float glass surfaces in solution phase differed less. The SE on the AS of M2 (2 %) was 49.8 mJ/m² and on the TS 49.5 mJ/m². The SE on the AS of M2 (8 %) was 62.2 mJ/m² and on the TS 62.3 mJ/m².

4. Results of DCA measurement

The following subsections show exemplarily the DCA measurements and evaluated data (advancing and receding contact angle, drop age, baseline diameter (BD), tilt base (TB) and hysteresis) of investigated surfaces by using the test fluid diiodomethane. The DCA results of the test fluid water are included in chapter 4.5 and show their relevance only on the tin side of APTES-functionalized float glass surfaces. Appendix shows all evaluated SCAs, corresponding SEs and DCA parameters, hysteresis and drop age, for test fluids diiodomethane and water used (Tables A1 to A5).

Table 7: Contact angles: median, min. and max. and deviation of 20 SCA measurements of test fluids used on the AS and TS of the M1 (8 h) APTES-functionalized float glass surfaces









SCA [°]	Water	Diiodomethane	Benzyl alcohol	Glycerol
AS	37.8	37.5	14.9	39.3
Min./Max.	35.6/40.6	35.5/40.7	11.7/17.7	37.3/43.7
Deviation	± 2.5	± 2.6	± 3.0	± 3.2
				
TS	22.2	36.1	10.3	39.4
Min./Max.	18.7/31.9	34.0/37.4	9.7/13.2	36.5/42.7
Deviation	± 6.6	± 1.7	± 1.8	± 3.1
				

Table 8: Contact angles: median, min. and max. and deviation of 20 SCA measurements of the test fluids used on the AS and TS of the M2 (2 %) APTES-functionalized float glass surfaces

















SCA [°]	Water	Diiodomethane	Benzyl alcohol	Glycerol
AS	50.3	40.7	11.5	44.0
Min./Max.	47.4/54.5	36.4/42.1	9.8/14.9	42.7/52.5
Deviation	± 3.6	± 2.9	± 2.6	± 4.9
				
TS	47.5	41.9	12.0	50.9
Min./Max.	43.5/52.8	39.8/43.5	7.5/16.8	46.4/53.9
Deviation	± 4.7	± 1.9	± 4.7	± 3.8
				

Table 9: Contact angles: median, min. and max. and deviation of 20 SCA measurements of the test fluids used on the AS and TS of the M2 (8 %) APTES-functionalized float glass surfaces

SCA [°]	Water	Diiodomethane	Benzyl alcohol	Glycerol
AS	36.5	31.5	2.0	33.9
Min./Max.	35.8/37.9	29.9/32.4	–	32.0/35.9
Deviation	± 1.1	± 1.3	–	± 2.0
				
TS	34.9	33.1	2.0	33.4
Min./Max.	31.6/38.5	32.2/34.0	–	30.9/36.6
Deviation	± 3.5	± 0.9	–	± 2.9
				

4.1 Results of DCA measurements on the EM-cleaned float glass surfaces

The DCA measurements on the EM-cleaned hydrophilic (polar) float glass surfaces with test fluid diiodomethane showed on the TS a higher hysteresis (39.8° to 42.0°) than on the AS (30.1° to 31.8°) (Figures 2, 3a; Table 10) and a longer drop age of the TS (72.9 s to 82.4 s) in comparison to the AS (59.9 s to 62.7 s) (Figure 3b; Table 10). The sharp drop part at the end of the advancing – and receding curves shows the incorrect polynomial fitting when the drop runs out of the measurement zone.

Out of the float glass manufacturing process, the TS (1–2 nm) is smoother than the AS (4–10 nm) as reported by Stiell (2002) and Silvestru, et al. (2018). The smoother surface results from the density differences between molten glass and tin. During the floating of molten glass on the tin bath, it is not unreasonable that the diffusing tin ions open the glass network by converting

bridging oxygens to non-bridging oxygens supported by the research of Šesták, Mareš and Hubík (2010) and Varshneya and Mauro (2019), just as network modifiers do. The alkaline cleaning bath used could attack the “weaker” TS more than the AS, which results in a higher surface roughness, an unsteady course of DCA measurements, and a larger hysteresis. This hypothesis can be supported by the research of Han, et al. (2016), which shows different Si wafer surface roughness after using different cleaning methods. AFM measurements showed on alkaline cleaned float glass surfaces the R_q roughness of 0.30 nm on the AS and 0.36 nm on the TS with relatively similar R_q roughness, but also assumed dust impurities, which complicate the evaluation of AFM measurements (Figure 4). An additional cleaning step with acetone and following ethanol ultrasonic bath led to better distinctions of roughness between AS and TS with 0.41 nm and 0.58 nm, respectively (Figure 5). The AFM results support the adoption of the “weaker” tin-side and the resulting larger hysteresis.

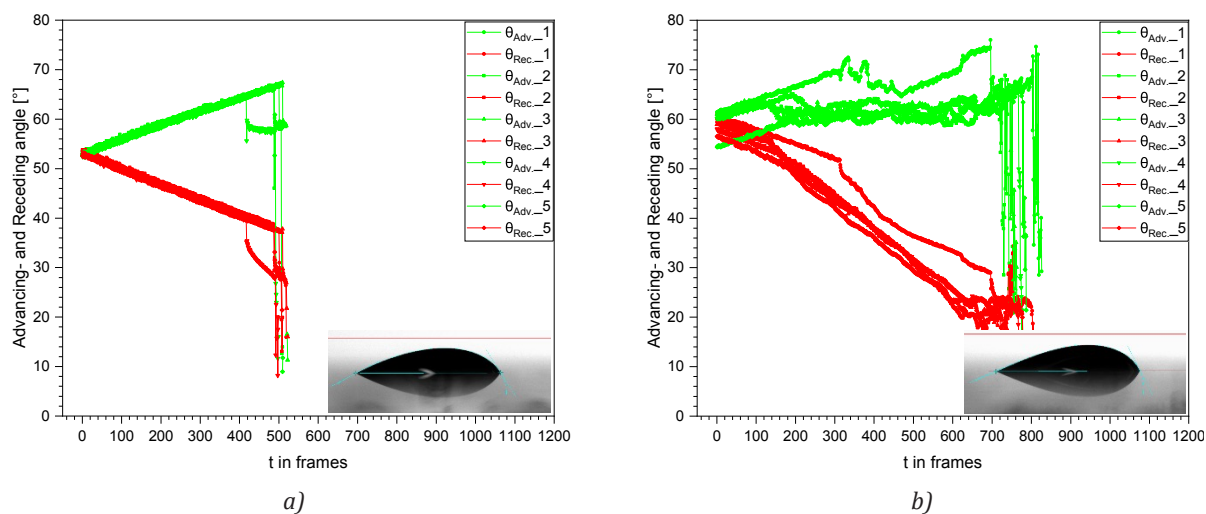


Figure 2: Dynamic contact angles on the EM-cleaned float glass surface, with the test fluid diiodomethane; air side (a), and tin side (b)

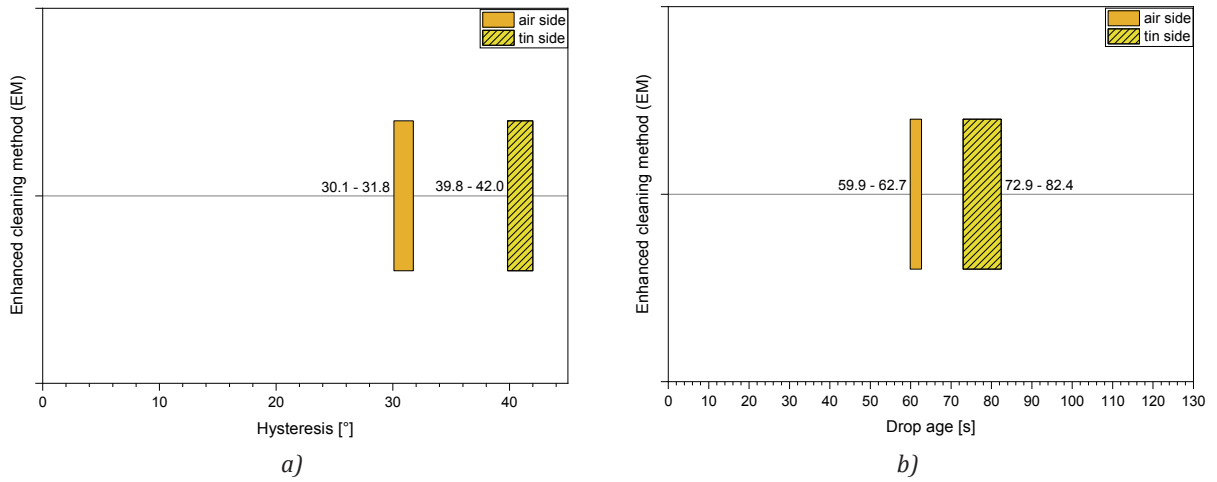
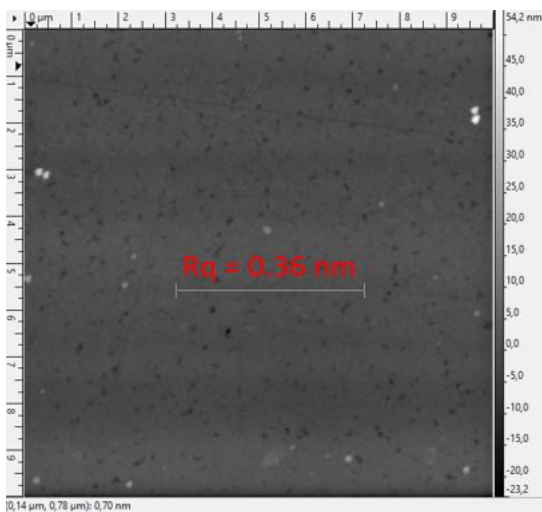


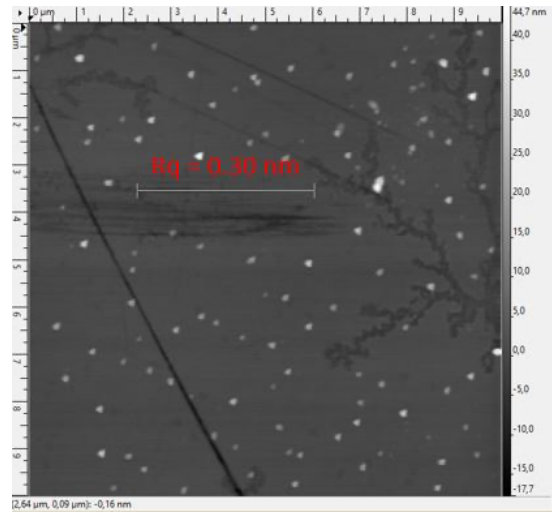
Figure 3: Diiodomethane drop (4 μl) on the EM-cleaned float glass (AS/TS), hysteresis (a), and drop age (b)

Table 10: Evaluated DCA parameters of the EM-cleaned float glass surface with the test fluid diiodomethane

DCA glass		Adv. CA [°]	Rec. CA [°]	Drop age [s]	BD [mm]	TB [°]	Hysteresis [°]
AS	1	58.9	27.5	62.20	4.01	27.1	31.4
	2	58.7	28.4	61.29	3.95	26.2	30.3
	3	58.7	26.9	62.70	4.04	27.1	31.8
	4	58.1	27.9	59.90	4.01	25.6	30.1
	5	58.1	27.7	61.60	4.01	26.3	30.4
TS	1	64.9	22.9	82.40	3.96	37.4	41.9
	2	59.9	19.8	72.99	4.33	32.7	40.1
	3	62.3	22.4	74.80	4.06	33.4	39.8
	4	63.5	22.9	76.00	4.01	33.8	40.6
	5	61.9	20.4	73.80	4.16	32.7	41.5



a)



b)

Figure 4: Atomic force microscopic measurement on the air and tin side after alkaline cleaning process with R_q roughness on the air side of 0.36 nm (a), and on the tin side 0.30 nm (b)

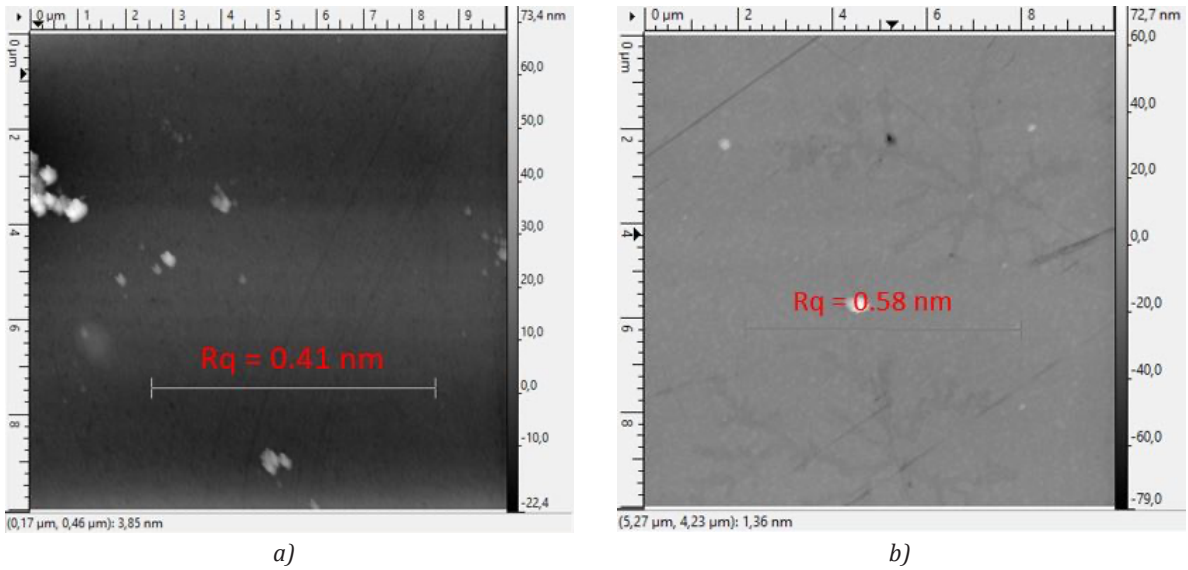


Figure 5: Atomic force microscopic measurement after alkaline cleaning process and afterwards following acetone and ethanol ultrasonic bath with R_q roughness on the air side of 0.41 nm (a), and on the tin side 0.58 nm (b)

The evaluated SEs of the AS (51.8 mJ/m²) and the TS (52.1 mJ/m²) seem to be first not sensitive to different surface properties of the EM-cleaned surfaces in comparison to the results of the DCA measurements.

4.2 Results of DCA measurements on the PE foil surface

The DCA measurements on the non-polar PE foil surface (WCA median: 101.8°) show, in contrast to the EM-cleaned float glass surfaces with assumed similar roughness, a low hysteresis (9.8° to 13.0°) (Figures 6, 7a; Table 11).

The unsteady course of DCA measurements at the end is caused by the unsteady position of the baseline during the contour fitting process.

The evaluation of the diiodomethane drop age on the PE foil surface is 28.9 s to 33.8 s (Figure 7b; Table 11), which is much shorter than on the EM-cleaned float glass surfaces. The DCA results of the hydrophilic float

glass surfaces and the hydrophobic PE foil surface confirm the suitability of using the DCA parameters hysteresis and drop age for indicating adhesion forces on functionalized float glass surfaces.

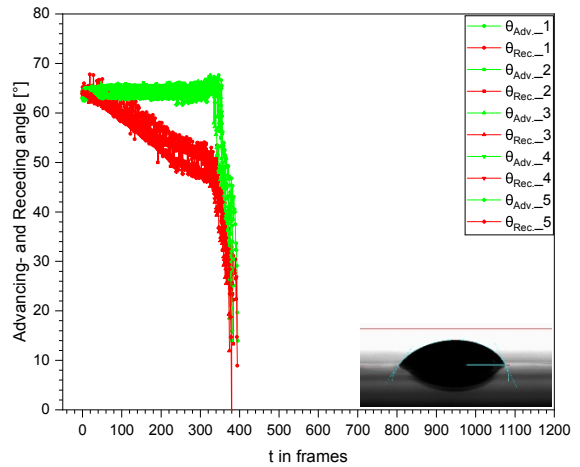
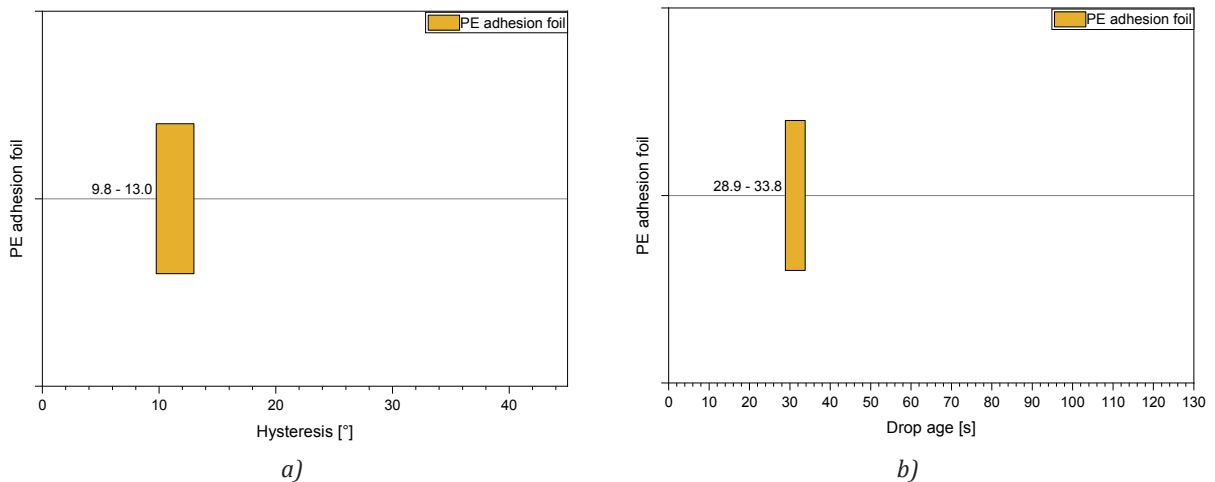


Figure 6: Dynamic contact angles on the PE foil surface with the test fluid diiodomethane

Table 11: Evaluated DCA parameters of the PE foil surface with the test fluid diiodomethane

DCA PE foil	Adv. CA [°]	Rec. CA [°]	Drop age [s]	BD [mm]	TB [°]	Hysteresis [°]
1	65.0	54.9	33.79	3.43	11.8	10.1
2	65.6	52.6	31.69	3.44	10.5	12.9
3	64.7	54.9	29.59	3.50	9.8	9.8
4	63.9	53.8	28.89	3.74	9.3	10.1
5	63.3	51.5	30.99	3.50	10.8	11.8



a) *Figure 7: Diiodomethane drop (4 μ l) on the PE foil surface, hysteresis (a), and drop age (b)*

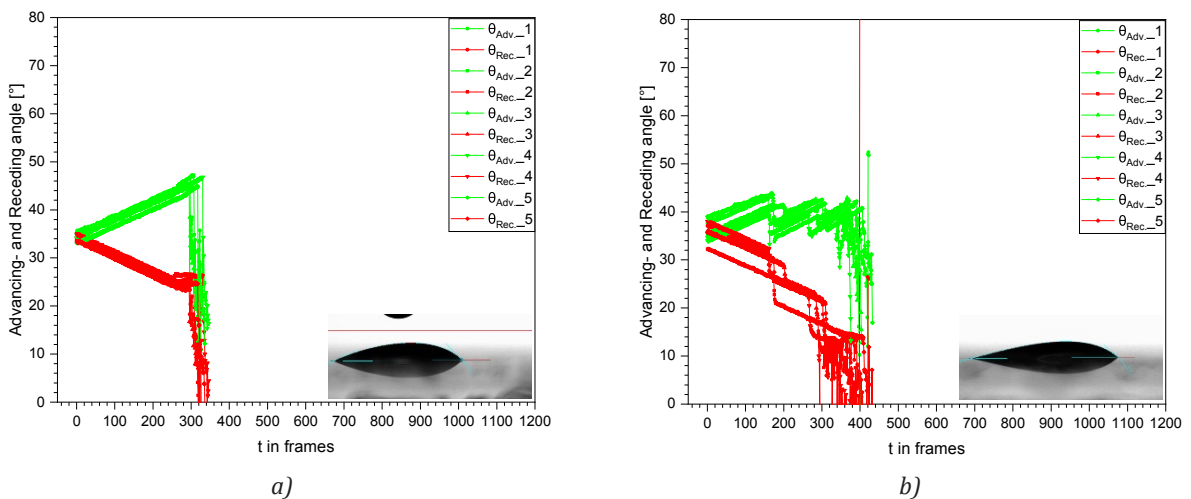
4.3 Results of DCA measurements of the M1 APTES-functionalized float glass surfaces in vapour phase

The DCA measurements and evaluated parameters of M1 APTES-functionalized float glass surfaces in the vapour phase are exemplarily shown for the test fluid diiodomethane and M1 (8 h) (Figure 8; Table 12). By ordering the evaluated DCA parameters, hysteresis and drop age, to increasing WCA medians, and differentiating between the AS and TS and the test fluids diiodomethane and water, of the investigated EM-cleaned float glass surfaces, M1 APTES-functionalized float glass surfaces, and the PE foil surface, partial inconsistencies in hysteresis and drop age are visible (Figure 9). A plausible explanation is incomplete functionalization, which leads to inhomogeneous surface properties. Despite these inconsistencies, the comparison of the polar

and non-polar surfaces is acceptable. For the further course, only the M1 (8 h) functionalization was taken into account for the final evaluations in section 4.5. Here, a completely functional surface can be expected.

4.4 Results of DCA measurements of the M2 APTES-functionalized float glass surfaces in solution phase

The DCA measurements and evaluated parameters of M2 APTES-functionalized float glass surfaces in the solution phase are exemplarily shown for the test fluid diiodomethane (Figures 10 to 12; Tables 13, 14). By ordering the evaluated DCA parameters, hysteresis and drop age, to increase WCA and differentiating between the AS and TS and the test fluids diiodomethane and water, of the investigated EM-cleaned float glass, M2 APTES-functionalized float glass, and the PE foil sur-



a) *Figure 8: Dynamic contact angles on M1 (8 h) APTES-functionalized float glass surface with the test fluid diiodomethane, air side (a), and tin side (b)*

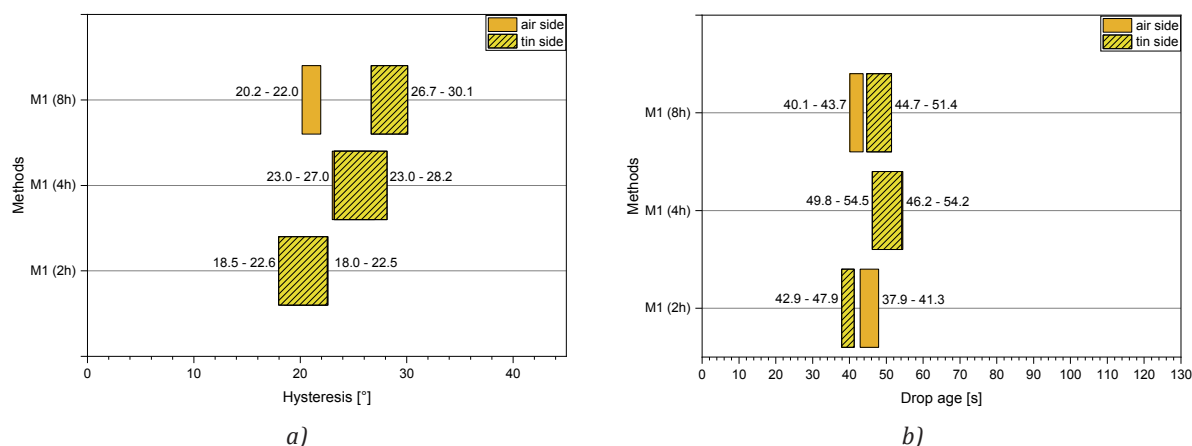


Figure 9: Diiodomethane drop (4 μ l) on the M1 APTES-functionalized float glass surfaces in vapour phase (AS/TS), hysteresis (a), and drop age (b)

Table 12: Evaluated DCA parameters of the M1 (8 h) APTES-functionalized float glass surfaces with the test fluid diiodomethane

DCA glass	Adv. CA [°]	Rec. CA [°]	Drop age [s]	BD [mm]	TB [°]	Hysteresis [°]	
AS	1	44.7	23.3	40.09	4.10	15.4	21.4
	2	47.1	25.2	41.60	4.10	15.8	21.9
	3	45.1	24.1	40.60	4.18	15.2	20.9
	4	46.8	26.3	43.70	4.00	17.2	20.6
	5	44.7	24.6	42.39	4.09	16.4	20.2
TS	1	41.9	13.2	49.90	5.00	20.3	28.7
	2	41.4	11.3	46.09	5.00	18.3	30.1
	3	42.1	13.9	48.70	4.77	19.3	28.2
	4	39.5	12.7	44.70	5.19	17.7	26.8
	5	40.7	14.1	51.39	4.71	21.2	26.7

face, the data show consistency and are plausible in comparison of the polar and non-polar surfaces, too. For the M2 (2 %) and M2 (8 %) variants of solution

phase functionalization are taken into account for the final evaluations. A completely functional surface can be expected.

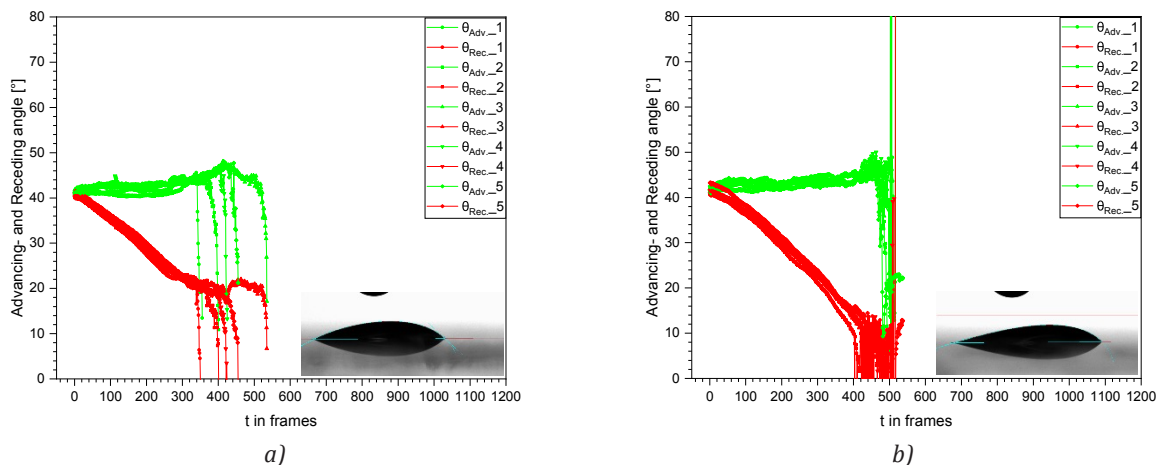


Figure 10: Dynamic contact angles on the M2 (2 %) APTES-functionalized float glass surface with the test fluid diiodomethane, air side (a), and tin side (b)

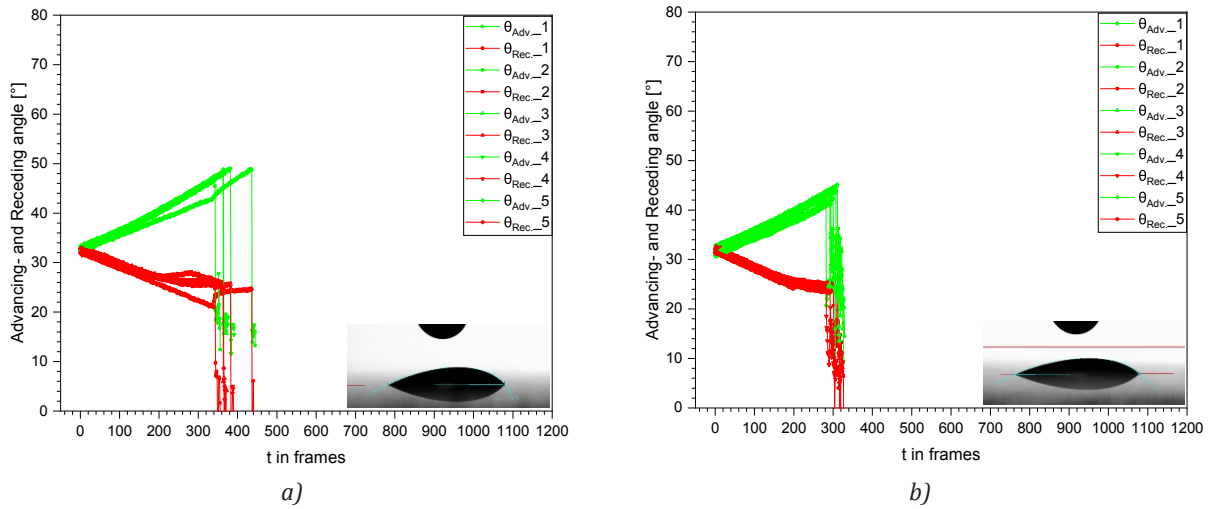


Figure 11: Dynamic contact angles on the M2 (8%) APTES-functionalized float glass surface with the test fluid diiodomethane, air side (a), and tin side (b)

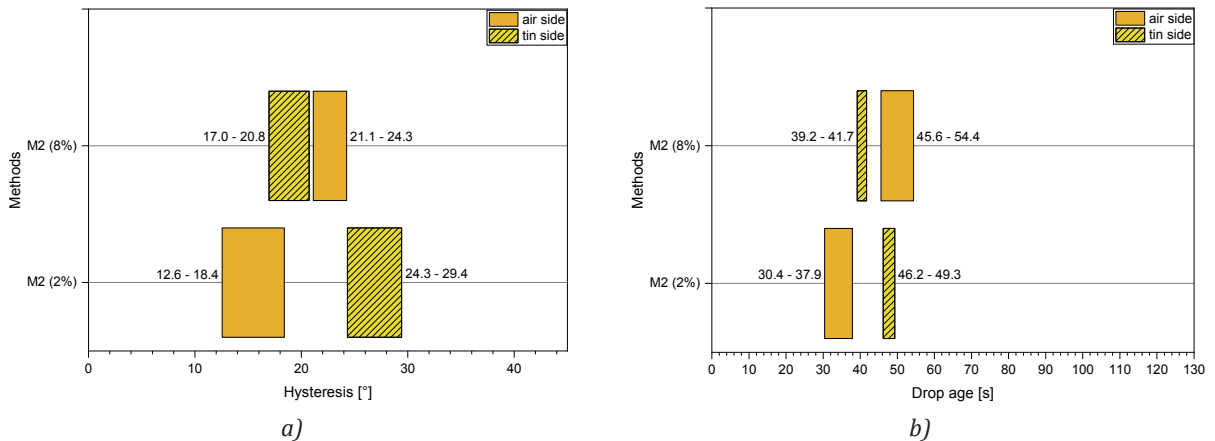


Figure 12: Diiodomethane drop (4 μl) on the M2 (8%) APTES-functionalized float glass surfaces (AS/TS), hysteresis (a), and drop age (b)

Table 13: Evaluated dynamic contact angle parameters of the M2 (2%) APTES-functionalized float glass surfaces with the test fluid diiodomethane

		Adv. CA	Rec. CA	Drop age	BD	TB	Hysteresis
DCA glass		[°]	[°]	[s]	[mm]	[°]	[°]
AS	1	41.7	27.1	30.99	4.40	10.6	14.6
	2	40.6	27.9	30.40	4.24	10.2	12.6
	3	42.8	25.2	37.90	4.30	13.8	17.6
	4	43.2	24.8	36.80	4.45	13.4	18.4
	5	43.0	25.6	36.79	4.25	13.3	17.4
TS	1	44.9	15.5	49.30	4.68	19.9	29.4
	2	43.3	14.2	47.60	4.93	18.9	29.1
	3	42.3	18.2	46.19	4.60	18.0	26.1
	4	42.9	18.6	46.20	4.65	18.1	24.3
	5	45.1	15.9	48.30	4.84	19.4	29.1

Table 14: Evaluated dynamic contact angle parameters of the M2 (8 %) APTES-functionalized float glass surfaces with the test fluid diiodomethane

DCA glass		Adv. CA [°]	Rec. CA [°]	Drop age [s]	BD [mm]	TB [°]	Hysteresis [°]
AS	1	48.9	24.6	54.39	3.66	22.8	24.3
	2	46.6	25.5	45.60	3.90	17.9	21.1
	3	47.8	25.9	47.19	3.91	18.7	21.9
	4	48.7	25.8	48.89	3.80	19.9	22.9
	5	48.3	24.8	47.19	3.90	18.8	23.5
TS	1	45.0	24.3	41.50	4.07	16.2	20.7
	2	42.4	25.4	40.69	3.92	15.6	16.9
	3	43.9	23.7	41.70	4.14	15.9	20.3
	4	43.2	25.2	39.19	4.12	14.8	17.9
	5	41.8	23.3	40.50	4.07	15.2	18.5

4.5 Results of DCA measurements under assumed complete functionalization of float glass surfaces

Tables 15 and 16 show the evaluated hysteresis and drop age ranges of M1 (8 h), M2 (2 %) and M2 (8 %) APTES-functionalized float glass surfaces. These variants are assumed to be completely functionalized and are plau-

sible in comparison with the polar and non-polar surfaces by ordering the DCA parameters with an increase of WCA median considering difference between the AS and TS and the test fluids diiodomethane and water.

The results show consistency by using the test fluid diiodomethane on the AS and the test fluid water on the TS.

Table 15: Comparison of assumed saturated APTES functionalization methods ordered after hydrophobization grade with the test fluid diiodomethane (AS)

	Polar surface	Dynamic contact angle measurements Hydrophobic direction →			Non-polar surface
		M2 (8 %)	M1 (8 h)	M2 (2 %)	
Material/Methods	EM-cleaned DCA: ~1.0° SE: 51.83 mJ/m ²	M2 (8 %) DCA: 36.5° SE: 62.10 mJ/m ²	M1 (8 h) DCA: 37.8° SE: 55.20 mJ/m ²	M2 (2 %) DCA: 50.3° SE: 49.80 mJ/m ²	PE DCA: 101.8° SE: 45.35 mJ/m ²
Parameter					
Hysteresis [°]	30.1–31.8	21.1–24.3	20.2–21.9	12.6–18.4	9.8–12.9
Drop age [s]	59.90–62.70	45.60–54.39	40.09–43.70	30.40–37.90	28.89–33.79

Table 16: Comparison of assumed saturated APTES functionalization methods ordered after hydrophobization grade with the test fluid water (TS)

	Polar surface	Dynamic contact angle measurements Hydrophobic direction →			Non-polar surface
		M1 (8 h)	M2 (8 %)	M2 (2 %)	
Material/Methods	EM-cleaned WCA: ~1.0° SE: 52.12 mJ/m ²	M1 (8 h) WCA: 22.2° SE: 59.90 mJ/m ²	M2 (8 %) WCA: 34.9° SE: 62.30 mJ/m ²	M2 (2 %) WCA: 47.5° SE: 49.50 mJ/m ²	PE WCA: 101.8° SE: 45.35 mJ/m ²
Parameter					
Hysteresis [°]	< 10	21.6–30.1	27.0–32.8	39.2–43.2	< 10
Drop age [s]	-	63.19–77.69	75.49–85.69	114.89–130.39	-

5. Conclusion

The dynamic contact angle measurement can be used as an indicator for adhesion forces on different APTES-functionalized float glass surfaces with different wetting properties.

The EM-cleaned hydrophilic polar float glass surfaces (WCA median: $\approx 1^\circ$) showed on the tin side a higher hysteresis between 39.8° and 42.0° than on the air side with a hysteresis between 30.1° and 31.8° of diiodomethane drop. The tin side also showed a higher drop age between 72.9 s and 82.4 s than the air side with a drop age between 59.9 s and 62.7 s. Despite very similar surface energies of 51.8 mJ/m^2 and 52.1 mJ/m^2 , the hysteresis and the drop age are parameters that showed clear tendencies for the EM-cleaned float glass surfaces. Both parameters indicated an increase in adhesion forces on the tin side of the float glass. AFM measurements showed a higher surface roughness on the tin side in comparison with the air side after the additional cleaning step with acetone and ethanol ultrasonic cleaning bath and explain the higher hysteresis and drop age on the tin side.

In contrast, the hydrophobic non-polar smooth PE foil surface (WCA median: 101.8°) showed a small hysteresis between 9.7° and 12.9° with a short drop age between 28.8 s and 33.7 s of diiodomethane drop in correlation with a low surface energy of 30.9 mJ/m^2 .

The DCA results of the hydrophilic float glass surfaces and the hydrophobic PE foil surface confirmed the suitability of using the DCA parameters hysteresis and drop age for indicating adhesion forces on functionalized float glass surfaces.

The float glass surfaces APTES-functionalized in the vapour phase were investigated with static and dynamic contact angle measurements with test fluids diiodomethane and water. The vapour-functionalized float glass surfaces clearly showed the two-sidedness of float glass. On the air side, the WCA median was between 35.7° and 41.1° and on the tin side, the WCA median was between 22.2° and 37.1° . These results

show the slower functionalization of tin side in comparison with the air side by using the vapour-phase method. The varying functionalization duration does not lead to a stronger hydrophobic wetting effect on the surfaces. The measurements of homogeneous functionalized float glass surfaces (preparation time of 8 h) showed a clear hysteresis and drop age difference between the air and tin side with the test fluid diiodomethane.

The float glass surfaces APTES-functionalized in the solution phase showed off clearly differentiable water contact angles dependent on the silane concentration. In contrast to the functionalization in the vapour phase the WCA medians of the air and tin sides differed not so much from each other. By evaluating the 2 % concentration, the static contact angle measurements showed an air side WCA median of 50.3° and a tin side WCA median of 47.5° . By evaluating the 8 % concentration, the static angle measurements showed on the air side a WCA median of 36.5° and on the tin side a WCA median of 34.9° .

The results of WCA median, surface energy, hysteresis, and drop age of EM-cleaned, vapour-phase functionalized (8 h), and solution-phase functionalized (2 % and 8 %) float glass surfaces, and the PE foil surface were shown in order of increasing water contact angle, separately for the air and tin sides, and test fluids diiodomethane and water. The application of the test fluid diiodomethane on the air side and the test fluid water on the tin side of functionalized float glass surfaces confirmed the prediction that an increased water contact angle leads to a clear decrease or increase of hysteresis and drop age. This confirmed again the suitability of using the DCA parameters hysteresis and drop age for indicating adhesion forces on functionalized float glass surfaces. Disperse and polar components of functionalized surfaces are not suitable for analysis of adhesion forces on APTES-functionalized float glass surfaces.

With this research a better understanding of e.g., UV-ink adhesion forces dependent on glass surface wetting properties could be reached.

References

- Acres, R.G., Ellis, A.V., Alvino, J., Lenahan, C.E., Khodakov, D.A., Metha, G.F. and Andersson, G.G., 2012. Molecular structure of 3-aminopropyltriethoxysilane layers formed on silanol-terminated silicon surfaces. *The Journal of Physical Chemistry C*, 116(10), pp. 6289–6297. <https://doi.org/10.1021/jp212056s>.
- Altmann, S. and Pfeiffer, J., 2003. The hydrolysis/condensation behaviour of methacryloyloxyalkylfunctional alkoxysilanes: structure-reactivity relations. *Monatshefte für Chemie / Chemical Monthly*, 134(8), pp. 1081–1092. <https://doi.org/10.1007/s00706-003-0615-y>.
- Argekar, S.U., Kirley, T.L. and Schaefer, D.W., 2013. Determination of structure-property relationships for 3-aminopropyltriethoxysilane films using x-ray reflectivity. *Journal of Material Research*, 28(8), pp. 1118–1128. <https://doi.org/10.1557/jmr.2013.54>.

- Arkles, B., Maddox, A., Singh, M., Zzyczny, J. and Matisons, J., 2014. *Silane coupling agents: connecting across boundaries*. 3rd ed. Morrisville, PA, USA: Gelest.
- Arslan, G., Ozmen, M., Gündüz, B., Zhang, X. and Ersöz, M., 2006. Surface modification of glass beads with an aminosilane monolayer. *Turkish Journal of Chemistry*, 30(2), pp. 203–210.
- Asenath Smith, E. and Chen, W., 2008. How to prevent the loss of surface functionality derived from aminosilanes. *Langmuir*, 24(21), pp. 12405–12409. <https://doi.org/10.1021/la802234x>.
- Canané, P., 2019. *Silanization by room temperature chemical vapor deposition and controlled roughness for wettability modification of microfabrication substrates*. [pdf] Available at: < <https://fenix.tecnico.ulisboa.pt/downloadFile/844820067126289/SilanizationbyRoomTemperatureChemicalVaporDepositionandControlledRoughnessforWettabilityModificationofMicro.pdf> > [Accessed August 2023].
- Chauhan, A.K., Aswal, D.K., Koiry, S.P., Gupta, S.K., Yakhmi, J.V., Sürgers, C., Guerin, D., Lenfant, S. and Vuillaume, D., 2008. Self-assembly of the 3-aminopropyltrimethoxysilane multilayers on Si and hysteretic current–voltage characteristics. *Applied Physics A*, 90(3), pp. 581–589., <https://doi.org/10.1007/s00339-007-4336-7>.
- Da Silva, L.F.M., Öchsner, A. and Adams, R.D. eds., 2011. *Handbook of adhesion technology*. Cham: Springer.
- Deetz, J.D. and Faller, R., 2015. Reactive modeling of the initial stages of alkoxy silane polycondensation: effects of precursor molecule structure and solution composition. *Soft Matter*, 11(34), pp. 6780–6789. <https://doi.org/10.1039/C5SM00964B>.
- Deutsche Institut für Normung, 2020. *DIN EN ISO 19403-7:2020-04 Paints and varnishes – Wettability – Part 7: Measurement of the contact angle on a tilt stage (roll-off angle)*. Berlin: DIN, Beuth Verlag.
- Deutsche Institut für Normung, 2023. *DIN EN ISO 19403-6:2023-10 Draft Paints and varnishes – Wettability – Part 6: Measurement of dynamic contact angle*. Berlin: DIN, Beuth Verlag.
- Fadeev, A.Y. and McCarthy, T.J., 1999. Trialkylsilane monolayers covalently attached to silicon surfaces: wettability studies indicating that molecular topography contributes to contact angle hysteresis. *Langmuir*, 15(11), pp. 3759–3766. <https://doi.org/10.1021/la981486o>.
- Fiorilli, S., Rivolo, P., Descrovi, E., Ricciardi, C., Pasquardini, L., Lunelli, L., Vanzetti, L., Pederzoli, C., Onida, B. and Garrone, E., 2008. Vapor-phase self-assembled monolayers of aminosilane on plasma-activated silicon substrates. *Journal of Colloid and Interface Science*, 321(1), pp. 235–241. <https://doi.org/10.1016/j.jcis.2007.12.041>.
- Han, Y., Mayer, D., Offenhäuser, A. and Ingebrandt, S., 2006. Surface activation of thin silicon oxides by wet cleaning and silanization. *Thin Solid Films*, 510(1–2), pp. 175–180. <https://doi.org/10.1016/j.tsf.2005.11.048>.
- Issa, A.A. and Luyt, A.S., 2019. Kinetics of alkoxy silanes and organoalkoxy silanes polymerization: a review. *Polymers*, 11(3): 537. <https://doi.org/10.3390/polym11030537>.
- Kaelble, D.H., 1970. Dispersion-polar surface tension properties of organic solids. *The Journal of Adhesion*, 2(2), pp. 66–81. <https://doi.org/10.1080/0021846708544582>.
- Kim, J., Holinga, G.J. and Somorjai, G.A., 2011. Curing induced structural reorganization and enhanced reactivity of amino-terminated organic thin films on solid substrates: observations of two types of chemically and structurally unique amino groups on the surface. *Langmuir*, 27(9), pp. 5171–5175. <https://doi.org/10.1021/la2007205>.
- Koç, F., Sert Çok, S. and Gizli, N., 2020. Tuning the properties of silica aerogels through pH controlled sol-gel processes. *Research on Engineering Structures and Materials*, 6(3), pp. 257–269. <http://dx.doi.org/10.17515/resm2019.166ma1203>.
- Lazauskas, A. and Grigaliūnas, V., 2012. Float glass surface preparation methods for improved chromium film adhesive bonding. *Materials Science / Medžiagotyra*, 18(2), pp. 181–186. <https://doi.org/10.5755/j01.ms.18.2.1924>.
- Liang, Y., Huang, J., Zang, P., Kim, J. and Hu, W., 2014. Molecular layer deposition of APTES on silicon nanowire biosensors: surface characterization, stability and pH response. *Applied Surface Science*, 322, pp. 202–208. <https://doi.org/10.1016/j.apsusc.2014.10.097>.
- Matinlinna, J.P., Lung, C.Y.K. and Tsoi, J.K.H., 2018. Silane adhesion mechanism in dental applications and surface treatments: a review. *Dental Materials*, 34(1), pp. 13–28. <https://doi.org/10.1016/j.dental.2017.09.002>.
- Metwalli, E., Haines, D., Becker, O., Conzone, S. and Pantano, C.G., 2006. Surface characterizations of mono-, di-, and tri-aminosilane treated glass substrates. *Journal of Colloid and Interface Science*, 298 (2), pp. 825–831. <https://doi.org/10.1016/j.jcis.2006.03.045>.
- Mittal, K.L. and O'kane, D.F., 1976. Vapor deposited silanes and other coupling agents. *The Journal of Adhesion*, 8(1), pp. 93–97. <https://doi.org/10.1080/00218467608075073>.
- Munief, W.-M., Heib, F., Hempel, F., Lu, X., Schwartz, M., Pachauri, V., Hempelmann, R., Schmitt, M. and Ingebrandt, S., 2018. Silane deposition via gas-phase evaporation and high-resolution surface characterization of the ultrathin siloxane coatings. *Langmuir*, 34(35), pp. 10217–10229. <https://doi.org/10.1021/acs.langmuir.8b01044>.
- Osterholtz, F.D. and Pohl, E.R., 1992. Kinetics of the hydrolysis and condensation of organofunctional alkoxy silanes: a review. *Journal of Adhesion Science and Technology*, 6(1), pp. 127–149. <https://doi.org/10.1163/156856192X00106>.
- Owens, D.K. and Wendt, R.C., 1969. Estimation of the surface free energy of polymers. *Journal of Applied Polymer Science*, 13(8), pp. 1741–1747. <https://doi.org/10.1002/app.1969.070130815>.

- Pasternack, R.M., Rivillon Amy, S. and Chabal, Y.J., 2008. Attachment of 3-(aminopropyl)triethoxysilane on silicon oxide surfaces: dependence on solution temperature. *Langmuir*, 24(22), pp. 12963–12971. <https://doi.org/10.1021/la8024827>.
- Patejdl, S., Jung, U. and Freieck, K., 2022. Wetting and adhesion phenomena of surface-treated float glass. In: C. Ridgway, ed. *Advances in Printing and Media Technology: Proceedings of the 48th International Research Conference of iarigai*. Greenville, USA, 19–21 September 2022. Darmstadt: iarigai. https://doi.org/10.14622/Advances_48_2022_03.
- Pilkington, L.A.B., 1969. *Review lecture: the float glass process. Proceedings of the Royal Society of London A*, 314(1516), pp. 1–25. <https://doi.org/10.1098/rspa.1969.0212>.
- Plueddemann, E.P., 1970. Adhesion through silane coupling agents. *The Journal of Adhesion*, 2(3), pp. 184–201. <https://doi.org/10.1080/0021846708544592>.
- Plueddemann, E.P., 1991. *Silane coupling agents*. 2nd ed. Boston, MA, USA: Springer US.
- Rabel, W., 1971. Einige Aspekte der Benetzungstheorie und ihre Anwendung auf die Untersuchung und Veränderung der Oberflächeneigenschaften von Polymeren. *Farbe und Lack*, 77, pp. 997–1005.
- Silberzan, P., Leger, L., Ausserre, D. and Benattar, J.J., 1991. Silanation of silica surfaces. A new method of constructing pure or mixed monolayers. *Langmuir*, 7(8), pp. 1647–1651. <https://doi.org/10.1021/la00056a017>.
- Silvestru, V.A., Drass, M., Englhardt, O. and Schneider, J., 2018. Performance of a structural acrylic adhesive for linear glass-metal connections under shear and tensile loading. *International Journal of Adhesion and Adhesives*, 85, pp. 322–336. <https://doi.org/10.1016/j.ijadhadh.2018.07.006>.
- Siqueira Petri, D.F., Wenz, G., Schunk, P. and Schimmel, T., 1999. An improved method for the assembly of amino-terminated monolayers on SiO₂ and the vapor deposition of gold layers. *Langmuir*, 15(13), pp. 4520–4523. <https://doi.org/10.1021/la981379u>.
- Stiell, W., 2002. *Haftverhalten von Dichtstoffen auf beschichtetem und unbeschichtetem Glas*. Rosenheim: ift Rosenheim.
- Šesták, J., Mareš, J. and Hubík, P. eds., 2010. *Glassy, amorphous and nano-crystalline materials: thermal physics, analysis, structure and properties*. Dordrecht, New York: Springer.
- Van Der Voort, P. and Vansant, E.F., 1996. Silylation of the silica surface a review. *Journal of Liquid Chromatography & Related Technologies*, 19(17–18), pp. 2723–2752. <https://doi.org/10.1080/10826079608015107>.
- Varshneya, A.K. and Mauro, J.C., 2019. *Fundamentals of inorganic glasses*. 3rd ed. Amsterdam, Netherlands: Elsevier.
- Wang, Y., Hansen, C.J., Wu, C.-C., Robinette, E.J. and Peterson, A.M., 2021. Effect of surface wettability on the interfacial adhesion of a thermosetting elastomer on glass. *RSC Advances*, 11(49), pp. 31142–31151. <https://doi.org/10.1039/D1RA05916E>.
- Wolf, A.T., 2022. Organofunktionelle Silane als Haftvermittler. *Chemie in unserer Zeit*, 56(1), pp. 22–33. <https://doi.org/10.1002/ciuz.202000038>.
- Yadav, A.R., Sriram, R., Carter, J.A. and Miller, B.L., 2014. Comparative study of solution-phase and vapor-phase deposition of aminosilanes on silicon dioxide surfaces. *Materials Science and Engineering C*, 35, pp. 283–290. <https://doi.org/10.1016/j.msec.2013.11.017>.
- Zhang, F., Sautter, K., Larsen, A.M., Findley, D.A., Davis, R.C., Samha, H. and Linford, M.R., 2010. Chemical vapor deposition of three aminosilanes on silicon dioxide: surface characterization, stability, effects of silane concentration, and cyanine dye adsorption. *Langmuir*, 26(18), pp. 14648–14654. <https://doi.org/10.1021/la102447y>.
- Zhang, K., Li, T., Zhang, T., Wang, C. and Wu, M., 2013. Adhesion improvement of UV-curable ink using silane coupling agent onto glass substrate. *Journal of Adhesion Science and Technology*, 27(13), pp. 1499–1510. <https://doi.org/10.1080/01694243.2012.746159>.
- Zhu, M., Lerum, M.Z. and Chen, W., 2012. How to prepare reproducible, homogeneous, and hydrolytically stable aminosilane-derived layers on silica. *Langmuir*, 28(1), pp. 416–423. <https://doi.org/10.1021/la203638g>.

Appendix: Overview of static and dynamic- contact angle results of test fluids diiodomethane and water, and surface energies (Tables A1 to A5).

Table A1: SCA, SE (with disperse (γ^d_s), and polar (γ^p_s) components) and DCA results on the AS of float glass with the test fluid diiodomethane

Methods	Static contact angle measurements (2 μ l) [°]				Surface energy [mJ/m ²]	Dynamic contact angle measurements (diiodomethane)	
	Water	Diiodomethane	Benzyl alc.	Glycerol		Hysteresis [°]	Drop age [s]
EM	1.0	45.2	28.9	18.9	51.83 γ^d_s : 30.36 γ^p_s : 21.47	30.09–31.76	59.90–62.70
M1 (2 h)	41.1	35.3	14.7	36.6	54.92 γ^d_s : 30.78 γ^p_s : 24.14	18.50–22.62	42.90–47.90
M1 (4 h)	35.7	39.7	18.5	32.7	56.36 γ^d_s : 28.34 γ^p_s : 28.02	23.01–26.97	49.79–54.49
M1 (8 h)	37.8	37.5	14.9	39.3	55.21 γ^d_s : 28.93 γ^p_s : 26.28	20.16–21.92	40.09–43.70
M2 (2 %)	50.3	40.7	11.5	44.0	49.81 γ^d_s : 31.05 γ^p_s : 18.77	12.56–18.40	30.40–37.90
M2 (8 %)	36.5	31.5	2.0	33.9	62.18 γ^d_s : 38.94 γ^p_s : 23.25	21.12–24.26	45.60–54.39

Table A2: SCA, SE (with disperse (γ^d_s), and polar (γ^p_s) components) and DCA results on the TS of float glass with the test fluid diiodomethane

Methods	Static contact angle measurements (2 μ l) [°]				Surface energy [mJ/m ²]	Dynamic contact angle measurements (diiodomethane)	
	Water	Diiodomethane	Benzyl alc.	Glycerol		Hysteresis [°]	Drop age [s]
EM	1.0	42.1	22.1	20.8	52.12 γ^d_s : 30.30 γ^p_s : 19.82	39.84–41.99	72.99–82.40
M1 (2 h)	23.1	36.5	15.0	31.3	60.92 γ^d_s : 27.74 γ^p_s : 33.18	17.96–22.54	37.89–41.30
M1 (4 h)	37.1	37.2	15.8	39.3	55.62 γ^d_s : 28.87 γ^p_s : 26.75	23.19–28.15	46.20–54.20
M1 (8 h)	22.2	36.1	10.3	39.4	59.89 γ^d_s : 27.23 γ^p_s : 32.65	26.66–30.09	44.70–51.39
M2 (2 %)	47.5	41.9	12.0	50.9	49.53 γ^d_s : 29.19 γ^p_s : 20.35	24.32–29.43	46.19–49.30
M2 (8 %)	34.9	33.1	2.0	33.4	62.29 γ^d_s : 37.83 γ^p_s : 24.46	16.95–20.73	39.19–41.70

Table A3: SCA, SE (with disperse (γ^d_s), and polar (γ^p_s) components) and DCA results on PE foil surface with the test fluid diiodomethane

Methods	Static contact angle measurements (2 μ l) [°]				Surface energy [mJ/m ²]	Dynamic contact angle measurements (diiodomethane)	
	Water	Diiodomethane	Benzyl alc.	Glycerol		Hysteresis [°]	Drop age [s]
PE foil	101.2	56.2	45.6	88.9	30.92 γ^d_s : 30.80 γ^p_s : 0.12	9.75–12.98	28.89–33.79

Table A4: SCA, SE (with disperse (γ^d_s), and polar (γ^p_s) components) and DCA results on the AS of float glass with the test fluid water

Methods	Static contact angle measurements (2 μ l) [°]				Surface energy [mJ/m ²]	Dynamic contact angle measurements (water)	
	Water	Diiodomethane	Benzyl alc.	Glycerol		Hysteresis [°]	Drop age [s]
EM	1.0	45.2	28.9	18.9	51.83 γ^d_s : 30.36 γ^p_s : 21.47	< 10	Not detectable
M1 (2 h)	41.1	35.3	14.7	36.6	54.92 γ^d_s : 30.78 γ^p_s : 24.14	18.20–24.08	51.39–53.69
M1 (4 h)	35.7	39.7	18.5	32.7	56.36 γ^d_s : 28.34 γ^p_s : 28.02	25.08–33.66	79.99–97.49
M1 (8 h)	37.8	37.5	14.9	39.3	55.21 γ^d_s : 28.93 γ^p_s : 26.28	21.88–27.54	61.00–75.40
M2 (2 %)	50.3	40.7	11.5	44.0	49.81 γ^d_s : 31.05 γ^p_s : 18.77	33.31–37.41	93.99–110.19
M2 (8 %)	36.5	31.5	2.0	33.9	62.18 γ^d_s : 38.94 γ^p_s : 23.25	24.23–29.31	62.19–73.49

Table A5: SCA, SE (with disperse (γ_s^d), and polar (γ_s^p) components) and DCA results on the TS of float glass with the test fluid water

Methods	Static contact angle measurements (2 μ l) [°]				Surface energy [mJ/m ²]	Dynamic contact angle measurements (water)	
	Water	Diiodomethane	Benzyl alc.	Glycerol		Hysteresis [°]	Drop age [s]
EM	1.0	42.1	22.1	20.8	52.12 γ_s^d : 30.30 γ_s^p : 19.82	< 10	Not detectable
M1 (2 h)	23.1	36.5	15.0	31.3	60.92 γ_s^d : 27.74 γ_s^p : 33.18	< 10	Not detectable
M1 (4 h)	37.1	37.2	15.8	39.3	55.62 γ_s^d : 28.87 γ_s^p : 26.75	32.62–38.14	90.30–102.29
M1 (8 h)	22.2	36.1	10.3	39.4	59.89 γ_s^d : 27.23 γ_s^p : 32.65	21.57–30.09	63.19–77.69
M2 (2 %)	47.5	41.9	12.0	50.9	49.53 γ_s^d : 29.19 γ_s^p : 20.35	39.19–43.15	114.89–130.39
M2 (8 %)	34.9	33.1	2.0	33.4	62.29 γ_s^d : 37.83 γ_s^p : 24.46	27.01–32.82	75.49–85.69

JPMTR-2310
DOI 10.14622/JPMTR-2310
UDC 004.891:004.423:025.352

Research paper | 185
Received: 2023-08-21
Accepted: 2023-12-26

TaxoCatalog: expert system for semantically personalizing paper-based product catalogs in omni-channel context using background knowledge

Heiko Angermann

Hochschule Darmstadt, Faculty of Design,
Olbrichweg 10, 64287 Darmstadt, Germany

heiko.angermann@h-da.de

Abstract

Taxonomies are a formal method of semantically structuring information using hierarchically ordered concepts. Those play a crucial role in omni-channel retailing to publish product catalogs across media channels, i.e. digital (portal-based, paper-based) media channels, and print media (paper-based) media channels. Portal-based media channels use taxonomies to structure product-related content by concepts to facilitate customers navigate through the e-commerce site. That are the product categories. Paper-based media channels require taxonomies for automatic layout setting using data-driven publishing software. When recommender systems are additionally used, products are published individually on the e-commerce site. Printed product catalogs, on the other hand, currently only display content regardless of dynamic preferences, unless the layout is set manually. That is, as in an industrial context, personalization is of no interest if the necessary processes cannot be automated. The only recent industrially relevant method of taking preferences into account is to print sub-catalogs. However, these only contain certain product categories, resulting in a loss of information and sales, as preferences change dynamically today. With TaxoCatalog, an expert system is presented in this paper, capable of semantically personalizing product taxonomies to layout printed product catalogs according to the dynamic preferences of customers. The proposed expert system considers three layers to achieve full automation of relevant processes. The first layer uses background knowledge to consider a memory-based analysis of preferences, and a content-based analysis of possible semantic modifications. The second layer infers semantically personalized taxonomies using different modification rules. The third layer transforms the individual taxonomy paths into XML. This allows that the output of TaxoCatalog can be processed by any standard data-driven publishing software for automatic layout setting. A case study and a comprehensive evaluation, which discusses the strengths and limitations of previous research in the field, as well as the expert system in terms of quantitative and qualitative criteria, underline the efficiency of TaxoCatalog.

Keywords: data-driven publishing, expert systems, page layout, cross-channel publishing, taxonomy

1. Introduction

Today, products are advertised on different media channels (Hänninen, Kwan and Mitronen, 2021). Formally, this is referred to as multi-channel retailing strategy, or as omni-channel retailing strategy when the different channels offered are connected to each other in one retail network (Herhausen, et al., 2019; Beck and Rygl, 2015). Digital media channels can be used in the form of internal and external operated sales portals (e-commerce, marketplaces), or in the form of paper-based digital documents. Paper-based printed media products can be used as documents

(Gao, Melero and Sese, 2020). All have their own advantages, but when using e-commerce, retailers can infer customer preferences in real time using recommender systems (Chen, et al., 2023). As a result, products can be individually displayed to customers based on their likelihood of ordering (Behera, et al., 2020). For example, suitable products are shown at the bottom of the product site, known as cross- and up-selling (Norvell, Kumar and Contractor, 2018). Paper-based digital product catalogs, on the other hand, display static content, even if the appearance is dynamic. Here, formats like EPUB, or (interactive) PDF are used. Printed product catalogs, also show static content, as individualization

affects the de-automation of processes (Hoffmann-Walbeck, 2022). Usually, the specific PDF file created with settings conforming to PDF/X is used for printing. Minimal individualization is possible for paper-based product catalogs using proven methods of print-on-demand, variable data printing, programmatic printing, and sub-catalogs.

Using print-on-demand, the catalog is produced on the basis of an interaction, e.g. an order. With variable data printing, single pages of the catalog are individualized, e.g. with an individual name (Lin, 2006). With programmatic printing, a combination of the before-mentioned possibilities is achieved, that has been possible since the advent of non-impact printing. For example, when an (online) shopping basket is not ordered, the customer receives a mailing with the products and a promotional code. Of course, programmatic printing is a major step forward in terms of multi- and omni-channel retailing, as now, preferences of digital channels can be used for the printing. However, the decisive factor is that the media that is produced shows a certain selection. This leads to a loss of information as a large number of products are not displayed. This is similar to the well-established paradigm of sub-catalogs (Angermann and Ramzan, 2016). Here, catalogs are printed that contain only products of certain categories (Xu, Du and Xu, 2014). For example, a sub-catalog is printed for a specific season, e.g. garden furniture for the summer. Sub-catalogs can also be used to filter the customers who receive the document (Mark, et al., 2019; de Melo, et al., 2019). For example, only customers who have bought garden furniture will receive the sub-catalog. However, dynamic preferences are not taken into account when producing the sub-catalogs (Angermann, 2022). It looks identical for all recipients, regardless of whether a customer lives in an apartment with a balcony, or in a house with a garden and pool. And maybe a homeowner is not only planning to buy new garden furniture, but also a garden kitchen. Unfortunately, kitchen appliances are not included in this sub-catalog, as those are logically part of an excluded product category. Like programmatic printing, this method results in a loss of information. And, in turn, both methods lead to a potential loss of sales. The homeowner may buy the kitchen appliances elsewhere or, in the worst case, the homeowner may look elsewhere to buy all the products at once. In summary, none of the existing methods provide a solution for paper-based product catalogs that takes into account individual preferences while still being able to include all products.

As a result, the only option for retailers that want to take customers preferences into account in the layout of the catalog is to layout the document manually using DTP software, or to accept a loss of potential sales.

To overcome above-mentioned limitations, the expert system (ES) TaxoCatalog is presented in this paper. The main difference to existing methods is that TaxoCatalog semantically personalizes the leading element for retailers regardless of branch or strategy, to publish content across channels. This is the product taxonomy, usually stored in a product information management (PIM) system. For portal-based media, the product taxonomy is used for product navigation on the e-commerce site. For paper-based media, the product taxonomy is used to structure documents for automatic layout setting of paper-based product catalogs using data-driven publishing. With TaxoCatalog, dynamic customer preferences can now be taken into account across channels based on this taxonomy, personalization is performed without loss of information, and automatic layout setting is still supported. To achieve this new approach to paper-based product catalogs, the proposed three-layered ES uses so-called background knowledge (BK).

The first layer of TaxoCatalog leverages two main sources of BK into its knowledge base (KB). These are the content-based BK of the taxonomy and possible semantic modifications, and the memory-based BK of customer preferences. Based on the first layer of BK, the second layer of TaxoCatalog infers semantically personalized taxonomies using a rule-based approach. For this purpose, different modification rules are provided by the included inference engine (IE). The third layer finally transforms the personalized taxonomy paths of the previous layer into the extensible markup language (XML) format.

The used architecture, especially because of the used BK, results in two other important advantages. Firstly, TaxoCatalog performs the computation of the semantically personalized taxonomy fully automatically, but the retailer is still able to customize the volume of personalization. And, the initial product taxonomy in the PIM remains consistent. In summary, the proposed ES TaxoCatalog provides three contributions to the data-driven publishing and printing industry:

- TaxoCatalog advances the interlinking of portal-based media, paper-based digital media, and printed media. This is achieved through the memory-based BK of customers' preferences.
- TaxoCatalog is the first solution for personalizing paper-based product catalogs without loss of information. This is achieved by using content-based BK of the taxonomy.
- TaxoCatalog is able to dynamically, yet fully automatically, scale the desired level of semantic personalization. This is achieved by using a rule-based IE.

The rest of the paper is organized as follows. Section Background describes the basic underlying methods necessary for the development of the proposed ES TaxoCatalog. After that, the ES is presented in detail in section TaxoCatalog. In section Case study, the ES is demonstrated in a real-world context. In section Evaluation, the ES is quantitatively and qualitatively evaluated from different perspectives. Finally, the conclusions are presented in the corresponding section.

2. Background

This section describes the methods necessary to develop the ES TaxoCatalog. Furthermore, this section will help to understand the use-case, methods, and implementation of the system presented in the following section. For this reason, four methods are necessary to be explained. These are the retail strategy paradigm called omni-channel retailing, the applications of taxonomy including its use in the context of omni-channel retailing, the principles of expert systems (ES) and the programming languages used, and the aim of data-driven publishing for the page-layout process.

2.1 Omni-channel retailing

The retail industry as a whole has been significantly impacted by digitization, particularly through the emergence of digital media channels (Hagberg, Sundstrom, and Egels-Zandén, 2016; Hübner, et al., 2021). This includes digital product distribution and sales channels (e.g. e-commerce, mobile commerce, external marketplaces), as well as digital marketing and hybrid marketing channels and techniques (e.g. social commerce, bots).

The demand to connect the heterogeneous channels into one single retail network represents the essential aspiration of today's retail industry (Hübner, Wollenburg and Holzapfel, 2016; Yrjölä, Saarijärvi and Nummela, 2018). The aim of networking the different channels is now to offer customers a so-called cross-channel customer experience (Asmare and Zewdie, 2022; Van Nguyen, McClelland and Thuan, 2022).

The most recent paradigm of maximum channel connectivity is called omni-channel retailing. This retail strategy is used by most of the leading retailers today (Jocevski, et al., 2019; Asmare and Zewdie, 2022; Li, et al., 2022). Compared to its predecessors, cross-channel and multi-channel, omni-channel retailing allows all channels that are part of the strategy to be supplied by a leading publishing source, and yet the channels can be interconnected without any barriers on the customer side (see Figure 1) (Verhoef, Kannan and Inman, 2015; Yrjölä, Saarijärvi and Nummela, 2018). In

most cases, a PIM system is used as the leading source, structuring the product information using a product taxonomy (see section Taxonomy applications). Omni-channel retailing opens up new opportunities for both the retailer and the customer. First, the retailer can explore knowledge about the customer across channels in real time using recommender systems (RS). The RS typically combine statistical methods to measure the likelihood of ordering products. In particular, they use content and memory-based methods (e.g. order history, product features) or collaborative filtering (e.g. similar customers, similar ordering behavior). The results of recommender systems indicate customer preferences. These, in turn, can be used to display product-related content in a personalized manner on digital portal-based channels (Roy and Dutta, 2022). This opens up new opportunities for customers to receive personalized content across channels, creating a new kind of shopping experience throughout the customer journey (Alexander and Kent, 2022). For example, the customer receives a promotional code from an influencer on social media, sees the product on the main landing page when entering the online store, and purchases the product.

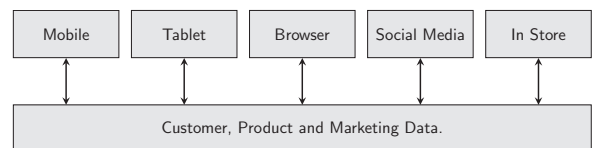


Figure 1: Omni-channel data integration schema (adapted from Cook, 2014)

2.2 Taxonomy applications

Taxonomies are a formal method of semantically structuring information using hierarchically ordered concepts (Angermann and Ramzan, 2017). The concepts can be described as a two-tuple: $\tau = \{\varphi, \rho\}$, where ρ is a set of edges for connecting partially ordered concepts of φ in taxonomy τ . Each edge represents a semantic hypernym–hyponym relationship between the concepts, expressed in simplified terms as a so-called *is-a* relationship. For example, 'Fish' *is-a* 'Seafood' (presented later in Figure 5).

Using the resulting string of *is-a* relationships, each concept can be uniquely defined by its so-called taxonomy path ρ_φ . Based on the unique paths for each concept, different concept types are distinguished. Concepts that share the same direct hypernym relationship are referred to as sibling concepts. For example, 'Fish' and 'Seaweed'. These concepts are also called sub concepts, as those specify the more general super concept. In our example, the super concept is 'Seafood'. Finally, the concept that is not further generalized is called the root concept, e.g. 'Products'.

Based on the number of φ that are part of ρ_φ , each path has a length, and each concept of the path has a depth. The deeper the position of one concept within the path, the more specific the concept is. The higher its position, the more general the concept is. Conversely, the path of one particular taxonomy with the maximum length defines the depth of the taxonomy. Formally, this is referred to as the number of levels N . In our example taxonomy, $N = 3$. Regardless of the depth and the underlying concept type, each concept is defined by a unique identifier (ID) and a label. This is usually a word or a multi-word in a natural language. Optionally, a concept can have a description, named gloss.

As taxonomies are able to semantically structure information based on the mentioned *is-a* principle, the represented information becomes knowledge (Bellinger, Castro and Mills, 2004). For this reason, taxonomies have many applications in information management (IM) (Angermann, 2017):

- In PIM, a taxonomy is used to hierarchically structure concepts in the form of product categories. This taxonomy is usually the leading element for all processes related to product information in the context of omni-channel retailing.
- In media asset management (MAM), the above-mentioned product categories are used to structure product-related media (e.g. images), and to assign those to the products.
- In e-commerce, content is usually provided by interfaces to other IM systems, e.g. PIM, MAM, enterprise resource planning (ERP), customer relationship management (CRM). Again, the product taxonomy is used as the leading element for data exchange.
- In data-driven publishing, the information from the PIM is used by the templates to automatically layout pages with dynamic content provided by the PIM and MAM.

As the examples above illustrate, the importance of taxonomy increases with the complexity of the IT landscape, which is the case with omni-channel retailing.

2.3 Expert systems

The ES are intelligent systems that aim to automatically infer decisions based on knowledge (Oleshchuk and Fensli, 2011). The main purpose of ES is to achieve a decision quality similar to that of a human expert (Mirmozaffari, 2019). Consequently, unlike machine learning (ML), the knowledge is not acquired by training an algorithm as for ML. However, ES have the abil-

ity to use, formally named consult, knowledge across expert systems. Thus, already defined knowledge can be consulted into the considered ES, as so-called BK (Angermann and Ramzan, 2017). These can be internally or externally generated BK from different sources.

In ES, the decisions are inferred using logic reasoning based on the mentioned knowledge, including BK (Merritt, 2012). This is another key difference from ML (Langley, 2011). The decision statements of ES are unambiguous (Ben-David and Frank, 2009). Each decision is true or false. A true statement states that the necessary knowledge is available to infer the decision, hence an unambiguous conclusion can be drawn. A false statement states that the necessary knowledge is not available to infer a decision. Before, all possible combinations of inferences are evaluated, called backtracking. Due to the binary answer spectrum, ES are well suited for taxonomic operations (Angermann and Ramzan, 2016). And, the ability of ES can be easily extended using BK (Angermann and Ramzan, 2017).

From a technical perspective, ES can be implemented using declarative programming languages (e.g. Python, Prolog). Prolog, in particular, is widely used for taxonomy-driven ES (Merritt, 2012). In Prolog, every program consists of two components (Bramer, 2005). These are a KB, and an IE. The KB represents knowledge in the form of fact predicates. The IE represents rule predicates to infer decisions based on the facts contained in the KB. Each rule uses facts, and/or other rules. Due to the interconnection between rules, and the backtracking, Prolog's inference mechanism can be time consuming. However, the computation can be accelerated using so-called dynamic facts. Then, the result of true statements is dynamically consulted into the KB as facts, formally called fact assert. The same is true for BK, as arbitrary sources can be easily consulted in the KB to further improve the Prolog program.

2.4 Page layout

The page-layout process is part of a print media production workflow (Angermann, 2023b). It aims to determine the layout of pages for paper-based documents, such as a printed product catalog. It involves the creative production of the design, depending on the desired format, the number of pages, and the graphical content to be included (Ambrose, Harris and Ball, 2019). Depending on the aforementioned criteria, this can be a time-consuming process when carried out manually using desktop publishing (DTP) software.

For this reason, different methods exist to automate the layout setting. These are methods known as scripting (e.g. JavaScript), or the database-driven methods (e.g. XML-based approaches).

Data-driven publishing, also known as database publishing, is a database-driven process that achieves the highest level of automation in the page-layout process. It is a rule-based technique for automatically setting the layout of paper-based documents using a layout generator. The software provides various data interfaces to databases of different formats, such as structured query language (SQL), comma separated values (CSV) and XML. In addition, the software provides a graphical user interface (GUI) for the designer to set up the data connections and to create the necessary components of the master page and templates (see Figure 2):

- The master page defines the dimensions of the paper-based document, and of the page frame(s). These frames are the areas of the paper that contain graphical content. Of course, each document can have multiple master pages.
- A template contains and defines so-called content frames for the page frames of master pages. The main purpose of the content frames is to include static and/or dynamic content, and to specify the design of this particular content. The main difference compared to other methods (DTP, scripting) is the use of dynamic content. This is content provided by a data source (e.g. a PIM). To do so, dynamic content is placed using data queries. For example, the product categories of products. A single content frame then consists of a rule that defines which content is to be dynamically queried and how this content should finally be designed. For example, the taxonomy path should be in 12 pt.
- A data source provides the dynamic content for each content frame as data stack. This stack is processed sequentially during the automatic generation of the document to be published. For example, a stack to query concepts as a sequence of paths.

The requirements for data-driven publishing logically lie in the data – more specifically, in the separation and structure of the data (Gündoğan, 2022). First, the data must be separated from channel-specific design, called media-neutral data storage. This allows the data to be later designed media-specific for different channels. Second, the data must be semi- or highly-structured. This results in the data marked using so-called tags. This means that the different data elements can be distinguished as distinct content types for data-driven publishing. For example, a content type ‘concept’ is used to filter out elements of the database (or data file) that are actually product categories. Based on this, all elements tagged as ‘concept’ are returned using the product path stack. Most omni-channel retailers fulfill data separation and data structure by using the hier-

archical database format XML. This has the advantage that the data is semi-structured, and the data can be individually specified in the form of customizable tags (van der Vlist, 2002). In addition, the structure required for a particular document can be validated using the data format doctype definition (DTD), or other XML-based techniques (e.g. XML Schema).

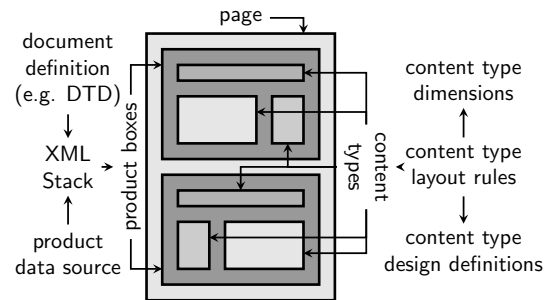


Figure 2: The concept and required components of data-driven publishing

In addition to data storage and structure, another important aspect of omni-channel retailing is data consistency. This means that all channels are based on the same (leading) data source. For example, the product information on the e-commerce site is based on the same data as the content displayed in the printed product catalog. In most cases, the PIM and product taxonomy is used as the leading element to publish consistent product information across online and offline channels (Angermann, 2022). In terms of product master data, the external procurement relationship (EPR) is usually the leading system.

3. TaxoCatalog

This section discusses the proposed ES TaxoCatalog for the semantic personalization of paper-based product catalogs in the context of omni-channel retailing. The comprehensive discussion starts by explaining the underlying use case, followed by the included methods, before explaining the implementation of the ES including its architecture using the logic programming language Prolog.

3.1 TaxoCatalog use-case

TaxoCatalog use-case is aimed at semantically personalizing product taxonomies for the layout setting of paper-based product catalogs based on customer preferences. These preferences are consolidated by a recommender system in an omni-channel context. This includes preferences derived from digital media, e.g. an e-commerce site, but it can also include preferences provided through other channels, e.g. a call-center, a local store or print media. For this reason, a current

order does not necessarily have to be an authoritative interaction to infer a personalized product taxonomy using TaxoCatalog. Rather, the TaxoCatalog use-case is based on providing the customer, at a selected time X , with a semantically personalized printed product catalog Y (see Figure 3). The actors in the use-case involved are indirectly the customer, and the retailers' professional who decides to layout and print a personalized product catalog:

1. An initial product taxonomy provided by a PIM forms the basis of the use-case. In addition, a content-based BK detailing the semantic correspondences of the included concepts is entered.
2. The customer places orders via channels, e.g. on the e-commerce site. These individual preferences are entered into the ES as memory-based BK. Based on the BK, and the intention to layout a semantically personalized paper-based product catalog, the retailer's professional (e.g. designer, marketing expert), starts the computation, i.e. the rule-based IE. Now, the professional has to define the customer, and the volume of personalization desired. Logically, semantic correspondences, preferences, and the volume, are now taken into account to compute the customer-specific path, combined into a taxonomy. Here, different modification rules are used depending on the preferences.
3. The personalized taxonomy is exported by TaxoCatalog in XML file format. Logically, it contains paths with a semantic weight according to the customer's preferences.
4. The XML file is now used by the professional to start the layout setting processes using data-driven publishing software. Based on the semantic weight of the paths according to the customer's preferences, the designer can use standard queries that filter accordingly.

3.2 TaxoCatalog methods

TaxoCatalog uses different methods to infer semantically personalized product taxonomies. These are a content-based analysis method to derive semantic correspondences of the initial product taxonomy, a memory-based analysis method to result individual customer preferences, a modification rule-based method to personalize the taxonomy without loss of information, and finally a schema-based method to derive an XML file to be used for data-driven publishing.

3.2.1 Content-based analysis

The content-based analysis method uses natural language processing (NLP) to produce semantic correspondences of the original concepts in the form of mediator concepts. In TaxoCatalog, the output is based on the work presented in Angermann, Pervez and Ramzan (2017) and Angermann (2022). These are latent concept types of dependencies and collections (see Figure 4).

The concept type Dependency further specifies a super concept φ_I , and at the same time, further generalizes a set of sibling sub concepts φ_{I_N} specifying φ_I . Thus, a dependency forms a further, but latent level between super and sub concepts that are more synonymous than other sub concepts. For example, in the initial product taxonomy, the sibling sub concepts 'Soft Drinks', 'Coffees', 'Teas', 'Beers', and 'Ales' are assigned to the super concept 'Beverages' (see Figure 5). The dependency 'Alcoholic Drinks' further generalizes the sibling concepts 'Beers' and 'Ales' (see Figure 6). Same for the dependency 'Hot Drinks', which generalizes 'Coffees' and 'Teas', and for the dependency 'Nonalcoholic Drinks', which generalizes 'Soft Drinks'. The concept type Collection works in a similar way, but between the root concept and the super concepts. For example, the initial product taxonomy contains the super concepts 'Meat Poultry' and 'Seafood'. These

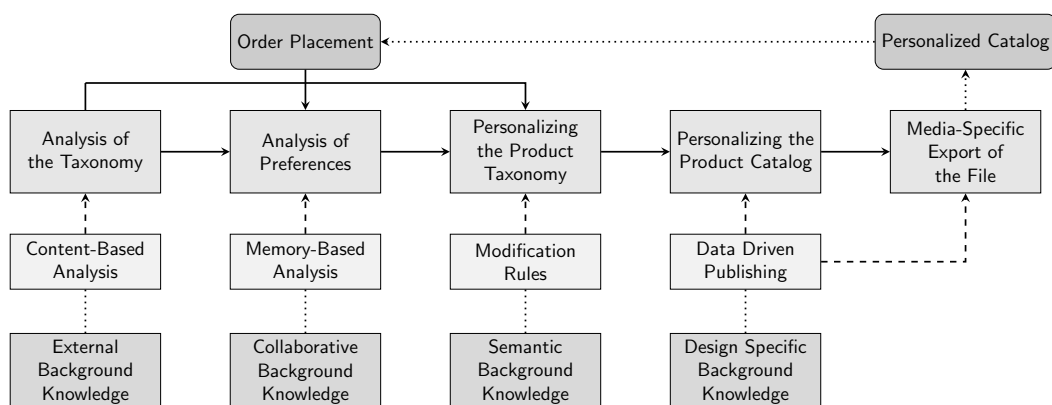


Figure 3: Use-case and methods of the ES TaxoCatalog

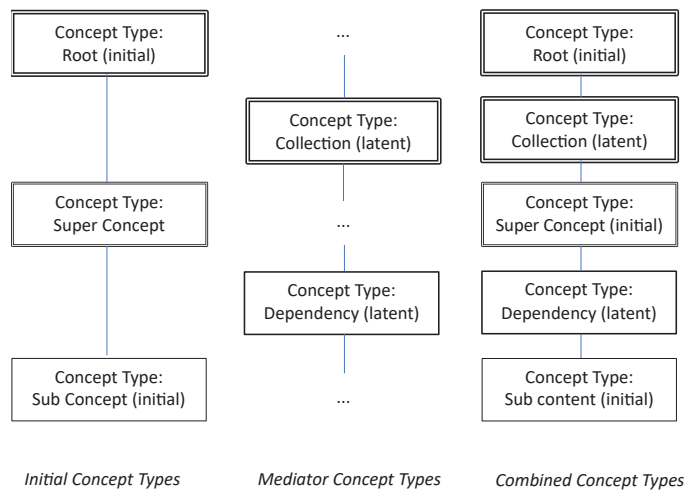


Figure 4: Hierarchical structure of a taxonomy using two mediator concept types

two super concepts can be generalized by a collection ‘Meat and Seafood’, etc. Both latent concept types, as well as the associated *is-a* relationships, are consulted in TaxoCatalog as external BK.

3.2.2 Memory-based analysis

The memory-based analysis method provides customer preferences using the recommender system as presented in the work of Angermann and Ramzan (2016). The method outputs preference statements. Each statement clarifies whether an individual customer has shown a low, medium, or high preference for similar product categories:

$$(\varphi_{I_{N_i}}, \varphi_{I_{NN}}) \rightarrow \text{preference (low; medium; high)} \quad [1]$$

The algorithm first divides the orders into epochs, where more recent epochs are assigned with a higher epoch rate R . The algorithm then calculates the preferences for the different epochs E before combining them using $[R_E]$. This is performed not only for one customer, but for customers sharing the identical customer group as well, known as collaborative filtering. This avoids over-specialization and the cold start problem (Desrosiers and Karypis, 2010). Again, the preference statements of the customers are consulted in TaxoCatalog as external BK. However, these preferences are further analyzed in TaxoCatalog using the above-mentioned method of latent concept types dependencies and collections. First, the preferences of the customers are consulted as a three-tuple:

$$\varepsilon_D = \{I, \rho_N, P\} \quad [2]$$

where I is the ID of the customer, ρ_N is a set of similar sub-concepts (dependency), and P is the preference statement (1 = low preference, 2 = medium prefer-

ence, 3 = high preference). Second, the preferences of dependencies that generalize a collection are combined accordingly:

$$\varepsilon = \sum[\varepsilon_D]/N_{\varepsilon_D} \quad [3]$$

This results in a second and more general preference statement (1 = low preference, 2 = medium preference, 3 = high preference).

3.2.3 Modification rules

In TaxoCatalog, each taxonomy path is personalized according to the customer’s preferences and the desired volume of personalization defined by the retailer’s professional:

$$\text{Path Modification}_I = (P_C, P_D, M_C, M_D) \quad [4]$$

where P_C is the preference of a latent concept type collection for path I , M_C is the desired volume of personalization for the entire catalog, P_D is the preference of a latent concept type dependency for path I , and M_D is again the desired volume of personalization. Parameter M can have three states, corresponding to the different states of preferences; by default, $M = P$.

However, when the retailer decides not to modify the taxonomy according to the preferences, or not to modify a set of particular taxonomy path at all, the retailer can override P with M :

$$P \neq M \rightarrow P = M \quad [5]$$

Based on the Equation 5, it is clear that each path is modified separately, and in addition, both latent mediator concept types can now be modified separately. This is an improvement over recent work on taxonomy

modification presented in Angermann (2022). For each latent mediator concept type, three modifications are available:

- $P = M = 1$ results in that the latent mediator concept is shown instead of showing the assigned more specific concepts. In terms of a collection, it means that the collection is shown instead of the super concepts. In terms of dependencies, it means that the dependency is shown instead of the sub concepts. In terms of $P_D = P_C = M_C = M_D = 1$, this means that the modified path considers the low preferences of the customer.
- $P = M = 2$ results in that the latent mediator concept is not shown, but the assigned more specific concepts are displayed. In terms of a collection, it means that the super concepts are shown instead of the collection. In terms of dependencies, it means that the sub concepts are shown instead of the dependency. In terms of $P_D = P_C = M_C = M_D = 2$, this means that the modified path considers the medium preferences of the customer.
- $P = M = 3$ results in that the latent mediator concept is shown, as well as the assigned more specific concepts. In terms of a collection, it means that the collection is shown, as well as the super concepts. In terms of dependencies, it means that the dependency is shown, as well as the sub concepts. In terms of $P_D = P_C = M_C = M_D = 3$, this means that the modified path considers the high preferences of the customers.

Of course, P_D and P_C of the individual paths can have different preference and volume statements (1, 2, 3). This results in that one single path can have nine possible modifications to be performed.

3.2.4 Schema export

TaxoCatalog is aimed to support automation of processes. For that reason, the personalized paths are transferred into an XML schema. This allows that the file can be processed using data-driven publishing software to automatically set the layout of the product catalogs to be printed. To transfer the single path into a valid well-formed XML, the following steps are performed:

1. The single concepts of one path are labelled with the tag `<concept>{Label}</concept>`. And, the ID of the concept is assigned to the start tag `<concept id="{ID Concept}">`.
2. The different concepts (3 to 5) of one path are assigned as sub-elements to the tag `<path>{Con-`

`cepts}</path>`. The assignment is performed according to the depth of the concept within the single taxonomy path. For example, the root is the first element. In addition, the starting tag `<path id="{ID+ID+ID+(ID;{})+(ID;{})}">` is assigned an ID in the form of a concatenation of the IDs of the individual concepts.

3. All single paths of the personalized taxonomy are assigned as sub-elements to the tag `<customer>{Paths}</customer>`. Logically, the customer ID is assigned to the start tag `<customer id="Customer ID">`.
4. An XML header is assigned before the start tag to uniquely describe the customer. Finally, the exported XML looks like shown in Listing 1.

```
<?xml version="1.0" encoding="UTF-8"?>
<!DOCTYPE customer SYSTEM "taxocatalog.dtd">
<customer id="1">
  <path id="1010000141001412014121">
    <concept id="10000">Products</concept>
    ...
  </path>
</customer>
```

Listing 1: An extract from an XML file produced by TaxoCatalog

3.3 TaxoCatalog implementation

TaxoCatalog is implemented using the logic programming language Prolog. Logic programming languages are assigned to the declarative programming paradigm, which is often used for artificial intelligence applications. For that reason, a Prolog code does not serve as a collection of instructions, but as a description of the KB to infer logic conclusions (see section Expert Systems). For describing the KB, predicates expressed in the form of horn clauses are used. Each predicate has two components:

- The first component is the functor. It serves as the name of the predicate. For example, the predicate `"concept(12000,"Trousers")"` has the functor `"concept"`.
- The second component are the arguments (1 to N), which stand in brackets behind the functor. The arguments are the knowledge assigned to the predicate. For example, the predicate `"concept(12000,"Trousers")"` has two arguments, referred to as arity. The first argument is a number, the second argument is a string. Besides numbers and strings, arguments can also be compound terms or lists. A predicate ends by writing a dot `"."` behind the enclosing bracket after the last argument.

Alternatively to the notation mentioned above, where the functor is mentioned with the arguments in detail, predicates can also be expressed by its short form. Then, the arity is written after the functor, separated by a slash, e.g. “concept/2”.

The predicate from the example given above is a so-called fact predicate. For example, the fact that a concept named “Trousers” exists with the identifier of 12000, is expressed using “concept(12000,“Trousers”)”. Besides fact predicates, so-called rule predicates exist in Prolog. A rule predicate consists of two components to infer knowledge:

- The first component of a rule predicate is its head. It has a similar structure as a fact predicate: a functor, and arguments standing in brackets. For example, the rule predicate “twoconcepts(A,B) :- ...” has a functor (“twoconcepts”) and two arguments (A,B). However, the arguments are usually not knowledge, but variables. In Prolog, variables are written with a capital initial letter.
- The second component is the body. Head and body are separated by a colon and hyphen “:-”. The body includes further rule and/or fact predicates, which are set in relation to each other using the logical *and* operator written as comma “;”, or by using the logical *or* operator written in the form of a semi-colon “;”. For example, the rule predicate “twoconcepts(A,B) :- concept(A,_),concept(B,_).” includes two fact predicates of type “concept/2” to investigate if two different concepts exist. As can be seen, the variables from the head are used again in the body of the rule. By using variables, all possible combinations of relevant predicates are evaluated to test if a solution for the given problem exists inside the KB (true) or not (false). To ignore arguments not required for a specific rule, those can be ignored. This is done by using so-called anonym variables written as underscore “_”. Analogous to a fact predicate, a rule predicate ends by writing a dot “.”.

3.3.1 Program architecture

The ES TaxoCatalog is implemented using different layers, as suggested in recent literature discussing these types of intelligent systems (van der Aalst, Bichler and Heinzl, 2018). For TaxoCatalog, this means a three-layer approach. Doing so, only the data required for setting the layout is personalized. The initial data (in the leading PIM system) remains consistent:

- The storage layer consults all the required BK resources as fact predicates into the KB. This is the external BK based on the content-based analysis

of the taxonomy and BK using the memory-based analysis of customer preferences. All resources of BK can be updated for each computation, if the underlying initial data changes in the leading systems. This is the product data in the PIM, but also the external BK mentioned before.

- The processing layer contains all the rule predicates within the IE necessary to compute a semantically personalized taxonomy for one customer. The main objective of the rules included is to create single and unique taxonomy path based on the customer’s preferences. Depending on the preferences, the semantics of the paths are adopted, resulting in combining concepts, splitting concepts, and changing levels.
- The publishing layer contains all the rule predicates within the IE of the ES that are necessary to export the semantically personalized catalog in a format that can be effectively input and processed by a layout generator software. For this reason, TaxoCatalog exports the semantically personalized taxonomy as an XML file. To do so, the different paths are transformed into XML tags, before the complete catalog is transformed into an enclosing custom XML tag, which is further enclosed by an enclosing customer XML tag.

As mentioned above, in Prolog the rules are related to each other. This is done using logical operators (*and* “;”, *and or* “;”),. To optimize the processing time, dynamic facts are generated in TaxoCatalog. After the XML export has taken place, these dynamic facts are deleted (retracted) so that the program can be used for a new computation.

3.3.2 Program Sequence

The program sequence is structured according to the layers mentioned in the previous section. The top level rule predicate taxocatalog/0 contains the required rule predicates in its body (see Listing 2).

```
taxocatalog:-
    storagelayer,
    processinglayer,
    publishinglayer.
```

Listing 2: The upper-level rule predicate in TaxoCatalog

Within the rule predicate storagelayer/0 and its contained rule predicate readknowledge/0, as well as its contained rule predicates, e.g. concepts/1, different resources of the BK are consulted (see Listing 3). This is the external BK based on the content-based analysis of the taxonomy, and the BK based on the storage-based analysis of customer preferences (preferences/1).

In addition, the rule `storagelayer/0` contains the rule predicate `gettimestamp/0`, which dynamically asserts the predicate `timeidentifier/1` to the KB based on the current time and date. This is necessary to calculate different catalogs for different customers.

```
storagelayer:-
  gettimestamp,
  readknowledge.

readknowledge:-
  directory(Directory),
  string_concat(Directory,'/Knowledge/',Folder),
  concepts(Folder),
  customers(Folder),
  dependencies(Folder),
  dependency mappings(Folder),
  collections(Folder),
  collection mappings(Folder),
  preferences(Folder).

concepts(Folder):-
  string_concat(Folder,"concepts.csv",File),
  csv_read_file(File,Rows,
  [functor(concept),arity(2)]),
  maplist(assert,Rows).
```

Listing 3: The rule predicates to consult used BK

After the rule `storagelayer/0` is executed, the KB consists of seven dynamic facts describing knowledge and external BK. The fact `concept/2` describes concepts of the initial product taxonomy using two arguments: ID and the concept's associated label. The `customer/2` fact describes customers with an ID and a name. The fact `dependency/2` describes dependency concepts with an ID and a label. The mapping of the different dependencies to the corresponding source concepts is done by the fact `dependencymapping/3`.

Each possible path extension is represented as a single fact using the ID of the super concept, the ID of the dependency and the ID of the sub concept (see Listing 4). Thus, the number of dependency mappings/3 is equal to the number of most specific concepts. Similarly to dependencies, two dynamic facts are used to represent the different collections: `collection/2` and `collectionmapping/3`. Finally, the fact `dependencypreferences/3` describes the individual customer preferences at the dependency level: Customer ID, Dependency ID, Preference.

Personalization of the catalog based on the dynamic BK fact predicates is performed within the rule predicate `processinglayer/0`, and the therein included rule predicates `definecustomer/0`, `getpreferences/0`, `definevolume/0`, and `createcatalog/0` (see Listing 5). The main aim of the included rules is to use the different mod-

ification rules for single paths of the catalog depending on the customers individual preferences and the desired volume of personalization.

```
dependency(ID_Dependency,Label) .

dependencymapping(ID_Super_Concept,
  ID_Dependency,ID_Sub-Concept) .

collection(ID_Collection,Label) .

collectionmapping(ID_Root_Concept,
  ID_Collection,ID_Super-Concept) .

dependencypreference (ID_Customer,
  ID_Dependency,Preference_Degree) .
```

Listing 4: The fact predicates for depicting mediator concepts and customers' preferences

```
processinglayer:
  definecustomer,
  getpreferences,
  definevolume,
  createcatalog.

getpreferences:-
  customer (ID_Customer) ,
  forall (collection (ID_Collection,_) ,
  collectionpreference (ID_Customer,
  ID_Collection)) .

collectionpreference (ID_Customer,
  ID_Collection,Preference_Degree) .

definevolume:-
  customer (ID_Customer) ,
  dependencyadaption (ID_Customer) ,
  collectionadaption (ID_Customer) ,
  setcustomerrules (ID_Customer) .

createcatalog:-
  customer (ID_Customer) ,
  possiblepaths (ID_Customer) ,
  modification (ID_Customer) ,
  validatepaths (ID_Customer) ,
  removeduplicates (ID_Customer) .
```

Listing 5: The rule predicates to infer semantically personalized Taxonomies

After the rule `processinglayer/0` has been performed, the KB consists of several dynamic facts describing personalized paths of the taxonomy. First, the rule predicate `definecustomer/0` asserts the current customer with an ID. Second, the rule predicate `getpreferences/0`, calculates and asserts the fact predicate `collectionpreference/3`, using `dependencypreference/3`.

Based on the two facts and the *is-a* relationships between the concepts of the initial taxonomy, it can be clearly stated which preference a customer has for one path of the initial taxonomy. Thirdly, the rule predicate `definevolume/0` states and asserts the fact predicates `dependencyadaptionrule/3` and `collectionadaptionrule/3` to the KB.

```
path(ID_Customer, ID_Root, ID_Collection,
    ID_Dependency) .

path(ID_Customer, ID_Root, ID_Collection,
    ID_Sub_Concept) .

path(ID_Customer, ID_Root, ID_Super_Concept,
    ID_Dependency) .

path(ID_Customer, ID_Root, ID_Super_Concept,
    ID_Sub_Concept) .

path(ID_Customer, ID_Root, ID_Collection,
    ID_Dependency, ID_Sub_Concept) .

path(ID_Customer, ID_Root, ID_Super_Concept,
    ID_Dependency, ID_Super_Concept) .

path(ID_Customer, ID_Root, ID_Collection,
    ID_Super_Concept, ID_Dependency) .

path(ID_Customer, ID_Root, ID_Collection,
    ID_Super_Concept, ID_Sub_Concept) .

path(ID_Customer, ID_Root, ID_Collection,
    ID_Super_Concept, ID_Dependency,
    ID_Sub_Concept) .
```

Listing 6: The fact predicates including personalized taxonomy paths

These rules define how a path should be treated based on the actual preferences and based on the desired degree of personalization. Consequently, for each type of mediator concept and for each type of possible preference degree, there is a fact with three arguments.

This is the degree of preference (1 to 3), the customer's ID and the desired modification. Based on this, two types of dynamic fact predicates are created to define the desired set, the dynamic fact predicates `collectionrule/3` and `dependencyrule/3`. These define the actual desired modification for each mediator concept using the arguments customer ID, mediator concept ID and modification state. Thirdly, the rule predicate `createcatalog/0` asserts the personalized path to the KB depending on the preferences and the desired scope of the modification. Paths are created for every possible and semantically correct combination. This results in

three different dynamic fact predicates: `path/4`, `path/5` and `path/6`. All three use the ID of the customer as the first argument and the ID of the root concept as the second argument. However, the other arguments, as well as the number of arguments, are different depending on the modification used (see Listing 6).

The XML export is achieved using the `publishinglayer/0` rule predicate (see Listing 7) and the `exportcatalog/0` rule predicate it contains. The `retractcatalog/0` rule predicate removes dynamic facts.

```
publishinglayer:-
    exportcatalog, retractcatalog.

exportcatalog:-
    customer(ID_Customer),
    createpaths(ID_Customer),
    combinepaths(ID_Customer),
    writexml(ID_Customer),
    writefile(ID_Customer) .
```

Listing 7: The fact predicates for exporting the personalized catalog in XML data format

Analogous to the other layers, dynamic fact predicates are asserted. First, the rule predicate `createpaths/1` infers and asserts the fact predicate `xmlpath/3` to the KB. Here, the first argument is the customer's ID, the second argument is the modification performed, and the third argument is paths in XML syntax. To do this, each concept of each path is assigned an associated XML tag. These elements are then collected and the collection is assigned an associated XML tag.

The result is a dynamic fact predicate called `combined-path/2`, where the first argument is again the customer's ID, and the second argument is the XML element containing the path tag and the contained concept tags. Finally, the individual XML path elements are collected again and given an associated XML tag. This tag identifies the customer. This finally represents the XML schema of a personalized catalog.

4. Case study

As a demonstration of TaxoCatalog, let us consider the omni-channel retail market Northwind (2017), and three customers. The initial taxonomy consists of three levels and 31 concepts (see Figure 5).

Based on a content-based analysis of the taxonomy, the mediator concepts were consulted as BK, as well as the necessary mappings with the concepts of the initial taxonomy (see Figure 6). In detail, there are four collections and 16 dependencies. The taxonomy now has a maximum of five levels.

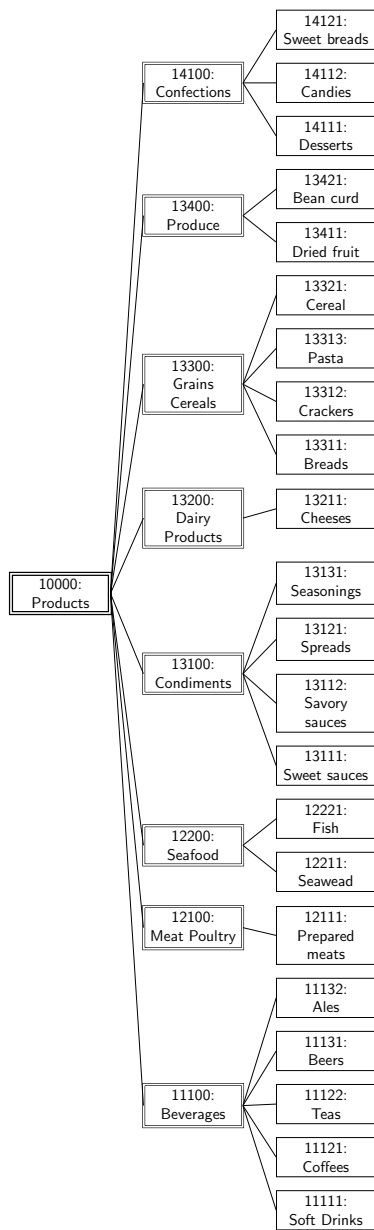


Figure 5: The initial product taxonomy of the omni-channel retailing market Northwind

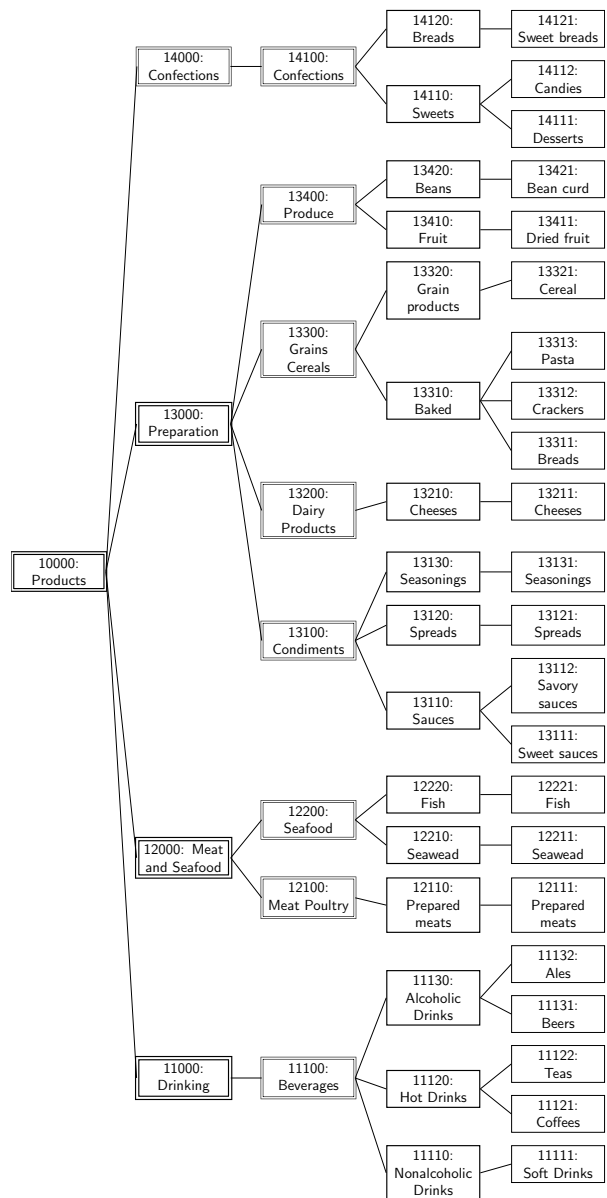


Figure 6: The initial product taxonomy of the omni-channel retailing market Northwind, including the two latent mediator concept types

4.1 Customers preferences

Before the personalization takes place, the preferences for the collections are inferred using TaxoCatalog’s processing layer. This inference is based on the preferences shown for the dependencies. The resulting preferences for collections, are listed in Table 1.

In addition to the mediator concepts, the customer preferences are used in TaxoCatalog as BK. The customers considered (ID = 1, 2, 3) have shown the preferences listed in Table 2.

Table 1: Customers (ID = 1, 2, 3) inferred preference regarding collections (degree 1 = low, degree 2 = medium, degree 3 = high)

Collection (ID, Label)	ID = 1 (degree)	ID = 2 (degree)	ID = 3 (degree)
11000, Drinking	2	1	2
12000, Meat and seafood	2	2	3
13000, Preparation	2	3	2
14000, Confections	2	1	2

Table 2: Customers (ID = 1, 2, 3)
consulted preferences regarding dependencies
(degree 1 = low, degree 2 = medium, degree 3 = high)

Dependency (ID, Label)	ID = 1 (degree)	ID = 2 (degree)	ID = 3 (degree)
1110, Nonalcoholic Drinks	2	1	1
11120, Hot drinks	2	1	1
11130, Alcoholic drinks	2	1	3
12110, Prepared meats	1	2	3
12210, Seaweed	2	2	3
12220, Fish	1	2	3
13110, Sauces	1	3	1
13120, Spreads	2	3	1
13130, Seasonings	1	3	1
13210, Cheeses	1	3	1
13310, Baked	1	2	2
13320, Grain products	2	2	3
13410, Fruit	1	1	2
13420, Beans	1	1	1
14110, Sweets	1	1	2
14120, Breads	3	1	1

4.2 Catalog personalization

Each path is personalized according to the preferences for the dependencies, for the collections, and the desired volume of personalization. For the case study, it was assumed that $P = M$.

4.2.1 Customer 1

One customer (ID = 1) has medium preferences for all four collections, so the super concepts are used as in the original taxonomy (see Figure 7).

The customer has different preferences for the dependencies. For the six dependencies with medium preferences, the sub-concepts of the initial taxonomy are shown instead of the semantically more general dependency. For the nine dependencies with low preferences, the dependencies are shown instead of the individual sub-concepts. For the one dependency with high preferences, the dependency is shown as well as the individual sub-concepts, resulting in an additional level.

Based on this customer’s preferences, a taxonomy of four levels and 28 concepts was created (Figure 7). Specifically, the semantically personalized taxonomy contains a root concept on level 1, eight super concepts on level 2, nine dependencies and eight sub concepts on level 2, and one sub concept on level 4. Compared to the initial taxonomy, the resulting personalized taxonomy consists of three fewer concepts and one additional level.

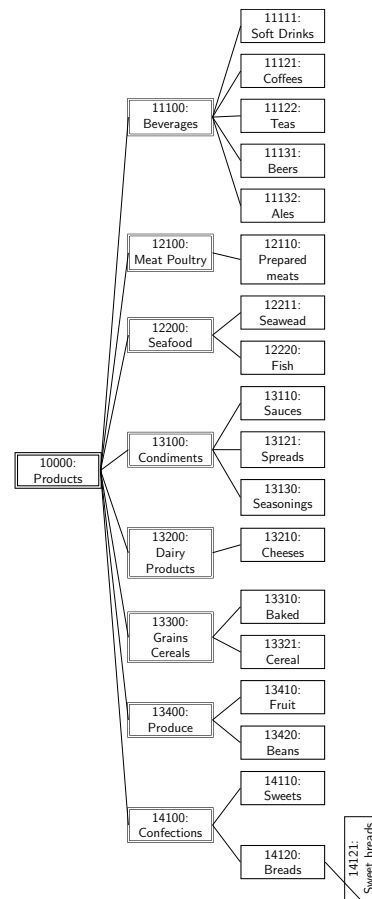


Figure 7: Semantically personalized taxonomy for Customer 1

4.2.2 Customer 2

Another customer (ID = 2) has different preferences for the four collections. For the two low preferred collections, those are shown instead of splitting those into semantically more general super concepts (see Figure 8). The opposite is inferred for the medium preferred collection. For the high preferred collection, the collection is shown, as well as the assigned super concepts. This adds a further level to the personalized taxonomy. For the dependencies, the customer has also heterogeneous preferences. Seven are low preferred; therefore here the dependencies are shown instead of the included sub concepts. Five are medium preferred, so here the sub concepts are shown without the dependencies. The remaining four dependencies are high preferred; this is the reason why those are shown and the sub concepts at a deeper level included. Now, the taxonomy has five levels.

Based on this customer’s preferences, a taxonomy consisting of five levels and 33 concepts was created (Figure 8). In detail, the semantically personalized taxonomy includes one root concept on level 1, three col-

lections and two super concepts on level 2, four super concepts, five dependencies and three sub concepts on level 3, six dependencies and four sub concepts on level 4, as well as finally, five sub concepts on level 5. Compared to the initial taxonomy, the resulting personalized taxonomy consists of two concepts more, and two additional levels.

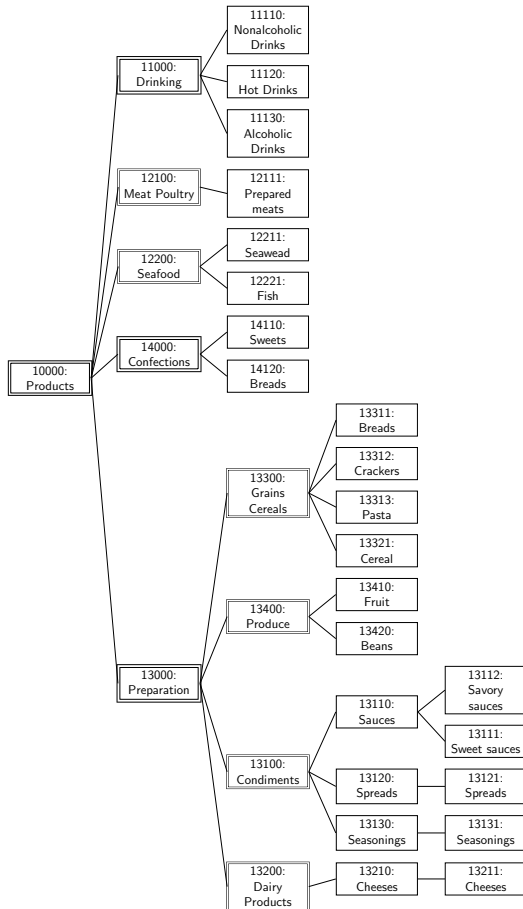


Figure 8: Semantically personalized taxonomy for Customer 2

4.2.3 Customer 3

The last customer (ID = 3) has different preferences for the four collections. For the high preferred collection, it is included in the paths, as well as the super concepts. This adds a further level to the personalized taxonomy (see Figure 9). For the three medium preferred collections, only the super concepts are shown. For the dependencies, the customer has also heterogeneous preferences. Eight are low preferred; therefore, here the dependencies are shown instead of the included semantically more specific sub concepts. Three are medium preferred, so the sub concepts are shown without the dependencies. Five, high preferred, are shown with the included sub concepts at a deeper level. Now, the taxonomy has five levels.

Based on this customer’s preferences, a taxonomy consisting of five levels and 34 concepts was created (Figure 9). In detail, the semantically personalized taxonomy includes one root concept on level 1, one collection and six super concepts on level 2, two super concepts, ten dependencies and three sub concepts on level 3, three dependencies and five sub concepts on level 4, and finally, three sub concepts on level 5. Compared to the initial taxonomy, the resulting personalized taxonomy consists of three concepts more, and two additional levels.

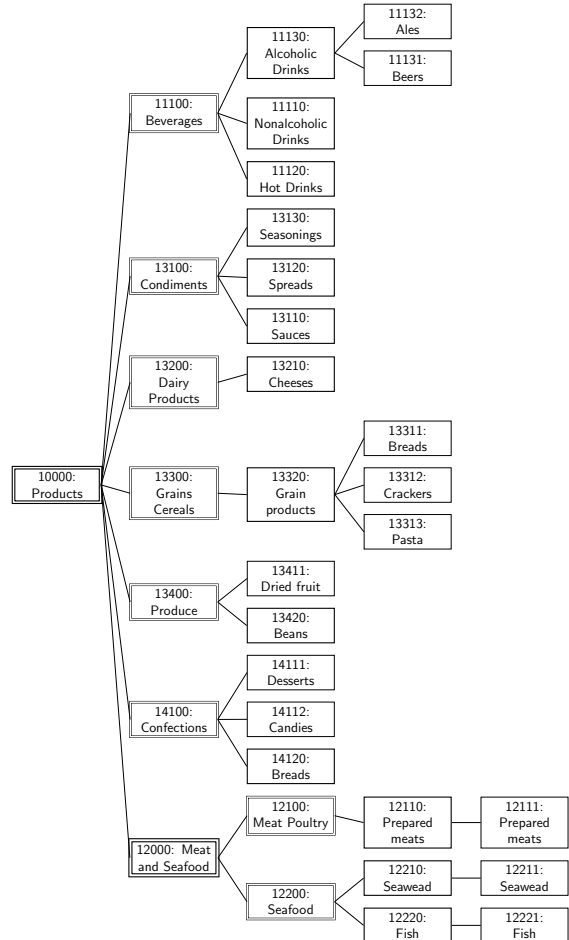


Figure 9: Semantically personalized taxonomy for Customer 3

4.3 Layout setting

The three personalized taxonomies are exported by TaxoCatalog as XML files. These files can be used for automatic layout generation using data-driven publishing software. For this project, the layout generator from the German software provider InBetween is used. All three files can be imported without any modifications compared to other XML files. The same template can be used for all customers, or an independent template can be created (see Figure 10). The template includes content frames with a query. In our example,

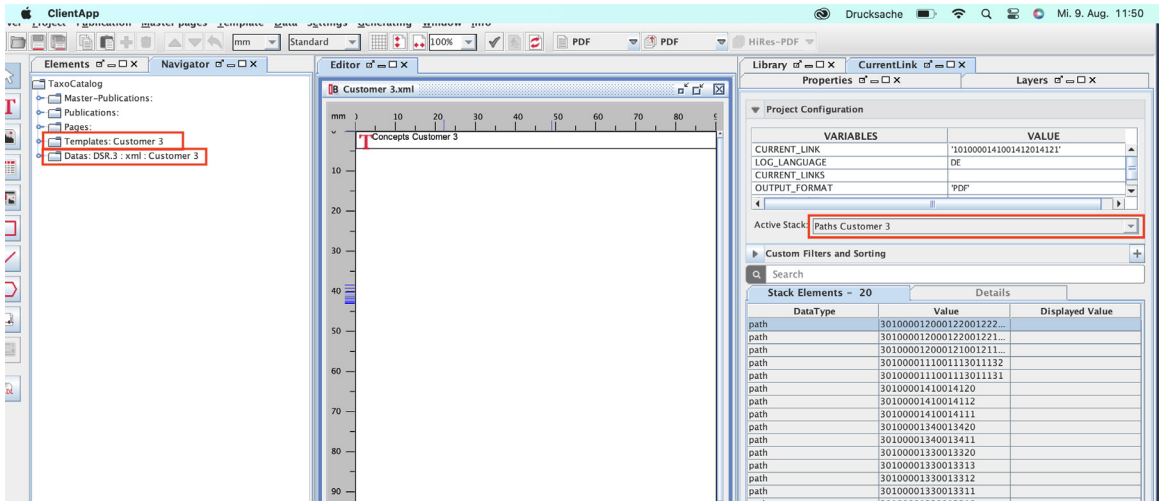


Figure 10: GUI of InBetween for layout setting using the XML output of TaxoCatalog

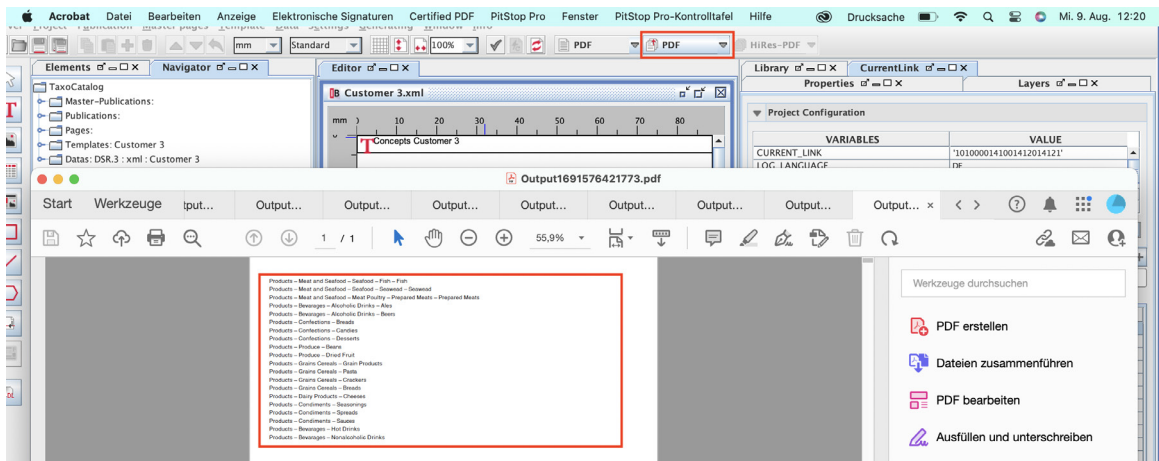


Figure 11: Dynamically generated publication using TaxoCatalog and InBetween

Scottish Longbreads
 12.5 EUR 10 boxes x 8 pieces

Pavlova HIGHLIGHT: This is an exemplary text describing how to use this particular product.
 17.45 EUR 32 - 500 g boxes
This is an exemplary product description.

Figure 12: Personalization of product elements depending on semantic context weight

this means querying concepts sequentially using the path-driven stack. Based on the semantic weight of the path, the paths having a deeper level are at the top. Each stack element is queried, which results in the generation of a dynamic publication containing the paths (see Figure 11). Other templates making a separate use of the personalized semantic weights can also be created. This is of course the ultimate usage of TaxoCatalog XML output, but the focus of future research. For example, product information (e.g. gloss) can be included and designed based on the different semantic weights (see Figure 12).

5. Evaluation

The evaluation of rule-based ES is known to be challenging (Ligèza, 2006). This is because ES are designed to automate individual processes as performed by a human domain expert. Consequently, the quality of the ES is highly dependent on the expert. And, the implementation of the ES is usually done by using BK. Obviously, the quantity and quality of the BK used has a significant impact on the quality of the inference. To address the above aspects, the ES TaxoCatalog is evaluated in five directions:

- First, a comparison with previous studies for the research paradigm of taxonomy personalization including taxonomy modification is performed. This comparison examines the strengths and limitations of prior research efforts to give context of the proposed ES TaxoCatalog.
- Next, the BK efficiency is measured to check whether the BK used most effectively supports the methods contained in TaxoCatalog. As the BK is provided as output from other systems, a summary of the results is presented as a basis for evaluation.
- Based on above, the catalog modification efficiency of the ES TaxoCatalog is discussed to identify if the included modification rules effectively support personalizing a paper-based catalog.
- Following, the workflow integration efficiency of TaxoCatalog is discussed to determine if the ES can be integrated into existing print media workflows without changing those workflows.
- Finally, the catalog personalization efficiency of TaxoCatalog is discussed to verify how the semantically personalized taxonomies are recently used by the system and how the semantically personalized taxonomies could also be used in terms of layout setting. Consequently, this discussion will reveal open directions for future research of the proposed expert system.

5.1 Comparison with previous studies

The comparison with previous studies examines the strengths and limitations of prior research efforts to give context of TaxoCatalog. Consequently, previous studies are discussed, which focus on the aspect of taxonomy personalization and modification.

The very first study discussing the need for taxonomy modification was presented in Joh and Lee (2003). The core element of the Prolog-based implementation is different taxonomy modification rules that have to be performed manually by a user. A study discussing the need of intelligent-driven modification was presented in Lin and Hong (2008). Here, a database model collects knowledge about the customer and the taxonomy, to help the expert manually generating new taxonomies. Two similar frameworks, but with the capability to analyze about the customers and the taxonomy, were presented in Pierrakos and Paliouras (2010), and Tao, Li and Zhong (2011). In 2015, the need of preference-based taxonomy was additionally discussed in Svee and Zdravkovic (2015), before the first work allowing a fully-automatic modification and personalization was presented in Angermann and Ramzan (2016). Here, an ES implemented in Prolog was provided. This ES is able to analyze customers shopping behavior for personalizing the taxonomy based on predefined modification rules. In addition to earlier approaches, the ES is additionally capable to consider the semantics of the taxonomy. This means that the information remains semantically consistent after modifying the taxonomy, by using so-called mediator concepts instead of only limiting the modification to the initial concepts. Analogous to all other above-mentioned studies, their ES is aimed for e-catalogs, meaning the modification of taxonomies to be used for digital publishing channels, especially e-commerce. This is the same for the subsequent work presented in Mao, et. al (2020). Here, a framework was presented that can enrich the taxonomy based on self-supervision. And, it is the same for the work presented in Pawlowski (2021). Here, a ML approach was presented to analyze customers word usage for personalizing the labels of the concepts inside the initial taxonomy. The very last study, and the first study discussing the need of personalizing taxonomies for non-digital channels as well, was presented in Angermann (2022). This work includes a set of different modification rules to modify the taxono-

Table 3: Phases and works on taxonomy personalization and modification

Phase	Description	Manual/ Automatic	References
1	Taxonomy modification rules	Manual	(Joh and Lee, 2003) (Angermann, 2022)
2	Taxonomy personalization using taxonomy modification rules	Manual	(Lin and Hong, 2008) (Pierrakos and Paliouras, 2010) (Tao, Li and Zhong, 2011)
3	Taxonomy personalization using taxonomy modification rules inside intelligent expert systems	Automatic	(Angermann and Ramzan, 2016) (Mao, et al., 2020) (Pawlowski, 2021)
4	Taxonomy personalization for different channels using taxonomy modification rules	Automatic	(Angermann, 2023a) TaxoCatalog

mies based on the capabilities of the different channels. In contrast to other works, the rule-based approach includes various interchangeable modifications, as well as the capability of mediator concepts. However, it has to be performed manually.

Summarizing the different previous studies on taxonomy personalization and modification, four phases or research can be identified (Table 3). In the first phase, the focus was on providing taxonomy modification rules that have to be performed manually. In the second phase, the focus was still on modifying taxonomies manually, but based on knowledge about the customers. In the third phase, user behavior and modification rules were combined to allow a fully-automatic personalization using intelligent systems. TaxoCatalog can therefore be considered as the fourth phase building upon the three previous phases of research on taxonomy modification and personalization. It performs taxonomy modification rules fully automatically based on the capabilities of phase three, but is implemented to perform in a cross-media context.

5.2 Background knowledge efficiency

The BK efficiency used in TaxoCatalog was evaluated with regard to a wide range of criteria and databases (see Table 4). Results for the two most relevant metrics are summarized in this section. These are the *F*-measure of the memory-based BK, and the semantic flexibility efficiency of the content-based BK regarding semantic correspondences.

The *F*-measure score indicates the decision quality of a recommender system for analyzing customer preferences compared to a human domain expert. A score of 1 means that the correct decision was made in all test cases. A score of 0 means the opposite. The average *F*-measure score of the memory-based BK used in TaxoCatalog is 0.94 for all three databases (Angermann and Ramzan, 2016): 0.90 (Northwind), 0.93 (Adventureworks), and 0.98 (Festool). It is particularly noteworthy that the score is similar for all three databases: $\sigma = 0.033$. This means that an equally good quality result can be achieved for a variety of product areas, i.e. for omni-channel retailers in different sectors.

Semantic flexibility efficiency is measured to verify the flexibility of using a taxonomy as the leading element for personalizing a product catalog. Two scores are important here. First, the reduction flexibility is calculated by identifying the maximum possible reduction of the taxonomy. This is done for mediator concepts (collections, dependencies) that are less preferred by a particular customer. Secondly, the extension efficiency is calculated to verify a maximum possible reduction of the taxonomy. This is done for mediator concepts (collections, dependencies) that are highly preferred by the same particular customer. The average reduction flexibility score of the content-based BK used in TaxoCatalog is 48.10 %, and the extension flexibility score is 51.26 % (Angermann, Pervez and Ramzan, 2017).

5.3 Catalog modification efficiency

In TaxoCatalog, the BK mentioned above is used as input for the KB. However, this BK is further processed in a separate IE. Consequently, this IE must also be evaluated. The discussion of its catalog modification efficiency aims at finding out whether the contained modification rules also support the semantic personalization of a paper-based printed product catalog in the most effective way. The discussion presented in this section is therefore the logical application-oriented evaluation based on the qualitative results presented above (see section Comparison with previous studies).

In TaxoCatalog, three path modifications are provided based on the two underlying mediator concept types: dependencies, collections. As each initial taxonomy path always contains both latent mediator concepts, each path can be modified using nine different options. Each mediator concept can be displayed without including the initially assigned concepts, each mediator concept can be hidden and the initially assigned concepts displayed, and each mediator concept can be displayed including the assigned concepts at the deeper level. Consequently, each path can be extended by two levels and by the number of mediator concepts ($N = N + 2$). In this way, all paths that share an *is-a* relationship (sibling concepts) can be combined by their included dependency and collection.

Table 4: Characteristics and parameters of the databases used for experimental results

<i>N</i>	Adventureworks	Northwind	Festool
Customers	700	93	500
Orders	31 464	829	1 400
Products	320	77	118
Concepts (initial)	$1 + 4 + 37 = 42$	$1 + 8 + 22 = 31$	$1 + 9 + 43 = 53$
Dependencies	14	16	23
Collections	2	4	3

Based on the modifications, each individual path is semantically correct on its own due to the external BK used. However, as shown in the case study (see section Catalog personalization), different concept types become concepts of the same level through the implemented rules. This leads to conceptual heterogeneity, even if each path is semantically correct (Angermann, Pervez and Ramzan, 2017). This is the case when concepts with different semantic weights are displayed at the same level. Whether this is actually a challenge for the customer would need to be examined separately in a user study.

5.4 Workflow integration efficiency

The use of TaxoCatalog promotes the linking of portal-based media, paper-based digital media and print media. But it does mean that new software has to be integrated into an existing workflow.

The discussion of workflow integration aims to determine whether the ES can be integrated into existing workflows without having to adapt these workflows. This is important because workflows in the printing industry can be complex, depending on variables such as product variety, technical heterogeneity and the degree of automation of the processes involved (Hofmann-Walbeck, 2022). The following discussion assumes that catalogs are printed using non-impact printing.

Firstly, the TaxoCatalog ES can be implemented in existing workflows without the need to adapt processes. This is the case for upstream and downstream processes that are set up as state of the art for publishing content in an omni-channel context. There are two main reasons for this. Firstly, TaxoCatalog uses external BK and knowledge as provided by the latest omni-channel publishing IT infrastructures. This is media-neutral data provided by a PIM system. Secondly, TaxoCatalog transforms the paths into the standard file format required for data-driven publishing. This is achieved by transforming them into XML format.

However, the ES assumes that the given workflow is as shown above. In other words, the ES requires structured, media-neutral data as provided by a PIM. And it assumes that the subsequent page-layout process is actually performed using data-driven publishing. If one of these aspects (structured data, data-driven publishing) is not taken into account in the workflow, it will not be supported. For example, if DTP is used instead.

5.5 Catalog personalization efficiency

The aim of TaxoCatalog is to provide an ES for semantically personalizing paper-based product catalogs in

omni-channel context using BK. Finally, its catalog personalization efficiency is discussed with respect to real retail scenarios.

Regardless of the media channel used (digital portal-based, digital paper-based, printed paper-based), in most cases the ultimate element for structuring the content to be included in a particular product catalog is the underlying product taxonomy. On an e-commerce site as well as for a printed catalog, the (identical) taxonomy is used as the main element for navigation and structuring. As a result, products are displayed in the corresponding catalog sections. This is because products are assigned to the concepts (product categories) of the taxonomy as so-called members – for example, on category-specific landing pages on an e-commerce site, or on category-specific pages in a printed product catalog. For this reason, the taxonomy is also the leading element when it comes to automatically setting the layout of paper-based product catalogs using data-driven publishing.

TaxoCatalog is used to perform semantic personalization, as mentioned above. This means that the initial product taxonomy is semantically personalized based on BK. This is knowledge about the customer and other knowledge about the initial taxonomy. The BK is used to combine, split and expand product categories according to the individual's preferences. As a result, the personalized catalog is structured according to these specific individual preferences. Thus, from a semantic point of view, even the most essential element of a catalog is personalized to the maximum extent that can be achieved with the help of TaxoCatalog. However, this personalization may not be enough for the customer. While the taxonomy is the essential element from a semantic point of view, the personalization of the content can be a compelling criterion for the customer in terms of personalization based on preferences.

In this regard, semantic context weighting will play a crucial role in subsequent research work. TaxoCatalog is not only designed to personalize taxonomies. It is also designed to personalize content using the personalized taxonomies. In concrete terms, this means that elements from a set of product information can be displayed in the catalog or not, depending on the semantic context weight. For example: a path that has been semantically enriched to the highest level will show products with all available information (e.g. title, description, price, sample application) and will also be highlighted by design. In contrast, a path that has been semantically reduced to the highest level shows only selected information (e.g. title, price). A corresponding example is already shown in this study (see section Layout setting). This potential will be explored in more detail in a later research project.

6. Conclusions

This work presented TaxoCatalog, an expert system for semantically personalizing paper-based product catalogs in an omni-channel retail context using background knowledge. Compared to the method of sub-catalogs, the presented expert system performs the personalization without any loss of information. This is achieved by using different sources of background knowledge and by applying different modification rules based on this background knowledge. The evaluation performed in different directions underlines the efficiency of the presented expert system – in terms of catalog modifica-

tion efficiency, workflow integration efficiency and catalog personalization efficiency. Compared to previous studies in the field, TaxoCatalog works fully automatically, without suffering from information loss, and can be used across publishing channels. On the basis of the extensive evaluations and the included case study, two main directions for future research could have been identified. Firstly, the resulting conceptual heterogeneity can be investigated in a user study. Secondly, the personalization of product information based on the proposed system should be further investigated. Here, the resulting semantic context weight can be used as a main starting point for future research projects.

Acknowledgements

Thanks to the Festool GmbH & Co. KG and the InBetween Deutschland GmbH for providing data and software for the presented research.

References

- Alexander, B. and Kent, A., 2022. Change in technology-enabled omnichannel customer experiences in-store. *Journal of Retailing and Consumer Services*, 65: 102338. <https://doi.org/10.1016/j.jretconser.2020.102338>.
- Ambrose, G., Harris, P. and Ball, N., 2019. *The fundamentals of graphic design*. 2nd ed. London: Bloomsbury Publishing.
- Angermann, H. and Ramzan, N., 2016. TaxoPublish: towards a solution to automatically personalize taxonomies in e-catalogs. *Expert Systems with Applications*, 66, pp. 76–94. <https://doi.org/10.1016/j.eswa.2016.08.058>.
- Angermann, H., and Ramzan, N., 2017. *Taxonomy matching using background knowledge: linked data, semantic web and heterogeneous repositories*. Cham: Springer.
- Angermann, H., Pervez, Z. and Ramzan, N., 2017. Taxo-Semantics: assessing similarity between multi-word expressions for extending e-catalogs. *Decision Support Systems*, 98, pp. 10–25. <https://doi.org/10.1016/j.dss.2017.04.001>.
- Angermann, H., 2017. *Manager's guide to SharePoint server 2016: tutorials, solutions, and best practices*. New York: Apress Media/Springer.
- Angermann, H. (2022). TaxoMulti: rule-based expert system to customize product taxonomies for multi-channel e-commerce. *SN Computer Science*, 3(2): 177. <https://doi.org/10.1007/s42979-022-01070-8>.
- Angermann, H., 2023a. TaxoCatalog: costless workflow integration of an expert system environment to personalize product catalogs in omni-channel context. In: C. Ridgway, ed. *Advances in Printing and Media Technology: Proceedings of the 49th Research Conference of iarigai*. Wuppertal, Germany, 18–20 September 2023. Darmstadt: iarigai.
- Angermann, H., 2023b. Interaction design for print media – Teaching print media workflows by emphasizing the great diversity of print media products. In: A. Politis, ed. *Proceedings of the 54th Scientific Conference of the International Circle of Graphic-Media Technology and Management*. Wuppertal, Germany, 18–20 September 2023. Athens, Greece: HELGRAMED.
- Asmare, A. and Zewdie, S., 2022. Omnichannel retailing strategy: a systematic review. *The International Review of Retail, Distribution and Consumer Research*, 32(1), pp. 59–79. <https://doi.org/10.1080/09593969.2021.2024447>
- Beck, N. and Rygl, D., 2015. Categorization of multiple channel retailing in multi-, cross-, and omni-channel retailing for retailers and retailing. *Journal of Retailing and Consumer Services*, 27, pp. 170–178. <https://doi.org/10.1016/j.jretconser.2015.08.001>.
- Behera, R.K., Gunasekaran, A., Gupta, S., Kamboj, S. and Bala, P.K., 2020. Personalized digital marketing recommender engine. *Journal of Retailing and Consumer Services*, 53: 101799. <https://doi.org/10.1016/j.jretconser.2019.03.026>.
- Bellinger, G., Castro, D., and Mills, A., 2004. *Data, information, knowledge, and wisdom*. [online] Available at: <<http://www.systems-thinking.org/dikw/dikw.htm>> [Accessed July 2023].
- Ben-David, A. and Frank, E., 2009. Accuracy of machine learning models versus “hand crafted” expert systems – a credit scoring case study. *Expert Systems with Applications*, 36(3), pp. 5264–5271. <https://doi.org/10.1016/j.eswa.2008.06.071>.
- Bramer, M., 2005. *Logic programming with Prolog*. Berlin: Springer Science+Business Media.
- Chen, J., Dong, H., Wang, X., Feng, F., Wang, M. and He, X., 2023. Bias and debias in recommender system: a survey and future directions. *ACM Transactions on Information Systems*, 41(3): 67. <https://doi.org/10.1145/3564284>.

- Cook, G., 2014. Customer experience in the omni-channel world and the challenges and opportunities this presents. *Journal of Direct, Data and Digital Marketing Practice*, 15(4), pp. 262–266. <https://doi.org/10.1057/dddmp.2014.16>.
- de Melo, T., da Silva, A.S., de Moura, E.S. and Calado, P., 2019. *OpinionLink: leveraging user opinions for product catalog enrichment. Information Processing & Management*, 56(3), pp. 823–843. <https://doi.org/10.1016/j.ipm.2019.01.004>.
- Desrosiers, C. and Karypis, G., 2010. A comprehensive survey of neighborhood-based recommendation methods. In: F. Ricci, L. Rokach, B. Shapira and P.B. Kantor, eds. *Recommender systems handbook*. New York: Springer Science+Business Media, pp. 107–144.
- Gao, L.(X.), Melero, I. and Sese, F.J., 2020. Multichannel integration along the customer journey: a systematic review and research agenda. *The Service Industries Journal*, 40(15–16), pp. 1087–1118. <https://doi.org/10.1080/02642069.2019.1652600>.
- Gündoğan, E., 2022. *Robotic Process Automation im Desktop-Publishing: Eine Einführung in softwaregestützte Automatisierung von Artwork-Processen*. Wiesbaden: Springer.
- Hagberg, J., Sundstrom, M. and Egels-Zandén, N., 2016. The digitalization of retailing: an exploratory framework. *International Journal of Retail & Distribution Management*, 44(7), pp. 694–712. <https://doi.org/10.1108/IJRDM-09-2015-0140>.
- Hänninen, M., Kwan, S.K. and Mitronen, L., 2021. From the store to omnichannel retail: looking back over three decades of research. *The International Review of Retail, Distribution and Consumer Research*, 31(1), pp. 1–35. <https://doi.org/10.1080/09593969.2020.1833961>.
- Herhausen, D., Kleinlercher, K., Verhoef, P.C., Emrich, O. and Rudolph, T., 2019. Loyalty formation for different customer journey segments. *Journal of Retailing*, 95(3), pp. 9–29. <https://doi.org/10.1016/j.jretai.2019.05.001>.
- Hoffmann-Walbeck, T., 2022. *Workflow automation: basic concepts of workflow automation in the graphic industry*. Cham: Springer Nature.
- Hübner, A., Wollenburg, J. and Holzapfel, A., 2016. Retail logistics in the transition from multi-channel to omni-channel. *International Journal of Physical Distribution & Logistics Management*, 46(6/7), pp. 562–583. <https://doi.org/10.1108/IJPDLM-08-2015-0179>.
- Hübner, A., Amorim, P., Fransoo, J.C., Honhon, D., Kuhn, H., Martinez de Albeniz, V. and Robb, D., 2021. Digitalization and omnichannel retailing: innovative OR approaches for retail operations. *European Journal of Operational Research*, 294(3), pp. 817–819. <https://doi.org/10.1016/j.ejor.2021.04.049>.
- Jocevski, M., Arvidsson, N., Miragliotta, G., Ghezzi, A. and Mangiaracina, R., 2019. Transitions towards omni-channel retailing strategies: a business model perspective. *International Journal of Retail & Distribution Management*, 47(2), pp. 78–93. <https://doi.org/10.1108/IJRDM-08-2018-0176>.
- Joh, Y.H. and Lee, J.K., 2003. Buyer's customized directory management over sellers' e-catalogs: logic programming approach. *Decision Support Systems*, 34(2), pp. 197–212. [https://doi.org/10.1016/S0167-9236\(02\)00081-7](https://doi.org/10.1016/S0167-9236(02)00081-7).
- Langley, P., 2011. The changing science of machine learning. *Machine Learning*, 82(3), pp. 275–279. <https://doi.org/10.1007/s10994-011-5242-y>.
- Lin, C. and Hong, C., 2008. Using customer knowledge in designing electronic catalog. *Expert Systems with Applications*, 34(1), pp. 119–127. <https://doi.org/10.1016/j.eswa.2006.08.028>.
- Lin, X., 2006. Active layout engine: algorithms and applications in variable data printing. *Computer-Aided Design*, 38(5), pp. 444–456. <https://doi.org/10.1016/j.cad.2005.11.006>.
- Li, Z., Wang, D., Yang, W. and Jin, H. S., 2022. Price, online coupon, and store service effort decisions under different omnichannel retailing models. *Journal of Retailing and Consumer Services*, 64: 102787. <https://doi.org/10.1016/j.jretconser.2021.102787>.
- Ligêza, A., 2006. *Logical foundations for rule-based systems*. 2nd ed. Heidelberg: Springer.
- Mao, Y., Zhao, T., Kan, A., Zhang, C., Dong, X.L., Faloutsos, C. and Han, J., 2020. Octet: online catalog taxonomy enrichment with self-supervision. In: *KDD '20 Proceedings of the 26th ACM SIGKDD International Conference on Knowledge Discovery & Data Mining*. Virtual event, CA, USA, 6–10 July, 2020. New York: ACM, pp. 2247–2257. <https://doi.org/10.1145/3394486.3403274>.
- Mark, T., Bulla, J., Niraj, R., Bulla, I. and Schwarzwäller, W., 2019. Catalogue as a tool for reinforcing habits: empirical evidence from a multichannel retailer. *International Journal of Research in Marketing*, 36(4), pp. 528–541. <https://doi.org/10.1016/j.ijresmar.2019.01.009>.
- Merritt, D., 2012. *Building expert systems in Prolog*. New York: Springer Science+Business Media.
- Mirmozaffari, M., 2019. Developing an expert system for diagnosing liver diseases. *European Journal of Engineering and Technology Research*, 4(3), pp. 1–5. <https://doi.org/10.24018/ejeng.2019.4.3.1168>.
- NorthWind, 2017. *NorthWind*. [online] Available at: <<https://github.com/cjlee/northwind>> [Accessed July 2023].
- Norvell, T., Kumar, P. and Contractor, S., 2018. Assessing the customer-based impact of up-selling versus down-selling. *Cornell Hospitality Quarterly*, 59(3), pp. 215–227. <https://doi.org/10.1177/1938965518762836>.
- Oleshchuk, V. and Fensli, R., 2011. Remote patient monitoring within a future 5G infrastructure. *Wireless Personal Communications*, 57(3), pp. 431–439. <https://doi.org/10.1007/s11277-010-0078-5>.

- Pawlowski, P., 2021. Non-deterministic logic of informal provability has no finite characterization. *Journal of Logic Language and Information*, 30(4), pp. 805–817. <https://doi.org/10.1007/s10849-021-09344-9>.
- Pierrakos, D. and Paliouras, G., 2009. Personalizing web directories with the aid of web usage data. *IEEE Transactions on Knowledge and Data Engineering*, 22(9), pp. 1331–1344. <https://doi.org/10.1109/TKDE.2009.173>.
- Roy, D. and Dutta, M., 2022. A systematic review and research perspective on recommender systems. *Journal of Big Data*, 9(1): 59. <https://doi.org/10.1186/s40537-022-00592-5>.
- Svee, E.-O. and Zdravkovic, J., 2015. Towards a consumer preference-based taxonomy for information systems development. In: R. Matulevičius and M. Dumas, eds. *Perspectives in Business Informatics Research: 14th International Conference, BIR 2015, Proceedings*. Tartu, Estonia, 26–28 August, 2015. Cham: Springer International Publishing, pp. 213–227. https://doi.org/10.1007/978-3-319-21915-8_14.
- Tao, X., Li, Y. and Zhong, N., 2011. A personalized ontology model for web information gathering. *IEEE Transactions on Knowledge and Data Engineering*, 23(4), pp. 496–511. <https://doi.org/10.1109/TKDE.2010.145>.
- van der Aalst, W.M.P., Bichler, M. and Heinzl, A., 2018. Robotic process automation. *Business & Information System Engineering*, 60(4), pp. 269–272. <https://doi.org/10.1007/s12599-018-0542-4>.
- van der Vlist, E., 2002. *XML schema: the W3C's object-oriented descriptions for XML*. Sebastopol, CA: O'Reilly Media.
- Van Nguyen, A.T., McClelland, R. and Thuan, N.H., 2022. Exploring customer experience during channel switching in omnichannel retailing context: a qualitative assessment. *Journal of Retailing and Consumer Services*, 64: 102803. <https://doi.org/10.1016/j.jretconser.2021.102803>.
- Verhoef, P.C., Kannan, P.K. and Inman, J.J., 2015. From multi-channel retailing to omni-channel retailing: introduction to the special issue on multi-channel retailing. *Journal of Retailing*, 91(2), pp. 174–181. <https://doi.org/10.1016/j.jretai.2015.02.005>.
- Xu, Z., Du, D. and Xu, D., 2014. Improved approximation algorithms for the max-bisection and the disjoint 2-catalog segmentation problems. *Journal of Combinatorial Optimization*, 27(2), pp. 315–327. <https://doi.org/10.1007/s10878-012-9526-3>.
- Yrjölä, M., Saarijärvi, H. and Nummela, H., 2018. The value propositions of multi-, cross-, and omni-channel retailing. *International Journal of Retail & Distribution Management*, 46(11–12), pp. 1133–1152. <https://doi.org/10.1108/IJRDM-08-2017-0167>.



JPMTR-2309
DOI 10.14622/JPMTR-2309
UDC 655.535.2:303.54:001.8-027.511

Research paper | 186
Received: 2023-07-25
Accepted: 2023-12-13

Global trends in the study of projection mapping technology using bibliometric analysis

Intan Permata Sari, Agus Juhana and Nurhidayatulloh Nurhidayatulloh

Multimedia Education Study Program,
Universitas Pendidikan Indonesia, Bandung, Indonesia

intanpermatasari@upi.edu
agus.juhana@upi.edu
nurhidayatulloh@upi.edu

Abstract

Projection mapping has emerged as a compelling new medium, experiencing continual growth due to technological innovations across diverse fields, including medicine, communication, and science. Consequently, the volume of articles addressing technological advancements in projection mapping has surged over the past two decades. This article conducts a comprehensive bibliometric analysis on projection mapping technology, employing statistical and publication characteristic analyses to offer insights into research progress and trends spanning from 2003 to 2022. The results, based on 440 documents (journal articles, conference papers, book chapters, conference reviews, reviews, and books) retrieved from the Scopus database on February 9, 2023, indicate a consistent increase in publications on projection mapping technology, although research remains somewhat limited. Utilizing VOSviewer, Microsoft Excel, and Tableau Public, the bibliometric analysis unveils notable authors in the field, highlighting metrics such as the number of citations, country productivity, and key periodicals publishing projection mapping technology content. Iwai, D., from Osaka University emerges as the most prolific author on projection mapping technology, while Ishikawa, M., stands out as the researcher with the highest citation frequency. Japan is identified as the most productive and cited country of origin for researchers in this domain. Notably, "IEEE Transactions on Visualization and Computer Graphics" holds significant influence, having the highest citation count and serving as a vital reference source. Empirical researchers can leverage articles from this journal to track the evolving research topics in projection mapping technology year by year.

Keywords: research trend, bibliometric analysis, Scopus database, citation

1. Introduction

Projection mapping is a novel medium capable of projecting optical illusion content in the form of images or videos onto various surfaces, including buildings, facades, structures, and complex 3D surfaces (Rodriguez, et al., 2015). Projection mapping has the potential to transform visual perception into something more captivating (Fujimoto, 2018). The concept of projection mapping continues to evolve, enabling users to interact directly with the mapping results; this is commonly referred to as interactive projection mapping. The rapid development of physical processing technologies, such as electronics, sensors, and digital projections, creates an immersive experience through projection mapping that enhances the user's comprehension and retention of the presented content (Nofal, et al., 2018). By combining technology and art,

projection mapping can stimulate visual perception and enable users to physically interact with the content (Krautsack, 2011).

Projection mapping enhances user engagement by creating a very immersive and participatory experience. Visual stimulation has the capacity to captivate, amuse, and convey fascinating knowledge (Krautsack, 2011). An immersive experience refers to a situation when the consumer experiences a deep sense of connection and integration with the technology being utilized (Handa, Aul and Bajaj, 2012). Immersive technology, which merges the boundaries between the physical and virtual realms, enables consumers to indulge in a delightful digital encounter. Immersive technologies encompass augmented reality (AR), virtual reality (VR), mixed reality (MR), and extended reality (XR) (Hein, Wienrich and Latoschik, 2021). Immersive tech-

nology allows users to actively participate in genuine explorations of the real world, making complicated subjects easier to understand. Additionally, immersive technology can motivate users to improve their abilities (Suzanna and Lumban Gaol, 2021).

A significant amount of research and development has been focused on studying projection mapping technology as a means of implementing recent breakthroughs in new media. Based on the studies conducted by Rodriguez, et al. (2015), Fujimoto (2018), Krautsack (2011), Degner, Moser and Lewalter (2022), and Nofal, et al. (2018), it can be inferred that no research has utilized bibliometric analysis methods in the domain of projection mapping. Projection mapping has emerged as a prominent immersive technology in the ongoing development of new media. The authors aim to comprehend the scope and advancement of projection mapping research, prevailing worldwide research patterns, and the prospects for future research expansion in this domain. Hence, it is important to consult scientific literature in order to ascertain any shortcomings in the field of projection mapping study. The aim of this analytical study is to present scientific literature using bibliometric analysis approaches related to projection mapping technology. The research topics examined in this analysis are as follows:

RQ 1: Who are the influential authors in projection mapping technology research?

RQ 2: Which nations frequently conduct research on projection mapping technology, and what outputs do they produce?

RQ 3: Which projection mapping technologies have been the subject of research?

2. Methods

The analysis utilized bibliometrics, focusing on evaluating individual and institutional scientific outputs through bibliographic databases (Baker, 1991). Documents for this study were extracted from the Scopus database. Since data mining is conducted on public databases, ethical board approval is unnecessary (Xie, et al., 2020). Scopus was chosen as it is the predominant database used by academics across various multidisciplinary fields for searching journal articles, conference proceedings, and book chapters (Mongeon and Paul-Hus, 2016; Singh, et al., 2021). As illustrated in Figure 1, the authors initiated a search of the Scopus database on February 9, 2023, using keywords (TITLE-ABS-KEY ("projection mapping" OR "video mapping" OR "interactive projection mapping" OR "projection mapping installation") AND (tech* OR "new media" OR "immersive tech*")

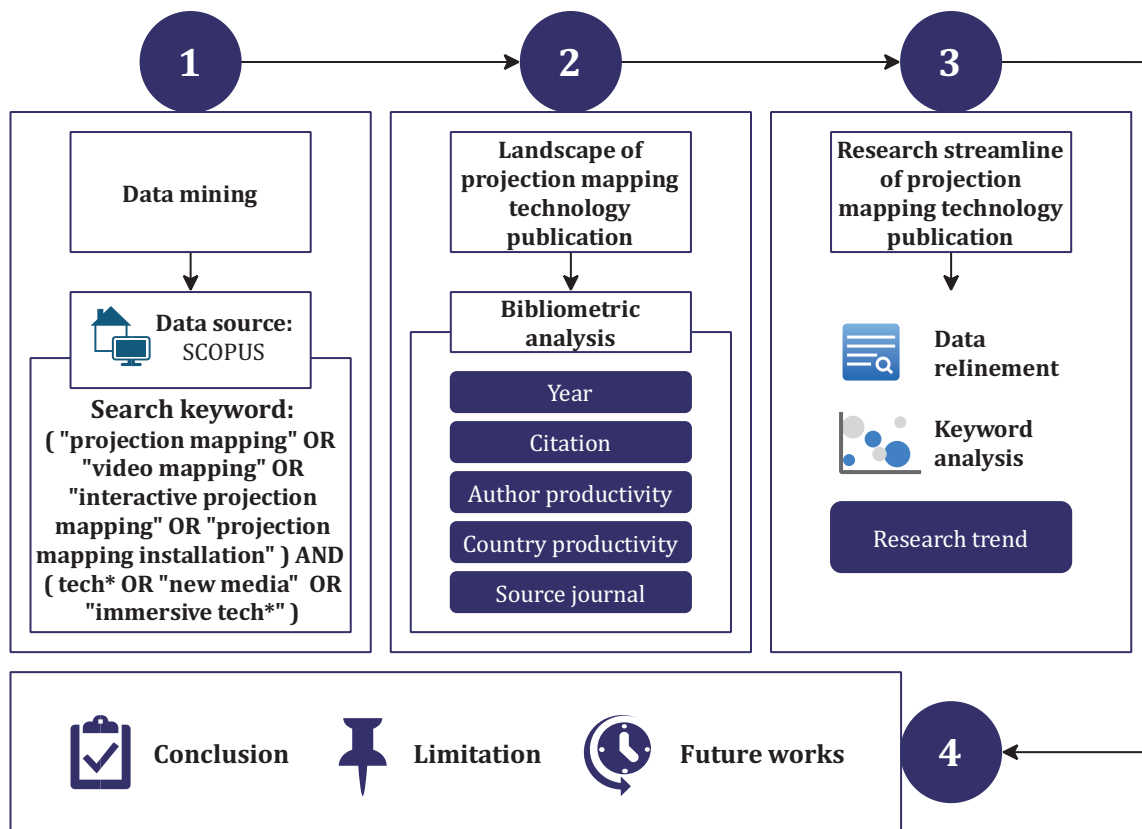


Figure 1: Research method

OR “interactive projection mapping” OR “projection mapping installation”) AND TITLE-ABS-KEY (tech* OR “new media” OR “immersive tech*”)) to identify research developments in projection mapping technology. Beyond trends, numerous intriguing findings requiring visualization and thorough analysis emerged. The data collection on this date yielded 440 documents (180 journal articles, 213 conference papers, 20 book chapters, 16 conference reviews, 8 reviews, and 3 books) on the topic. The metadata for these 440 documents were then downloaded as comma-separated value (CSV) files. This study restricts the search time period to the last 20 years in order to identify the most recent research trends. The literature data sources were limited to the Scopus database. The inclusion of other databases, such as Web of Science or Google Scholar, and other types of documents, such as patents, might have revealed further insights that were not included in this study.

The second stage involves conducting a bibliometric analysis to explore the research landscape of projection mapping technology. VOSviewer, Microsoft Excel, and Tableau Public are utilized for this analysis, focusing on factors such as annual publication trends, citations, author productivity, country productivity, and publications on projection mapping technology. Following the analytical strategy of Qin, et al. (2022), the analysis considers yearly publication trends and citations based on total publications (TP), their total citations (TC), and resulting average citations per publication ($AC = TC/TP$).

The third stage is dedicated to identifying keywords and streamlining research on projection mapping technology. Keywords are identified by analyzing their frequency of use and relationships with one another. Before analysis, author keywords and indexed keywords are refined using Open Refine to reduce bias, preventing the separate counting of keywords with the same meaning. The enhanced database is then used for analysis. The outcomes of this research streamlining analysis will help ascertain thematic evolution and the most recent trends in projection mapping technology research, aiding empirical researchers in identifying research gaps and novelties.

3. Results and discussion

3.1 Landscape of projection mapping technologies publications

3.1.1 Characteristics of projection mapping technology publications

This analysis utilized a total of 440 documents from the Scopus database, containing the searched phrases (see 2. Methods) and covering the time period from 2003 to 2022. An analysis was conducted to study the progression of publications on the topic of projection mapping technology, utilizing metrics including TP, TC, and AC. Figure 2 shows the growth of publications on this topic.

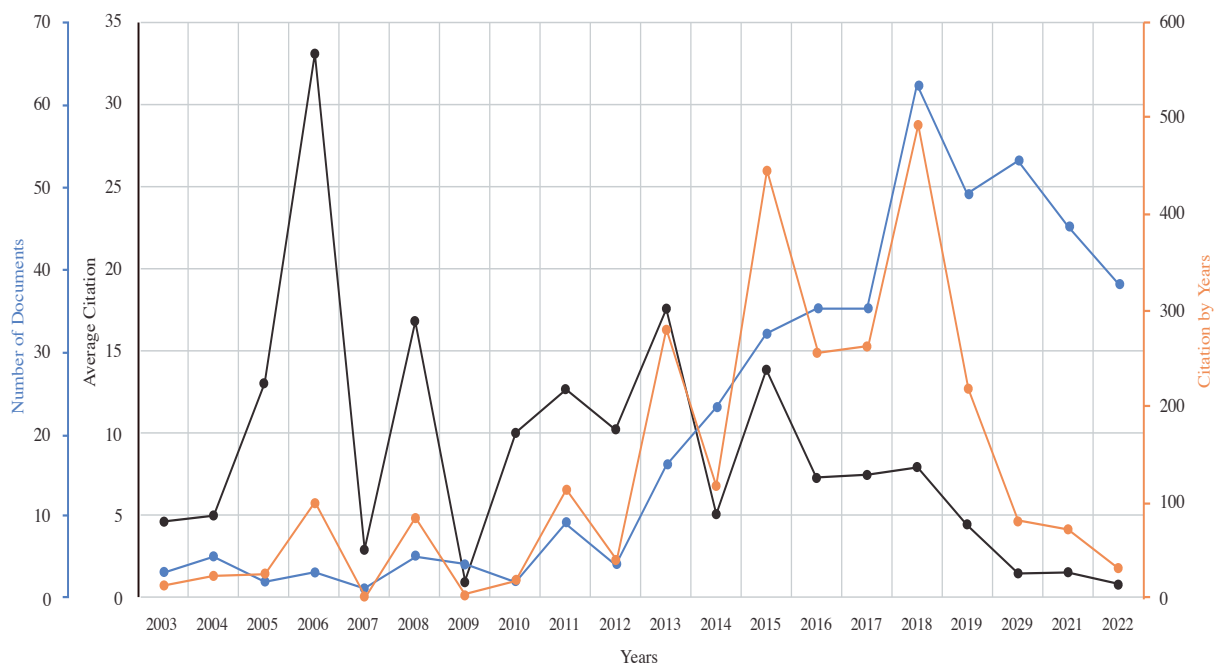


Figure 2: Trend distribution of publications from individual years and their citations in projection mapping technology

Analysis of the data on the number of publications (the blue line in Figure 2) reveals a moderate development of publications on projection mapping technology between 2003 and 2012. However, from 2012 to 2018, the average annual publication count was increasing on average by 95 %, related to the first year of this period. The number of scientific articles on projection mapping technology saw a significant surge between 2017 and 2018, aligning with rapid advancements in the discipline. Post-2018, research on projection mapping technology shows a declining trend, possibly influenced by factors such as the COVID-19 pandemic, which has impacted empirical research and development (Tuttle, 2020; Riccaboni and Verginer, 2022).

Over the last two decades, 440 documents were published, with 388 in the last ten years, indicating that publication productivity in the last decade contributed 88 % of the total during the developmental period of projection mapping technology research. This underscores the rapid development in the field, with an acceleration of research in recent years.

Similarly to the increasing trend in the number of publications, total citations of documents published in individual years (orange line in Figure 2) also show an upward trajectory till 2018. For documents from 2013, there were 280 citations; for those from 2015, the count rose to 444 citations, and for 2018 publications, it reached 492 citations. Researchers worldwide have conducted numerous studies on projection mapping technology in recent years. However, post-2018, the citation trend tends to decrease, possibly due to factors such as a decline in studies related to this topic and a reduced need for references among researchers. Additionally, the average number of citations reached its peak for publications from 2006, with 33.

3.1.2 Characteristics of projection mapping technology publications based on author productivity and number of citations

Scientists, innovators, practitioners, and academics conduct research to discover new things or to test something already in existence so that it can be eval-

Table 1: Top 5 authors by number of documents

Author/ No	Institution	Country	Number of documents	Number of citations
1	Iwai, D./ Osaka University	Japan	20	132
2-3	Hashimoto, N./ The University of Electro-Communications	Japan	13	37
2-3	Sato, K./ Osaka University	Japan	13	82
4	Ishikawa, M./ The University of Tokyo	Japan	12	206
5	Watanabe, Y./ Tokyo Institute of Technology	Japan	10	198

Table 2: Top 5 authors by number of citations

Author/ No	Institution	Country	Number of documents	Number of citations
1	Ishikawa, M./ The University of Tokyo	Japan	12	206
2	Watanabe, Y./ Tokyo Institute of Technology	Japan	10	198
3	Huang, C.-C., Sugino, K., Shima, Y., Guo, C., Bai, S., Mensch, B.D., Nelson, S.B., Hantman, A.W./ Howard Hughes Medical Institute and Brandeis University	United States	1	153
4	Iwai, D./ Osaka University	Japan	20	132
5	Ofek, E./ Microsoft Research Lab – Redmond	United States	2	115

uated and implemented in their respective fields of work. Research publications serve as a chronicle of a specialist's accomplishments. Numerous researchers in the field of projection mapping technology have developed, evaluated, and implemented this concept in various contexts. The authors have compiled a list of researchers whose works have been published and are listed in the Scopus index in order to determine who are the most productive and influential researchers in projection mapping technology research.

In Table 1, the authors are ranked based on the number of published works, with Iwai, D., leading the list with a total of 20 published documents, cited by 132 other works. The second and third positions are held by Hashimoto, N. and Sato, K., both with 13 documents. Sato, K., has 82 citations, while Hashimoto, N., has

37 citations. Notably, Iwai, D., often collaborates with Sato, K., who shares the same affiliation at the Graduate School of Engineering Science, Osaka University, Japan. Their research discusses the latest technologies developed in the field of projection mapping, such as the use of convolutional neural networks (Kageyama, Iwai and Sato, 2022), visuo-haptic augmented reality (VHAR) systems and tactile display control signals (Miyatake, et al., 2021), computational imaging (Iwai, 2019), visual markers for geometric registration (Asayama, Iwai and Sato, 2018), distributed optimization framework (Tsukamoto, Iwai and Kashima, 2017), and monocular projector-camera system (Yamamoto, et al., 2022).

Frequently cited studies often indicate greater influence. In the topic of projection mapping technology research, the authors have compiled a list of the ten

Table 3: Top 10 articles with the highest number of citations

Authors (Year)/ Title	Year	Source title / Quartile	Document type
Huang, et al. (2013)/ Convergence of pontine and proprioceptive streams onto multimodal cerebellar granule cells	2013	eLife / Q1	Article
Pejsa, et. al. (2016)/ Room2Room: Enabling life-size telepresence in a projected augmented reality environment	2016	Proceedings of the ACM Conference on Computer Supported Cooperative Work, CSCW	Conference Paper
Narita, Watanabe and Ishikawa (2017)/ Dynamic projection mapping onto deforming non-rigid surface using deformable dot cluster marker	2017	IEEE Transactions on Visualization and Computer Graphics	Article
Ishikawa, Shimuta and Häusser (2015)/ Multimodal sensory integration in single cerebellar granule cells in vivo	2015	eLife / Q1	Article
Nishino, et al. (2018)/ Real-time navigation for liver surgery using projection mapping with indocyanine green fluorescence: development of the novel medical imaging projection system	2018	Annals of Surgery / Q1	Article
Chee, Arrigoni and Maratos-Flier (2015)/ Melanin-concentrating hormone neurons release glutamate for feedforward inhibition of the lateral septum	2015	Journal of Neuroscience / Q1	Article
Bonaventura, et. al. (2019)/ High-potency ligands for DREADD imaging and activation in rodents and monkeys	2019	Nature Communications / Q1	Article
Chen, et al., (2018)/ Efficient in situ barcode sequencing using padlock probe-based BaristaSeq	2018	Nucleic Acids Research / Q1	Article
Grundhöfer and Iwai (2018)/ Recent advances in projection mapping algorithms, hardware and applications	2018	Computer Graphics Forum / Q1	Article
Rodriguez, et al. (2015)/ Developing a mixed reality assistance system based on projection mapping technology for manual operations at assembly workstations	2015	Procedia Computer Science / Q2	Conference Paper

most frequently cited researchers over the past two decades, presented in Table 2. Serving as a valuable reference for researchers in the field, this table supplements the existing literature. Ishikawa, M., tops the list, cited in 206 other documents based on his 12 publications. His research delves into technological applications in projection mapping, particularly high-speed image processing (Ishikawa, 2014; 2019), high-speed vision (Ishikawa, 2022), high-speed focal tracking projection (Wang, et al., 2020), intelligent imager and GPU (Miyashita and Ishikawa, 2020), MIDAS projection (Miyashita, Watanabe and Ishikawa, 2018), high-speed projector (Mikawa, et al., 2018), dot cluster marker (Narita, Watanabe and Ishikawa, 2017; Watanabe, Kato and Ishikawa, 2017), and mirror-based robust high-speed tracking (Sueishi, Oku and Ishikawa, 2016). Watanabe, Y., has 10 documents that have been cited by 198 other documents, while the authors in third place have 1 document that has been cited by 153 other documents. These authors are incorporated in one document that discusses the use of projection mapping technology in the medical field (Huang, et al., 2013).

Table 3 reveals that the most cited papers are published in Scopus Q1-indexed international journals, indicating that articles in Q1 journals are a primary source for scientific advancement, particularly in the field of projection mapping technology. The size of a

journal cluster correlates with the difficulty of publishing within it, reflecting the caliber of the research and articles. Analyzing a database of research publications on projection mapping technology from 2003 to 2022, the ten articles with the highest citations were published between 2013 and 2019, amassing a total of 832 citations, equivalent to 31 percent of the total citations over the past two decades. Subsequently, we will provide a brief analysis of some of these highly-cited articles on projection mapping technology.

The first among the ten articles with the highest citations was published in 2013 by Huang, et al. (2013), accumulating a total of 153 citations. This article explores the application of projection mapping technology in the medical field, specifically for viewing synaptic resolution cell activity. The second article, published in 2016 by Pejsa, et al. (2016), employs projection mapping as a tool for long-distance teleconferencing, displaying the interlocutor’s object at its actual scale. The investigation utilized three ceiling-mounted camera projector units (procam), projectors, and Kinect. The third article, published by Narita, Watanabe and Ishikawa (2017), addresses a challenge in projection mapping, namely its inability to project onto dynamic objects. The authors propose the use of the deformable dot cluster marker (DDCM) to track non-rigid surfaces at high-speed using high frame rate cameras, enabling

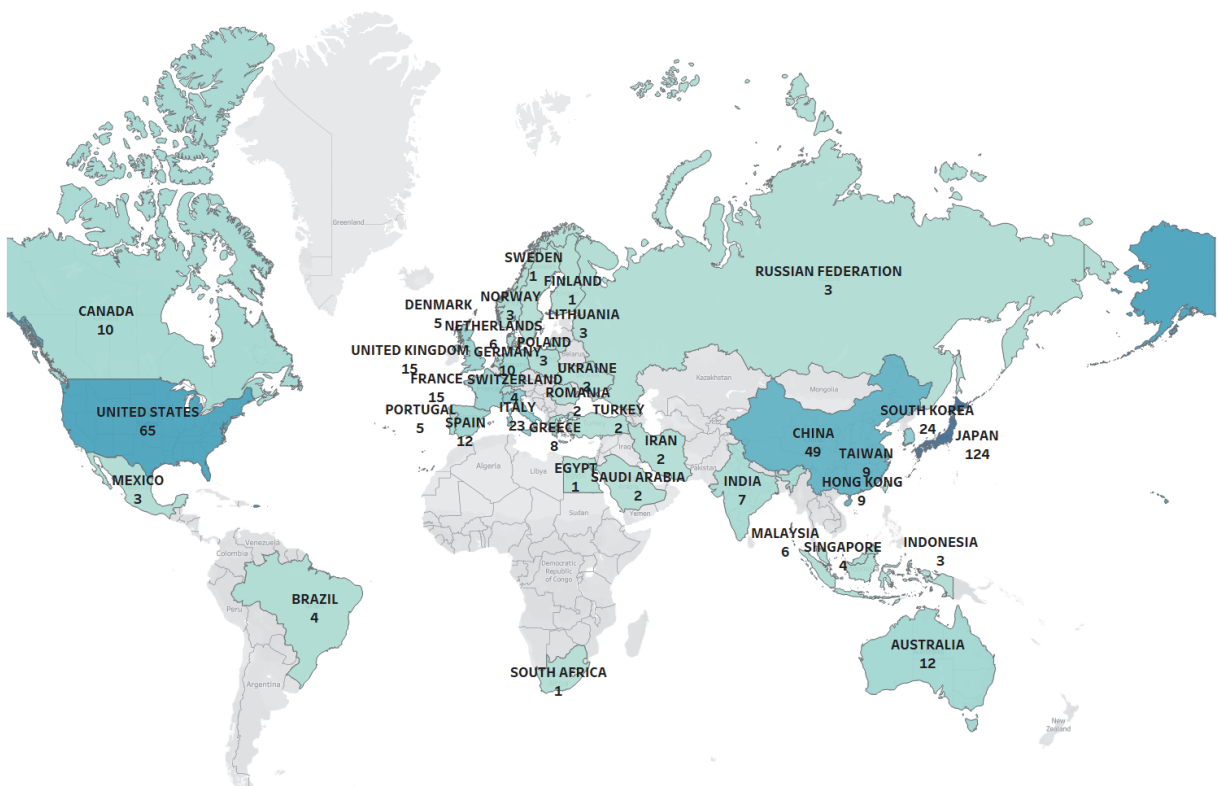


Figure 3: Distribution of the number of documents based on the country of origin of the researcher

that are frequently used as references in research about projection mapping technology.

The journal *IEEE Transactions on Visualization and Computer Graphics* is classified as a Q1 journal. It contains 9 documents that pertain to projection mapping technology. However, it is not as extensive as *Lecture Notes in Computer Science* (including subseries *Lecture Notes in Artificial Intelligence* and *Lecture Notes in Bioinformatics*), which is ranked fifth and has 14 documents. Despite this, the *IEEE Transactions on Visualization and Computer Graphics* journal has received the highest number of citations, specifically 149 citations, compared to *Lecture Notes in Computer Science*, which has only been cited 16 times. The second most often referenced source was the proceedings of the *Conference on Human Factors in Computing Systems*, cited 95 times. Following that, *IEEE Access* was cited 59 times, and the *ACM International Conference Proceedings* series was cited 35 times.

3.2 Research streamline of projection mapping technology publications

Author keyword analysis is a crucial component of bibliometric research as it identifies the most significant research topics (Kumar Kar and Harichandan, 2022).

In this subparagraph, authors present the research process for publications on projection mapping technology, conducting an in-depth analysis of author keywords and current topic trends (see Figure 4).

In Cluster 1, marked in red, additional research focuses on the projection mapping technology tool processing system. Keywords in this cluster include camera, actuator, adaptive control, calibration, slide mode control, stereoscopic device, computational display, digital fabrication, digital projection mapping, human vision, screen correction, digital sculpture, spatially enriched reality, tracking control, high speed, and others.

Cluster 2, denoted in green, emphasizes research on projection mapping related technology and content. Keywords in this cluster encompass 3D construction, animation, photogrammetry, computer graphics, entertainment computing, GPS, VR, MR, projection mapping installation, laser scanning, and transducer sensors, among others.

In projection mapping technology, the interaction between content and technology is crucial. The technology employed influences the content created, resulting in engaging concepts for immersive experiences. An example in this cluster is *OptiSpace*, developed by Fender, et al. (2018), a system used to optimize the positioning of interactive projection mapping con-

tent in a physical environment for human-computer interaction. This reflects research focused on developing interactive systems that utilize projection mapping technology to enhance users' immersive experiences.

In Cluster 3, denoted in cyan, additional research focuses on techniques, maintenance, and interactive tools for developing content on projection mapping media. Keywords in this cluster include 3D modeling, dynamic objects, flexible shapes, projection mapping interactions, interactive surfaces, reverse perspective mapping, motion capture, multi-touch, performance, real-time masking, real interaction, texture mapping, virtual reconstruction, and human-computer interaction.

This cluster represents research that concentrates on the development of interactive techniques for projection mapping. The use of interactive technologies based on projection mapping, such as augmented reality, can result in more precise, stable, and natural information delivery. In the study of Yuan, et al. (2021), an appealing interaction design concept tailored to the intended audience resulted in an enhanced user experience.

The application of dynamic and adaptable projection mapping content is characterized by the use of interactive devices, a defining feature of the new media concept. Utilized interactive devices include motion capture, human-robot interaction, multi-touch, and interactive projection. Techniques and content used in this context include real-time masking, 3D modeling, dynamic objects, flexible forms, texture mapping, etc. *Pmomo*, created by Zhou, et al. (2016), is a prime example of interactive device development. *Pmomo* can project objects in real-time and directly interact with 3D objects in 360 degrees, employing sensors, depth cameras, and tracking algorithms to provide users with an interactive experience.

In Cluster 4, marked in yellow, the research focuses on the implementation of projection mapping in the fields of history and culture. Keywords in this cluster include augmented heritage, audiovisual production, design practices, cultural heritage, museum exhibitions, digital narratives, storytelling, improvement of error-resistant video coding, historical monuments, holographic techniques, mixed media installations, multimedia communications, coding with multiple descriptions, multiple input, multiple output (MIMO) systems, physical computing, and video mapping.

In these studies, projection mapping has been implemented in informal spaces such as museums and historical monuments to introduce knowledge about cultural and historical heritage. This is achieved through projection mapping installations or mixed media installa-

tions, applying audiovisual content, digital narratives, and storytelling. The goal is to create immersive experiences and interact with visitors, enriching the way they understand and appreciate culture and history.

In Cluster 5, colored violet, there is additional discussion of the medical applications of projection mapping. Keywords in this cluster include breast cancer, fluorescence, generalized mixed equilibrium problem, indocyanine green, infrared, Lyapunov functional, mixed reality technology, navigation surgery, neural network, optogenetics, photometric stereo, sentinel lymph node biopsy, uniformly smooth Banach space, and variational inequalities. According to Rodriguez, et al. (2015) research, the implementation of mixed reality using projection mapping can assist the operation process, allowing real-time control visualized directly in the operator's workplace.

4. Conclusions

This study conducted a comprehensive bibliometric analysis on the research topic of projection mapping technology using VOSviewer, Microsoft Excel, and Tableau Public. The analysis was based on the Scopus

database, focusing on the growth of the number of publications from 2003 to 2022, prolific authors, citation analysis, country productivity, sources publishing documents on projection mapping technology, and research trends. Over the period from 2003 to 2022, the annual number of articles on projection mapping technology in international journals, proceedings, and publications has consistently increased. However, there are variations in the total and average number of citations to documents published in individual years. Iwai, D., from Osaka University emerged as the most prolific author in projection mapping technology, while Ishikawa, M., received the highest number of citations for his works. Japan is identified as the most productive country of origin for researchers in this field. The journal with the highest number of citations, making it a crucial reference, is "IEEE Transactions on Visualization and Computer Graphics." Empirical researchers can use articles from this journal to track the evolution of research subjects and the ongoing development of the projection mapping technology research topic. The analysis suggests that projection mapping technology, currently evolving, has potential applications in education and entertainment, in addition to the medical and telecommunications fields discussed in the analyzed articles.

References

- Asayama, H., Iwai, D. and Sato, K., 2018. Fabricating diminishable visual markers for geometric registration in projection mapping. *IEEE Transactions on Visualization and Computer Graphics*, 24(2), pp. 1091–1102. <https://doi.org/10.1109/TVCG.2017.2657634>.
- Baker, D.R., 1991. On-line bibliometric analysis for researchers and educators. *Journal of Social Work Education*, 27(1), pp. 41–47. <https://doi.org/10.1080/10437797.1991.10672168>.
- Bonaventura, J., Eldridge, M.A.G., Hu, F., Gomez, J.L., Sanchez-Soto, M., Abramyan, A.M., Lam, S., Boehm, M.A., Ruiz, C., Farrell, M.R., Moreno, A., Galal Faress, I.M., Andersen, N., Lin, J.Y., Moaddel, R., Morris, P.J., Shi, L., Sibley, D.R., Mahler, S.V., Nabavi, S., Pomper, M.G., Bonci, A., Horti, A.G., Richmond, B.J. and Michaelides, M., 2019. High-potency ligands for DREADD imaging and activation in rodents and monkeys. *Nature Communications*, 10(1): 4527. <https://doi.org/10.1038/s41467-019-12236-z>.
- Chee, M.J.S., Arrigoni, E. and Maratos-Flier, E., 2015. Melanin-concentrating hormone neurons release glutamate for feedforward inhibition of the lateral septum. *Journal of Neuroscience*, 35(8), pp. 3644–3651. <https://doi.org/10.1523/JNEUROSCI.4187-14.2015>.
- Chen, X., Sun, Y.-C., Church, G.M., Lee, J.H. and Zador, A.M., 2018. Efficient in situ barcode sequencing using padlock probe-based BaristaSeq. *Nucleic Acids Research*, 46(4): e22. <https://doi.org/10.1093/nar/gkx1206>.
- Degner, M., Moser, S. and Lewalter, D., 2022. Digital media in institutional informal learning places: a systematic literature review. *Computers and Education Open*, 3: 100068. <https://doi.org/10.1016/j.caeo.2021.100068>.
- Fender, A., Herholz, P., Alexa, M. and Müller, J., 2018. Optispace: automated placement of interactive 3D projection mapping content. In: *Proceedings of the 2018 CHI Conference on Human Factors in Computing Systems*. Montreal, QC, Canada, 21–26 April 2018. New York, NY, USA: Association for Computing Machinery. <https://doi.org/10.1145/3173574.3173843>.
- Fujimoto, Y., 2018. Projection mapping for enhancing the perceived deliciousness of food. *IEEE Access*, 6, pp. 59975–59985. <https://doi.org/10.1109/ACCESS.2018.2875775>.
- Grundhöfer, A. and Iwai, D., 2018. Recent advances in projection mapping algorithms, hardware and applications. *Computer Graphics Forum*, 37(2), pp. 654–675. <https://doi.org/10.1111/cgf.13387>.
- Handa, M., Aul, E.G. and Bajaj, S., 2012. Immersive technology – uses, challenges and opportunities. *International Journal of Computing & Business Research*. [pdf] Available at: <<http://www.researchmanuscripts.com/isociety2012/12.pdf>> [Accessed July 2023].

- Hein, R.M., Wienrich, C. and Latoschik, M.E., 2021. A systematic review of foreign language learning with immersive technologies (2001-2020). *AIMS Electronics and Electrical Engineering*, 5(2), pp. 117–145. <https://doi.org/10.3934/ELECTRENG.2021007>.
- Huang, C.-C., Sugino, K., Shima, Y., Guo, C., Bai, S., Mensh, B.D., Nelson, S.B. and Hantman, A.W., 2013. Convergence of pontine and proprioceptive streams onto multimodal cerebellar granule cells. *eLife*, 2: e00400. <https://doi.org/10.7554/eLife.00400>.
- Ishikawa, M., 2014. Interactive display technologies using high-speed image processing. In: *21st International Display Workshops (IDW'14)*. Niigata, Japan, 3/5 December 2014. Society for Information Display, pp. 812–813.
- Ishikawa, M., 2019. Interactive dynamic projection mapping using high-speed display and high-speed image processing. In: *Proceedings of Optics & Photonics International Congress (OPIC 2019)*. Yokohama, Japan, 22–25 April 2019. SPIE Digital Library.
- Ishikawa, M., 2022. High-speed vision and its applications toward high-speed intelligent systems. *Journal of Robotics and Mechatronics*, 34(5), pp. 912–935. <https://doi.org/10.20965/jrm.2022.p0912>.
- Ishikawa, T., Shimuta, M. and Häusser, M., 2015. Multimodal sensory integration in single cerebellar granule cells in vivo. *eLife*, 4: e12916. <https://doi.org/10.7554/eLife.12916>.
- Iwai, D., 2019. Computational imaging in projection mapping. In: S. Tominaga, R. Schettini, A. Trémeau and T. Horiuchi, eds. *Computational Color Imaging: Proceedings of 7th International Workshop (CCIW 2019)*. Chiba, Japan, 27–29 March 2019. Cham: Springer Verlag, pp. 14–25. *Lecture Notes in Computer Science*, 11418. https://doi.org/10.1007/978-3-030-13940-7_2.
- Kageyama, Y., Iwai, D. and Sato, K., 2022. Online projector deblurring using a convolutional neural network. [online] *IEEE Transactions on Visualization and Computer Graphics*, 28(5), pp. 2223–2233. <https://doi.org/10.1109/TVCG.2022.3150465>.
- Krautsack, D., 2011. 3D Projection mapping and its impact on media & architecture in contemporary and future urban spaces. *Journal of the New Media Caucus*, 7(1).
- Kumar Kar, S. and Harichandan, S., 2022. Green marketing innovation and sustainable consumption: a bibliometric analysis. *Journal of Cleaner Production*, 361: 132290. <https://doi.org/10.1016/j.jclepro.2022.132290>.
- Mikawa, Y., Sueishi, T., Watanabe, Y. and Ishikawa, M., 2018. VarioLight: hybrid dynamic projection mapping using high-speed projector and optical axis controller. In: *Proceedings of SA'18: SIGGRAPH Asia 2018 Emerging Technologies*. Tokyo, Japan, 4–7 December 2018. New York, NY, USA: Association for Computing Machinery. <https://doi.org/10.1145/3275476.3275481>.
- Miyashita, L. and Ishikawa, M., 2020. Wearable DPM system with intelligent imager and GPU. In: *Proceedings of 2nd IEEE International Conference on Artificial Intelligence Circuits and Systems (AICAS)*. Genova, Italy, 31 August – 2 September 2020. IEEE, pp. 129–130. <https://doi.org/10.1109/AICAS48895.2020.9073788>.
- Miyashita, L., Watanabe, Y. and Ishikawa, M., 2018. MIDAS projection: markerless and modelless dynamic projection mapping for material representation. *ACM Transactions on Graphics*, 37(6): 196. <https://doi.org/10.1145/3272127.3275045>.
- Miyatake, Y., Hiraki, T., Iwai, D. and Sato, K., 2021. HaptoMapping: visuo-haptic augmented reality by embedding user-imperceptible tactile display control signals in a projected image. *IEEE Transactions on Visualization and Computer Graphics*, 29(4), pp. 2005–2019. <https://doi.org/10.1109/TVCG.2021.3136214>.
- Mongeon, P. and Paul-Hus, A., 2016. The journal coverage of Web of Science and Scopus: a comparative analysis. *Scientometrics*, 106(1), pp. 213–228. <https://doi.org/10.1007/s11192-015-1765-5>.
- Narita, G., Watanabe, Y. and Ishikawa, M., 2017. Dynamic projection mapping onto deformable non-rigid surface using deformable dot cluster marker. *IEEE Transactions on Visualization and Computer Graphics*, 23(3), pp. 1235–1248. <https://doi.org/10.1109/TVCG.2016.2592910>.
- Nishino, H., Hatano, E., Seo, S., Nitta, T., Saito, T., Nakamura, M., Hattori, K., Takatani, M., Fuji, H., Taura, K. and Uemoto, S., 2018. Real-time navigation for liver surgery using projection mapping with indocyanine green fluorescence: development of the novel medical imaging projection system. *Annals of Surgery*, 267(6), pp. 1134–1140. <https://doi.org/10.1097/SLA.0000000000002172>.
- Nofal, E., Stevens, R., Coomans, T. and Vande Moere, A., 2018. Communicating the spatiotemporal transformation of architectural heritage via an in-situ projection mapping installation. *Digital Applications in Archaeology and Cultural Heritage*, 11: e00083. <https://doi.org/10.1016/j.daach.2018.e00083>.
- Pejsa, T., Kantor, J., Benko, H., Ofek, E. and Wilson, A., 2016. Room2Room: enabling life-size telepresence in a projected augmented reality environment. In: *Proceedings of the 19th ACM Conference on Computer-Supported Cooperative Work & Social Computing*. San Francisco, CA, USA, 27 February – 2 March 2016. Association for Computing Machinery, pp. 1716–1725. <https://doi.org/10.1145/2818048.2819965>.
- Qin, Y., Xu, Z., Wang, X. and Škare, M., 2022. Green energy adoption and its determinants: a bibliometric analysis. *Renewable and Sustainable Energy Reviews*, 153: 111780. <https://doi.org/10.1016/j.rser.2021.111780>.
- Riccaboni, M. and Verginer, L., 2022. The impact of the COVID-19 pandemic on scientific research in the life sciences. *PLoS ONE*, 17(2): e0263001. <https://doi.org/10.1371/journal.pone.0263001>.

- Rodriguez, L., Quint, F., Gorecky, D., Romero, D. and Siller, H.R., 2015. Developing a mixed reality assistance system based on projection mapping technology for manual operations at assembly workstations. *Procedia Computer Science*, 75, pp. 327–333. <https://doi.org/10.1016/j.procs.2015.12.254>.
- Singh, V.K., Singh, P., Karmakar, M., Leta, J. and Mayr, P., 2021. The journal coverage of Web of Science, Scopus and Dimensions: a comparative analysis. *Scientometrics*, 126(6), pp. 5113–5142. <https://doi.org/10.1007/s11192-021-03948-5>.
- Sueishi, T., Oku, H. and Ishikawa, M., 2016. Lumipen 2: dynamic projection mapping with mirror-based robust high-speed tracking against illumination changes. *Presence: Teleoperators and Virtual Environments*, 25(4), pp. 299–321. https://doi.org/10.1162/PRES_a_00275.
- Suzanna, S. and Lumban Gaol, F., 2021. Immersive learning by implementing augmented reality: now and the future. *Jurnal Ilmu Komputer dan Desain Komunikasi Visual*, 6(1), pp. 22–28.
- Tsukamoto, J., Iwai, D. and Kashima, K., 2017. Distributed optimization framework for shadow removal in multi-projection systems. *Computer Graphics Forum*, 36(8), pp. 369–379. <https://doi.org/10.1111/cgf.13085>.
- Tuttle, K.R., 2020. Impact of the COVID-19 pandemic on clinical research. *Nature Reviews Nephrology*, 16, pp. 562–564. <https://doi.org/10.1038/s41581-020-00336-9>.
- Wang, L., Xu, H., Tabata, S., Hu, Y., Watanabe, Y. and Ishikawa, M., 2020. High-speed focal tracking projection based on liquid lens. In: *ACM SIGGRAPH 2020 Emerging Technologies (SIGGRAPH '20)*. Virtual event, 17 August 2020. New York, NY, USA: Association for Computing Machinery. <https://doi.org/10.1145/3388534.3408333>.
- Watanabe, Y., Kato, T. and Ishikawa, M., 2017. Extended dot cluster marker for high-speed 3D tracking in dynamic projection mapping. In: *Proceedings of the 2017 IEEE International Symposium on Mixed and Augmented Reality (ISMAR)*. Nantes, France, 9–13 October 2017. Institute of Electrical and Electronics Engineers, pp. 52–61. <https://doi.org/10.1109/ISMAR.2017.22>.
- Xie, L., Chen, Z., Wang, H., Zheng, C. and Jiang, J., 2020. Bibliometric and visualized analysis of scientific publications on atlantoaxial spine surgery based on Web of Science and VOSviewer. *World Neurosurgery*, 137, pp. 435–442.e4. <https://doi.org/10.1016/j.wneu.2020.01.171>.
- Yamamoto, K., Iwai, D., Tani, I. and Sato, K., 2022. A monocular projector-camera system using modular architecture. *IEEE Transactions on Visualization and Computer Graphics*, 29(12), pp. 5586–5592. <https://doi.org/10.1109/TVCG.2022.3217266>.
- Yuan, Q., Wang, R., Pan, Z., Xu, S., Gao, J. and Luo, T., 2021. A survey on human-computer interaction in spatial augmented reality. *Journal of Computer-Aided Design & Computer Graphics*, 33(3), pp. 321–332. <https://doi.org/10.3724/SP.J.1089.2021.18445>.
- Zhou, Y., Xiao, S., Tang, N., Wei, Z. and Chen, X., 2016. Pmomo: projection mapping on movable 3D object. In: *Proceeding of the 2016 CHI Conference on Human Factors in Computing Systems*. San Jose, CA, USA, 7–12 May 2016. New York, NY, USA: Association for Computing Machinery, pp. 781–790. <https://doi.org/10.1145/2858036.2858329>.



TOPICALITIES

Edited by Markéta Držková

CONTENTS

News & more	233
Bookshelf	235
Events	241

News & more

Recent news from CIE



In 2023, the International Commission on Illumination made the overview of the CIE datasets included in various CIE Technical Reports and International Standards available online. A dedicated CIE website provides the list of the datasets with links to their details, including brief descriptions, metadata files and references to the CIE publications where they were originally published. Some datasets are provided open access, such as for the CIE indoor daylight illuminant ID50 or the new CIE reference spectrum L41 – see the report CIE 251:2023 presented on the next page.

Also, CIE released two technical notes, which are, as usual, freely downloadable from the CIE website. The first one, CIE TN 014:2023, was prepared under Division 3, Interior Environment and Lighting Design. It is related to the discomfort caused by glare; namely, it provides an example HDR luminance image measurement setup for UGR (Unified Glare Rating). The method to determine the glare source area for luminaires with a non-uniform source luminance, which is typical for light-emitting diodes, is provided in the technical report CIE 232:2019.

The other, CIE TN 015:2023, prepared under Division 6, Photobiology and Photochemistry, reports on the Second International Workshop on Circadian and Neurophysiological Photoreception, held in 2019. Among other details, it provides the resulting thresholds for healthy day-active adults expressed in terms of the melanopic EDI, i.e. equivalent daylight (D65) illuminance defined in the standard CIE S 026, see also JPMTR Vol. 7 No. 4. The recommended minimum melanopic EDI during the daytime is 250 lx, while the recommended maxima are 10 lx during the evening (at least three hours before bedtime) and 1 lx during the night. Further, a new Joint Technical Committee, CIE JTC 20, was formed under Division 6 and Division 2, Physical Measurement of Light and Radiation. It deals with the current wearable α -opic dosimetry and light logging methods, as well as related limitations, device calibration, metadata and data schemes. Its work builds on the α -opic metrology defined in the standard CIE S 026, which provides the spectral sensitivity functions describing the ability of optical radiation to stimulate each of the five photoreceptor classes and has introduced α -opic as a common term for S-cone-opic, M-cone-opic, L-cone-opic, rhodopic and melanopic.

Another newly established Technical Committee, TC 3-63 under Division 3, aims to define a method for determining the indoor lighting requirements for different visual tasks while considering aspects beyond those usually covered in existing standards, such as personal and contextual variables. At the same time, the definition of a decision scheme to tailor the design values according to the specific lighting needs is in line with the approaches recently adopted in guidelines and standards for the lighting of indoor workplaces. In the summer months, a call of CIE TC 4-50 Road Surface Characterization for Lighting Application was open to collect data for the reflectance tables to be included in the update of CIE 144:2001 to represent modern pavements and road surfaces better. Several other standards also are currently under development. The two released in 2023 are presented on the next page.

An update on Fogra research projects in 2023



The projects with the timescale ending in 2023 cover all six main areas of Fogra research. The project in the field of security applications aimed to develop standardised performance tests in near-field communication technology based on ISO/IEC 14443 Cards and security devices for personal identification – Contactless proximity objects and in cooperation with the relevant card and reader manufacturers to identify all tasks essential for smart cards functionality. The standardised performance tests can be used for individual transponders and readers as well as for testing the interoperability of a particular transponder–reader combination.

Three projects concerned the areas of offset printing with materials and environment and were solved jointly by the corresponding Fogra Technical Committees. The project dealing with the on-demand inactivation of microbial contamination in the fountain solution circuit of offset printing presses was carried out in cooperation with the wfk – Cleaning Technology Institute. The need to solve this issue substantially increased with the reduced use of isopropanol and biocide additives in the fountain solution. The proposed system capable of dosing a tailored amount of antimicrobial substances is based on 3D-printed, biodegradable hydrogels with antimicrobial peptides in microcapsules that can be degraded by contamination and thus release the active substances when and where appropriate. This year, a new project on this topic was started with the same partner, aiming to develop a system for optical monitoring and minimising microbial contamination in the fountain solution circuit using photosensitisers with the aggregation-induced fluorescence emission and photodynamic inactivation of bacteria.

Another project studied, in partnership with the Technical University of Darmstadt, coldset inks formulated without mineral oils to gain insight into their deinkability, which is essential for paper recyclability, and the compatibility with elastomers to avoid damage of printing press components. The third project from the areas of offset printing and materials comprised a comprehensive characterisation of orange, green and violet printing inks together with folding boxboard and label papers to create the basis for the seven-colour offset packaging printing standard. The commercially available materials were tested in laboratory conditions and on the sheet-fed offset press with different process parameters and using linearisation based on the spot colour tone value (SCTV) defined in ISO 20654.

Further, two projects dealt with print finishing. One was dedicated to film lamination and aimed to develop a prediction model to help identify and prevent possible production risks. The quality of film lamination can be adversely affected due to shortened production times and the use of inks and adhesives optimised with respect to other properties; in particular, time-delayed delamination is an issue. The project involved designing the laboratory laminating system and appropriate stress tests and thorough characterisation of relevant material and process parameters of film-laminated products and their resulting mechanical and thermal resistance. The second finishing project was also concerned with digital printing. It focused on the development of a method for evaluating the perfect binding capability of uncoated printing papers for high-speed inkjet printing used in book production. It paid attention to characterising the specific types of uncoated paper and process influences and comparison of model predictions and practical results. In addition, Fogra participated in the EU-funded ApPEARS project (Appearance Printing – European Advanced Research School), which shall be included in the regular overview of the EU research projects in JPMTR Vol. 13 No. 2.

ISO/CIE 23539:2023

Photometry – The CIE system of physical photometry

This edition from March 2023 is the first published as an ISO/CIE standard. It cancels and replaces ISO 23539:2005 (CIE S 010:2004), which has been technically revised to incorporate the photometric units as defined in the International System of Units (SI) since 2019 and other changes implemented in the report providing the basis of physical photometry, CIE 018:2019, see also JPMTR Vol. 8 No. 4, as well as in CIE 170-2:2015, which deals with the fundamental chromaticity diagram with coordinates corresponding to physiologically significant axes. In particular, the current version includes the reformulated definition of the candela, the spectral luminous efficiency functions for mesopic and 10° photopic vision, and the cone-fundamental-based spectral luminous efficiency functions for 2° and 10° field size. Also, a list of normative references and requirements on using units, tabulated values and interpolating intermediate values have been added.

CIE 251:2023 – LED Reference Spectrum for Photometer Calibration

This report was prepared under Division 2 and provides the tabulated data of CIE reference spectrum L41, which is based on new LED illuminants published in CIE 015:2018 Colorimetry (4th Edition), together with a quality metric for the selection of white LEDs for physical LED standard sources. This reference spectrum comprises the theoretical spectral distribution of a white LED with a correlated colour temperature of 4 103 K. It is intended as a complement to the reference spectrum of CIE standard illuminant A used in photometer calibration, reflecting the rapidly increasing use of lighting products based on light-emitting diodes and thus also their photometric measurement. According to the comprehensive analyses of the corresponding Technical Committee (CIE TC 2-90), the spectral errors in measurements of LED sources are reduced by a factor of two on average with this calibration as compared to the standard illuminant A. However, the measurement with photometers calibrated to L41 is not limited to LEDs.

The 9th drupa Global Trends report



This edition was published approximately a year after the 8th one, so, hopefully, the pause due to the pandemic can be considered a history. Also, the number of respondents has increased to more than 600, which is still less than in the 2010s but is an increase of over 20 % compared to the previous report. The surveys were circulated to printers and suppliers in May and June 2023. The main message is the return of economic confidence, with its levels growing in almost all regions and across all print industry markets, which is particularly good news for the commercial and publishing sectors. However, the data sets for the Middle East and Australia/Oceania are small, and the same applies to functional printing. The key findings include the rising prices and planned capital investments reported by printers for the second time in a row. Concerning printing technology, the most pronounced increase in print volume overall was reported for colour electrophotography, although in the case of packaging, it was outperformed by both flexography and sheetfed offset. The highest increase of the latter was achieved in the publishing sector. For web-to-print solutions, the situation remains stable, with installations reported by 25 % of printers, which is the same percentage as in the first report almost ten years ago. Besides other challenges, recruiting the conventional press operators and finishing staff is an issue; the perceived socio-economic risks are region-specific.

Bookshelf

Springer Handbook of Augmented Reality

This new reference book brings a comprehensive, up-to-date account of augmented reality, i.e. the technologies that convey a sense of virtual and real environments blended to varying extents and provide a new interface to digital information. The publication reflects the recent significant progress achieved in this area thanks to the intensified research and development efforts in both academic and commercial spheres and a growing range of applications in different domains. At the same time, many challenges remain to be solved for augmented reality to deliver a truly immersive experience without the current limitations. Thus, this handbook, contributed by many leading experts in the field and covering the topic from the beginning to the development towards the so-called metaverse, can also be seen as a solid ground for further inventions. The text is supported by extensive references (however, some are repeating), complemented by numerous tables, schemes and other illustrations, and accompanied by a detailed index.

The content is organised into seven parts, where the first three provide the necessary background. Part I explains the fundamental concepts and elucidates the confusing taxonomies of virtual, augmented, mediated, multimediated, mixed, extended and other realities. Then, it brings a historical overview of augmented reality. Part II details the principles of object tracking and mapping, estimating a 3D pose for a hand and an object, mixed reality interaction techniques and interacting with characters controlled by artificial intelligence. Also, it discusses privacy and security issues and solutions. Part III is dedicated to hardware and peripherals for augmented reality, namely the optics of displays, calibration, hardware, and peripherals of tracking systems, the so-called embodied interaction on constrained interfaces, and networking and cyber foraging for mobile augmented reality.

The following three parts present the applications of augmented reality for various purposes. Part IV covers education and training in different areas, from arts to sports, serious games, cultural heritage, holocaust museums and memorials, live theatrical performances and tourist services. Engineering and science applications of augmented reality described in Part V include its use in aerospace and aviation, military and defence, shipbuilding, building maintenance and operation, maintenance, repair and troubleshooting of machinery and other products, remote assistance, and also for interactive finite element analysis. Part VI deals with augmented reality applications in health science, such as computer-guided interventions, healthcare exercise systems, and assistive systems for the cognitively impaired, as well as with considerations specific to its use by children and young adults. Finally, the last part explores the convergence of augmented reality with other emerging technologies, especially artificial intelligence, ubiquitous computing and the Internet of Things, and the potential of digital twins with strategies for their wider adoption, aspects to consider and example implementations.



Editors: Andrew Y. C. Nee, Soh K. Ong

Publisher: Springer
1st ed., January 2023
ISBN: 978-3-030-67821-0
948 pages, 526 images
Hardcover
Available also as an eBook



Innovative Technologies for Printing and Packaging

*Editors: Min Xu, Li Yang,
Linghao Zhang, Shu Yan*

Publisher: Springer
1st ed., March 2023
ISBN: 978-9811990236
677 pages, 473 images
Hardcover
Also as an eBook



This book includes over 80 peer-reviewed research papers from the 13th China Academic Conference on Printing and Packaging (Jinan, China, November 2022). Similarly to previous editions, the contributions cover technology related to colour science, digital media, printing, packaging, mechanical and information engineering, artificial intelligence, printing inks and substrates, and special functional materials. The papers deal e.g. with the calibration of grey balance for fluorescent inkjet image based on spectral calculation, spectral reflectance reconstruction of organic tissue from camera responses, structure design of 3D-printed Braille puzzles, preparation of durable superhydrophobic coating, research on control algorithm of solvent-free compound mixing ratio based on feedforward control, intelligent design of packaging layout using reinforcement learning, ink for electron-beam curing, and hyperelasticity of photosensitive resin plate, to name a few.

Image and Video Color Editing

Author: Shiguang Liu

Publisher: Springer
1st ed., March 2023
ISBN: 978-3031260292
86 pages, 16 images
Hardcover
Also as an eBook



This concise book is a part of the series called Synthesis Lectures on Visual Computing: Computer Graphics, Animation, Computational Photography and Imaging. It covers the advances in image and video colour editing, highlighting the fast

Advanced Technology in Textiles Fibre to Apparel

Current textile production is highly automated and efficient; nevertheless, there is still significant room for improvement, especially concerning the environmental impacts, from source materials to chemical treatments in individual processing steps up to solid waste management. This book brings an overview of the latest innovations in the field.

After introducing the basics of textiles and textile fibres, one chapter discusses various aspects of the management and maintenance of textile machinery necessary for achieving the required quality. The following five chapters present the advanced technology in fabric manufacturing, textile dyeing, textile printing, fabric finishing, and apparel manufacturing. With respect to textile printing technology, the text covers innovative screen printing, transfer printing, cool transfer printing, inkjet printing and 3D printing processes, including state-of-the-art as well as emerging methods, tools and machinery. Next, the book deals with non-woven materials, their unique features, manufacturing and applications, the recent research on applying structural colours to textiles, waste management and the use of biochemical engineering in the textile industry. The last chapter reviews the use of nanomaterials for special treatment in the finishing of textile materials.



*Editors: Md. Mizanur Rahman,
Mohammad Mashud, Md. Mostafizur Rahman*

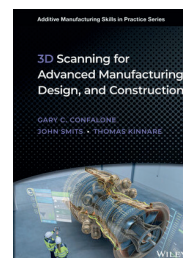
Publisher: Springer
1st ed., June 2023
ISBN: 978-981-99-2141-6
357 pages, 137 images
Hardcover
Available also as an eBook

3D Scanning for Advanced Manufacturing, Design, and Construction

The authors of this new book share their expertise in 3D scanning technology, which expands into various industries, together with 3D printing and other cutting-edge technologies. The text begins with the history of metrology and systems of units, the basics of lasers and their use for 3D scanning, including the principles, limitations and accuracy. Then, it describes scanning equipment and data acquisition and processing software, explaining the procedures and related terms, such as point cloud and polygonal mesh, and the importance of appropriate post-processing. Two chapters deal with reverse engineering for industrial and consumer applications and for architecture, engineering and construction. The text concludes with future directions, incl.

*Authors: Gary C. Confalone,
John Smits, Thomas Kinnare*

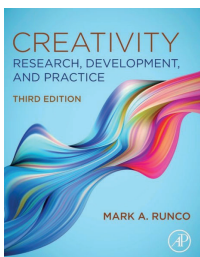
Publisher: Wiley
1st ed., March 2023
ISBN: 978-1-119-75851-8
224 pages
Hardcover
Available also as an eBook



extended reality, autonomous and unmanned aerial vehicles, and industry trends. At the end, an overview of resources and references and a glossary of metrology terms are provided.

Creativity Research, Development, and Practice

The content of this textbook reflects that, due to the nature of creativity, its studying and understanding require combining diverse perspectives. The third edition brings reorganised text with many updated, extended and added parts. First, it discusses the relationships with cognition, personality and motivation. The new chapter on the psychometrics of creativity stresses the need for validity and reliability; recently, quality control in considering new information gained even more importance. The next one brings many new biological insights thanks to the intensive neuroscientific research; on the other hand, their applicability in different contexts is often uncertain. Four chapters deal with clinical, social, attributional, organisational, cultural and historical perspectives. The coverage of relationships with politics is extended not only in the dedicated chapter. There, the deliberately harmful, malevolent creativity is also analysed. Further, age differences, developmental trajectories and educational perspectives are discussed, as are creative potential and prerequisites of its fulfilment and enhancement. The last two chapters review philosophical perspectives and refine the definition of creativity and other concepts, such as intelligence, invention, innovation, imagination and adaptability; computer and animal creativity are also explored.



Author: Mark A. Runco

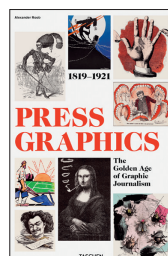
Publisher: Academic Press
3rd ed., March 2023
ISBN: 978-0-08-102617-5
612 pages
Hardcover
Available also as an eBook

History of Press Graphics 1819–1921

Spanning over a hundred years considered the golden age of graphic journalism, this collection showcases the influential magazine and newspaper illustrations, from those documenting events to political agitations to sharp caricatures, that inspired the art then – and still do today. Besides the works of famous artists, it brings to light many less-known ones and puts the role and evolution of press graphics into context.

Author: Alexander Roob

Publisher: Taschen
1st ed., April 2023
ISBN: 978-3-8365-0786-8
604 pages
Hardcover
Available also as an eBook



and easy-to-use techniques developed in the 21st century thanks to the rapid development of computer graphics, digital cameras and mobile phones. The chapters present colour transfer, emotional colour transfer, colourisation, decolourisation, style transfer, and enhancement of low-exposure image and video assets.

Communication Design and Branding A Multidisciplinary Approach

Editors: Nuno Martins, Daniel Raposo



Publisher: Springer
1st ed., August 2023
ISBN: 978-3031353840
374 pages, 144 images
Hardcover
Also as an eBook

This book includes 20 peer-reviewed contributions presenting the current knowledge and main research directions in communication design and branding. Combining theoretical and practical perspectives, it highlights the benefits of design and branding synergy in business as well as for academic purposes.

Advances in Design and Digital Communication III

Editors: Nuno Martins, Daniel Brandão



Publisher: Springer
1st ed., October 2022
ISBN: 978-3031203633
844 pages, 298 images
Hardcover
Also as an eBook

This volume presents the Proceedings of the 6th International Conference on Design and Digital Communication (Barcelos, Portugal, November 2022). It collects almost 70 papers in the areas of digital and interaction design, societal challenges and concerns of communication and design, graphic design and branding, and audiovisual design and communication. The topics include, for example, the artistic use of dynamic typography and the role of data visualisation in science communication.

Handbook of Biopolymers

Editors: Sabu Thomas, A. R. Ajitha,
Cintil J. Chirayil, Bejoy Thomas

Publisher: Springer
1st ed., April 2023
ISBN: 978-9811907098
1568 pages, 390 images
Hardcover
Also as an eBook



This extensive handbook, printed in two volumes, covers a wide range of biopolymers, their preparation, properties and applications. After the brief introductory part, the second one presents biopolymers from renewable sources, bacterial nanocellulose, marine prokaryotes, humus oils and soy protein, the third one describes their piezoelectric, optical, mechanical, thermal, gas barrier, structural, morphological and textural properties, and the fourth one deals with modifications to tune their hydrophilic or hydrophobic behaviour. The fifth part reviews biopolymer-based blends, interpenetrating polymer networks, gels and composites. The main part of the second volume is dedicated to applications of different types of biopolymers, including printing (especially printed electronics, 3D printing and bioprinting). The last part outlines the future scope, where biodegradation, waste management, safety, environmental and health effects and other challenges are discussed.

Natural Dyes for Sustainable Textiles

Authors: Padma S. Vankar,
Dhara Shukla

Publisher: Woodhead Publishing
1st ed., September 2023
ISBN: 978-0323852579
220 pages, Softcover
Also as an eBook



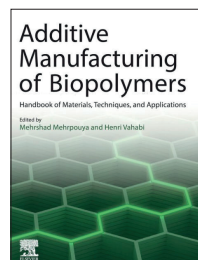
This book covers various aspects of natural dyeing to increase sustainability in textiles, including the application of inks by both traditional and modern printing techniques.

Additive Manufacturing of Biopolymers Handbook of Materials, Techniques, and Applications

This volume, contributed by 36 researchers affiliated with universities across the world, brings an overview of the state of the art in the area of rising importance due to the rapidly growing use of additive manufacturing and related sustainability concerns. The first three chapters introduce and then detail additive manufacturing and 3D printing techniques, considerations specific to printing biopolymers, and recent advances in biopolymer materials, both natural and synthesised. The following chapters deal with 3D printing of biopolymer hydrogels, fire-retardant biopolymers, biopolymer composites and nanocomposites, shape-switching biopolymers, and 4D printing of biopolymers in general. Principles and mechanisms, suitable 3D printing techniques, and example applications are discussed, among others. One chapter presents post-processing methods, which are usually needed to achieve the required mechanical and surface properties of 3D-printed biopolymers. Two chapters then focus on 3D-printed biopolymers and hydrogels for tissue engineering, medical applications and devices; attention is paid to mechanochemistry, mechanical deterioration and degradation of biopolymers, products under development to be adapted to clinical routine and the regulatory questions. The last two chapters discuss potential applications of 3D and 4D printing of biopolymers and the development towards a circular economy.

Editors: Mehrshad Mehrpouya, Henri Vahabi

Publisher: Elsevier
1st ed., April 2023
ISBN: 978-0-323-95151-7
422 pages
Softcover
Available also as an eBook

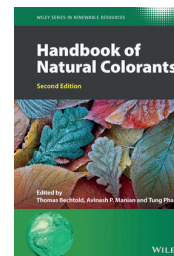


Handbook of Natural Colorants

The current edition builds on recent intensive research in the field of natural dyes and pigments, driven by the significantly increased environmental awareness and the need for industrial solutions based on renewable resources as compared to 15 years ago when the original edition was written. Contributed by over 40 experts, the reorganised text in 20 chapters presents historical uses of natural colourants, their sources in different geographical regions and the production and properties of specific types. The remaining ten chapters deal with analytical methods, colouration of wood, textiles and plastics, the role of mordants, natural colourants in printing and packaging, production processes, product standardisation, and environmental, economic, toxicologic and safety aspects of natural dyes and pigments.

Editors: Thomas Bechtold,
Avinash P. Manian, Tung Pham

Publisher: Wiley
2nd ed., July 2023
ISBN: 978-1-119-81171-8
688 pages
Hardcover
Available also as an eBook



Bookshelf

Academic dissertations

Multimaterial 3D/4D Printing by Integrating Digital Light Processing and Direct Ink Writing

This work addresses the challenges of developing a multi-material 3D printing system for high-resolution printing of a wide range of materials with different colours and functional properties at a reasonable price and with time efficiency. The approach is based on integrating digital light processing, which enables creating a matrix with high detail, complex geometry and multi-colour appearance, and direct ink writing as a technique capable of printing various functional materials, including conductive inks, shape memory photopolymers, and liquid crystal elastomers.

First, the dissertation briefly introduces the two 3D printing techniques considered, i.e. digital light processing and direct ink writing, the state of the art regarding multi-material and hybrid 3D printing, including the multicolour and multi-material 3D printing using single or more printing techniques, and the stimuli-responsive materials, namely liquid crystal elastomers (LCE). Next, it describes the design and control of the proposed hybrid 3D printer and printing process, which arbitrarily combines digital light processing and direct ink writing steps. It also discusses the types of inks and printing conditions for achieving the required print quality. Then, the applicability is demonstrated by hybrid printing of different multicolour prototypes, soft robots based on LCE fibres as an active component, and electronic elements. Further, the system was used for 4D printing of freestanding LCE with the ink developed for rapid curing by an in-situ laser-curing module and the utilisation of stretching by the nozzle movement to enhance actuation. The text discusses the influence of printing parameters and presents the printing of the LCE-embedded lattices, active tensegrity structures, actuator with tunable structural stability, and freestanding spatial LCE lattices. Finally, the multicolour 3D printing using single-vat, single-batch grayscale digital light processing without the need of post-processing, based on the Solvent Blue 104 and precisely controlled exposure, is shown with example applications.

Text Comprehension Across Print and Audio: A Person-Centered Mixed Methods Study

The research within this thesis focused on comparing textual information provided as print (in a digital form) or as audio, where the latter is the medium that has recently regained considerable popularity in general and also for academic use. The study systematically combined several methods to collect and analyse quantitative and qualitative data to provide insight into the differences between the two delivery methods and resulting reading and listening comprehension in the case of undergraduate college students. The qualitative data allowed putting the quantitatively identified profiles into context and helped their better understanding.

The introduction of the dissertation defines the objectives and research questions and explains the chosen approach, building on the existing knowledge and identified gaps in terms of learner characteristics, text and test features, and research design and analysis. The literature review provides

Doctoral thesis – Summary

Author:

Xirui Peng

Speciality field:

Mechanical Engineering

Supervisor:

H. Jerry Qi

Defended:

18 August 2022, Georgia Institute of Technology, George W. Woodruff School of Mechanical Engineering Atlanta, Georgia, USA

Contact:

aaronpeng@gatech.edu

Further reading:

<http://hdl.handle.net/1853/70102>

Doctoral thesis – Summary

Author:

Anisha Singh

Speciality field:

Educational Psychology

Supervisor:

Patricia A. Alexander

Defended:

28 March 2023, University of Maryland, Department of Human Development and Quantitative Methods College Park, Maryland, USA

Contact:
asingh56@sfsu.edu

Further reading:
 DOI: [10.13016/dspace/maco-ke3d](https://doi.org/10.13016/dspace/maco-ke3d)

Doctoral thesis – Summary

Author:
Yong-Woo Kang

Speciality field:
Materials Science and Engineering

Supervisor:
Jeong-Yun Sun

Defended:
 14 June 2023, Seoul National
 University, College of Engineering,
 Department of Materials Science and
 Engineering

Contact:
yongwoo.kang@northwestern.edu

Further reading:
<https://hdl.handle.net/10371/196361>

the background on comprehension, delivery of textual content by print and audio media, the related neuroscience research, reading on paper or on screen, and the relationship of comprehension with learner characteristics, including age, prior knowledge of the topic, self-efficacy, reading and listening habits, as well as text and test processing behaviours. The main part details the extent and conditions of the study and measures investigated in both phases, from demographics questionnaire to self-reported task experience and cued retrospective interviews, and presents the results together with their in-depth discussion. Three reader profiles and three listener profiles were identified and validated. In both cases, the depth of text processing differed among the groups. In addition, reader profile groups differed on digital reading strategies and listener profile groups on attention regulation and preferences. One of the key findings concerns the role of printed content in education. While similar performance levels of recall and inference were achieved when reading print and listening to audio, print showed an advantage over audio for understanding the main idea and incidental vocabulary learning.

A Study on Electrically Driven Hydrogel-Based Soft Robots: Turgor Actuator and 3D-Printed Modular Robot

This thesis contributed to the development of electrical soft actuators. The approaches were based on hydrogels. In particular, the work focused on two functional principles that complement each other in terms of their benefits and limitations. Actuators made from electroactive hydrogels utilise electroosmotic swelling and operate at low voltages. Meanwhile, dielectric elastomer actuators, which compress the elastomer using hydrogel stretchable electrodes, operate with high forces and speed. The research addressed the low actuation force and speed of the former and the fabrication complexity of the latter for more efficient production of configurable soft robotic systems.

After a brief introduction, the main content is organised into three chapters. One deals with modifying 3D-printable electroactive hydrogels to enhance their mechanical properties in terms of stretchability and toughness while preserving their electroactivity. It was achieved by using glycidyl methacrylated hyaluronic acid as a long-chain crosslinker for poly(3-sulfopropyl acrylate, potassium salt) hydrogels. Fabricated hydrogels were characterised regarding their mechanical properties and electroactivity and then two different models were successfully 3D-printed and electroactuated. The next chapter presents a turgor actuator inspired by plant cells that make use of a strong turgor (hydrostatic) pressure by utilising high osmotic pressure of hydrogel. The swelling accelerated by electroosmosis enables fast and strong actuations to be achieved. The text describes the fabrication of turgor actuators with hydrogels enclosed within selectively permeable membranes, measurement of osmotic pressure of hydrogel and analysis of electroosmosis, blocking stress and compression testing of turgor actuators. The resulting actuators could generate MPa driving stresses at high speeds. Their functionality was demonstrated by breaking solid bricks and constructing underwater structures. Finally, one chapter is dedicated to the design of agile, modular robots based on dielectric elastomer actuators. Different modules, including body modules, foot modules for diverse terrains and head modules for communication, were fabricated using multi-material 3D printing, analysed and assembled into various on-demand soft robotic devices. The dissertation demonstrates robotic locomotion on smooth or rough solid surfaces and water, emitting or detecting light, as well as extending the speed and force of robots or changing their moving direction by combining multiple bodies.

Events

Electronic Imaging 2024

Burlingame, California, USA
21–25 January 2024



The programme of this symposium is rich as usual. It offers 18 conferences and almost the same number of short courses, of which six are new. The keynote speakers include Norman Koren introducing image information metrics evaluated from slanted edges, Gordon Wetzstein presenting the capabilities of neural radiance fields and scene representation networks for a photorealistic output, Aaron Parry discussing next steps towards immersion entertainment, Thomas Wischgoll providing practical insight into immersive technologies for interactive visualisation, Grace Kuo dealing with holographic displays, Robin Atkins reviewing the state of the art in HDR imaging, Mohamed Wahib identifying the routes to next-generation high-performance imaging, Anjul Patney highlighting the relationship between vision science principles and advances in graphics algorithms based on artificial intelligence, Vivek K. Goyal demonstrating quantitative secondary electron yield mapping in ion-beam microscopy, Youzo Lin addressing the applicability and challenges of computational wave imaging, Patrick Le Callet explaining the concept of Quality of Experience, and Márton Orosz exploring the approaches of György Kepes to bridge aesthetics and engineering.

SPiE Events

Photonics West 2024

SPiE. PHOTONICS WEST San Francisco, California, USA
27 January – 1 February 2024

For this edition, the contributions related to printing deal e.g. with advanced digital light processing and femtosecond laser stereolithography for multi-material printing, photoinitiator depletion to expand printing capability of single-photon 3D printing, 3D printing through highly scattering media using upconversion nanoparticles, holographic beam shaping for volumetric 3D printing, in-situ shape monitoring during multi-photon 3D laser printing, dry printing multi-material electronic and functional devices, and 4D printing of optics and photonics using hybrid polymers and nanomaterials.

Smart Structures / Nondestructive Evaluation 2024

SPiE. SMART STRUCTURES+ NONDESTRUCTIVE EVALUATION Long Beach, California, USA
25–28 March 2024

The programme of this event also offers many applications of printing, such as fully inkjet-printed dielectric elastomer actuators, multi-material 4D printing for two-stage morphing in self-actuating structures, in-space manufacturing of morphing electronics, and all-printed multifunctional sensors for structural health monitoring of inflatable habitats.

Advanced Inkjet Technology 2024

Fribourg, Switzerland
29–31 January 2024



This event is held by the iPrint Institute of the University of Applied Sciences and Arts Western Switzerland and IS&T. It builds on one of the IS&T 2022 Advances in Printing Technology series sessions. The programme begins with a keynote, 'A Helicopter View of Ink Jet Printing' by Stephen Temple. The sessions cover droplet generation and visualisation, new application domains of inkjet-based processes, novel printing and micro-manufacturing technologies, inkjet printheads, closed-loop control based on piezo self-sensing, and key aspects of inks and substrates. In addition, the one-day Advanced Inkjet Workshop is offered on 1 February.

C!print

Lyon, France
6–8 February 2024



The 11th edition of this tradeshow introduces the C!Factory, a demonstration space covering a complete production chain. It complements the Software Village introduced in 2022 to present solutions for web-to-print, automation, personalisation, etc.

9th Colour Management Symposium

 Munich, Germany
21–22 February 2024

The topics of this edition include colour management approaches in various modern workflows to meet customer and standard requirements, contract proofing, the trends in using artificial intelligence, and more.

VISIGRAPP 2024

19th International Joint Conference on Computer Vision, Imaging and Computer Graphics Theory and Applications

Rome, Italy
27–29 February 2024

In 2024, the participants of this event that traditionally



joins four international conferences can also attend the co-located 4th International Conference on Robotics, Computer Vision and Intelligent Systems (25–27 February) and 10th International Conference on Information Systems Security and Privacy (26–28 February), as non-speakers without the additional fee.

The keynote speakers include Fahad Khan on deep-learning visual recognition networks and models with limited human supervision, Mel Slater on virtual reality in mental health, Gerhard Rigoll on multi-modal human-machine interaction, and Alvitta Ottley on the parallels between human reasoning and artificial intelligence models, substantial for facilitating effective human-AI interaction.

44th CIP4 InterOp Meeting

Munich, Germany
11–15 March 2024

This is the last in-person meeting before the upcoming drupa fair, dedicated to testing and discussing the next steps in developing JDF, XJDF and PrintTalk specifications.

The London Book Fair 2024

London, UK
12–14 March 2024



This edition includes e.g. the Research and Scholarly

Publishing Forum on the last day, focused on the influence of artificial intelligence on scientific authorship and research, transformation towards open access and other strategies or trends in academic publishing.

innoLAE 2024

Innovations in Large-Area Electronics

Cambridge, UK
20–22 February 2024



innoLAE

For the 10th annual conference, which is dedicated to innovations in printed, flexible, hybrid, plastic, organic and bioelectronics, the number of half-day courses offered on the first day was increased to four. The main programme for the next two days features the keynotes of Alberto Salleo, providing an insight into the possibilities to modulate the charge density in electrochemically active polymers over a wide range by ion insertion and the development towards so-called iontronics based on the modulation of electronic properties via electrolytes, Jonathan Rivnay, presenting new classes of organic mixed ionic/electronic conductors for bioelectronics, Ana C. Arias, discussing the options of distributing printed sensors over large areas to create a distributed network of nitrate sensors in soil, and Carl Naylor, focusing on 2D materials, such as transition metal dichalcogenides at angstrom thicknesses, and their possible role as next-generation materials in future electronic devices. The conference sessions deal with manufacturing methods, high-performance materials, novel devices, systems and applications, bioelectronics, sustainability and energy efficiency. Traditionally, the oral presentations are complemented by a poster display and exhibition of the industry partners.

LOPEC 2024



LOPEC
DRIVING THE FUTURE
OF PRINTED ELECTRONICS

Munich, Germany
5–7 March 2024

The Large-area, Organic & Printed Electronics Convention keeps the proven format for 2024. The conference schedule includes presentations in up to five parallel tracks. In plenary sessions, the invited lectures focus on steps taken towards sustainability thanks to printed electronics in general and smart and circular medical products in particular, the development of printed electronics solutions, flexible and printed electronics manufacturing in China from the perspectives of leading researchers, the role printed sensors can play in orthopaedic rehabilitation, transferring the experiences from silicon semiconductor industry to scale up the production of flexible integrated circuits, business development for next-generation telecommunications, and accelerating emerging photovoltaic technologies.

PRINTING United Technical Event Series



PRINTING UNITED
TECHNICAL EVENT SERIES

Dallas, Texas, USA
12–14 March 2024

In 2024, PRINTING United Alliance combines the COLOR and TAGA Conferences into a new series of technical events, bringing the former two months later than was its usual schedule. The announced programme features three keynote speakers – Peggy Van Allen, highlighting the power of colour and suggesting how to predict future trends for a longer period reliably; Don Hutcheson, presenting G7+ calibration; and Craig Bushman, sharing practical examples of packaging innovations improving recycling compatibility, lowering greenhouse gas emissions, and supporting reuse applications.

Call for papers

The Journal of Print and Media Technology Research is a peer-reviewed periodical, published quarterly by **iarigai**, the International Association of Research Organizations for the Information, Media and Graphic Arts Industries.

JPMTR is listed in Emerging Sources Citation Index, Scopus, DOAJ – Directory of Open Access Journals, Index Copernicus International, NSD – Norwegian Register for Scientific Journals, Series and Publishers.

Authors are invited to prepare and submit complete, previously unpublished and original works, which are not under review in any other journals and/or conferences.

The journal will consider for publication papers on fundamental and applied aspects of at least, but not limited to, the following topics:

- ⊕ **Printing technology and related processes**
Conventional and special printing; Packaging; Fuel cells, batteries, sensors and other printed functionality; Printing on biomaterials; Textile and fabric printing; Printed decorations; 3D printing; Material science; Process control
- ⊕ **Premedia technology and processes**
Colour reproduction and colour management; Image and reproduction quality; Image carriers (physical and virtual); Workflow and management
- ⊕ **Emerging media and future trends**
Media industry developments; Developing media communications value systems; Online and mobile media development; Cross-media publishing
- ⊕ **Social impact**
Environmental issues and sustainability; Consumer perception and media use; Social trends and their impact on media

Submissions for the journal are accepted at any time. If meeting the general criteria and ethic standards of scientific publishing, they will be rapidly forwarded to peer-review by experts of relevant scientific competence, carefully evaluated, selected and edited. Once accepted and edited, the papers will be published as soon as possible.

There is no entry or publishing fee for authors. Authors of accepted contributions will be asked to sign a Licensing agreement (CC-BY-NC 4.0).

Authors are asked to strictly follow the guidelines for preparation of a paper (see the abbreviated version on inside back cover of the journal).

Complete guidelines can be downloaded from: <http://iarigai.com/publications/journals/guidelines-for-authors/>
Papers not complying with the guidelines will be returned to authors for revision.

Submissions and queries should be directed to: journal@iarigai.org



Vol. 13, 2024

Prices and subscriptions

Since 2016, the journal is published in digital form; current and archive issues are available at:
<<https://iarigai.com/publications/journals/>>.

Since 2020, the journal is published as “open access” publication, available free of charge for **iarigai** members, subscribers, authors, contributors and all other interested public users.

A print version is available on-demand. Please, find below the prices charged for the printed Journal, for four issues per year as well as for a single issue

Regular prices

Four issues, print JPMTR (on-demand)	400 EUR
Single issue, print JPMTR (on-demand)	100 EUR

Subscription prices

Annual subscription, four issues, print JPMTR (on-demand)	400 EUR
---	---------

Prices for **iarigai** members

Four issues, print JPMTR (on-demand)	400 EUR
Single issue, print JPMTR (on-demand)	100 EUR

Place your order online at: <<http://www.iarigai.org/publications/subscriptions-orders/>>
Or send an e-mail order to: office@iarigai.org

Guidelines for authors

Authors are encouraged to submit complete, original and previously unpublished scientific or technical research works, which are not under reviews in any other journals and/or conferences. Significantly expanded and updated versions of conference presentations may also be considered for publication. In addition, the Journal will publish reviews as well as opinions and reflections in a special section.

Submissions for the journal are accepted at any time. If meeting the general criteria and ethical standards of the scientific publication, they will be rapidly forwarded to peer-review by experts of high scientific competence, carefully evaluated, and considered for selection. Once accepted by the Editorial Board, the papers will be edited and published as soon as possible.

When preparing a manuscript for JPMTR, please strictly comply with the journal guidelines. The Editorial Board retains the right to reject without comment or explanation manuscripts that are not prepared in accordance with these guidelines and/or if the appropriate level required for scientific publishing cannot be attained.

A – General

The text should be cohesive, logically organized, and thus easy to follow by someone with common knowledge in the field. Do not include information that is not relevant to your research question(s) stated in the introduction.

Only contributions submitted in English will be considered for publication. If English is not your native language, please arrange for the text to be reviewed by a technical editor with skills in English and scientific communications. Maintain a consistent style with regard to spelling (either UK or US English, but never both), punctuation, nomenclature, symbols etc. Make sure that you are using proper English scientific terms. Literal translations are often wrong. Terms that do not have a commonly known English translation should be explicitly defined in the manuscript. Acronyms and abbreviations used must also be explicitly defined. Generally, sentences should not be very long and their structure should be relatively simple, with the subject located close to its verb. Do not overuse passive constructions.

Do not copy substantial parts of your previous publications and do not submit the same manuscript to more than one journal at a time. Clearly distinguish your original results and ideas from those of other authors and from your earlier publications – provide citations whenever relevant.

For more details on ethics in scientific publication consult Guidelines, published by the Committee on Publication Ethics (COPE): <https://publicationethics.org/resources/guidelines>

If it is necessary to use an illustration, diagram, etc. from an earlier publication, it is the author's responsibility to ensure that permission to reproduce such an illustration, diagram, etc. is obtained from the copy-right holder. If a figure is copied, adapted or redrawn, the original source must be acknowledged.

Submitting the contribution to the Journal, the author(s) confirm that it has not been published previously, that it is not under consideration for publication elsewhere and – once accepted and published – it will be disseminated and made available to the public in accordance to the Creative Commons Attribution-NonCommercial 4.0 International Public License (CC-BY-NC 4.0), in English or in any other language. The publisher retains the right to publish the paper online and in print form, and to distribute and market the Journal containing the respective paper without any limitations.

B – Structure of the manuscript Preliminary

Title: Should be concise and unambiguous, and must reflect the contents of the article. Information given in the title does not need to be repeated in the abstract (as they are always published jointly), although some overlap is unavoidable.

List of authors: I.e. all persons who contributed substantially to study planning, experimental work, data collection or interpretation of results and wrote or critically revised the manuscript and approved its final version. Enter full names (first and last), followed by the present address, as well as the E-mail addresses. Separately enter complete details of the corresponding author – full mailing address, telephone number, and E-mail. Editors will communicate only with the corresponding author.

Abstract: Should not exceed 500 words. Briefly explain why you conducted the research (background), what question(s) you answer (objectives), how you performed the research (methods), what you found (results: major data, relationships), and your interpretation and main consequences of your findings (discussion, conclusions). The abstract must reflect the content of the article, including all keywords, as for most readers it will be the major source of information about your research. Make sure that all the information given in the abstract also appears in the main body of the article.

Keywords: Include three to five relevant scientific terms that are not mentioned in the title. Keep the keywords specific. Avoid more general and/or descriptive terms, unless your research has strong interdisciplinary significance.

Scientific content

Introduction and background: Explain why it was necessary to carry out the research and the specific research question(s) you will answer. Start from more general issues and gradually focus on your research question(s). Describe relevant earlier research in the area and how your work is related to this.

Methods: Describe in detail how the research was carried out (e.g. study area, data collection, criteria, origin of analyzed material, sample size, number of measurements, equipment, data analysis, statistical methods and software used). All factors that could have affected the results need to be considered. Make sure that you comply with the ethical standards, with respect to the environmental protection, other authors and their published works, etc.

Results: Present the new results of your research (previously published data should not be included in this section). All tables and figures must be mentioned in the main body of the article, in the order in which they appear. Make sure that the statistical analysis is appropriate. Do not fabricate or distort any data, and do not exclude any important data; similarly, do not manipulate images to make a false impression on readers.

Discussion: Answer your research questions (stated at the end of the introduction) and compare your new results with published data, as objectively as possible. Discuss their limitations and highlight your main findings. At the end of Discussion or in a separate section, emphasize your major conclusions, pointing out scientific contribution and the practical significance of your study.

Conclusions: The main conclusions emerging from the study should be briefly presented or listed in this section, with the reference to the aims of the research and/or questions mentioned in the Introduction and elaborated in the Discussion.

Note: Some papers might require different structure of the scientific content. In such cases, however, it is necessary to clearly name and mark the appropriate sections, or to consult the editors. Sections from Introduction until the end of Conclusions must be numbered. Number the section titles consecutively as 1., 2., 3., ... while subsections should be hierarchically numbered as 2.1, 2.3, 3.4 etc. Only Arabic numerals will be accepted.

Acknowledgments: Place any acknowledgements at the end of your manuscript, after conclusions and before the list of literature references.

References: The list of sources referred to in the text should be collected in alphabetical order on at the end of the paper. Make sure that you have provided sources for all important information extracted from other publications. References should be given only to documents which any reader can reasonably be expected to be able to find in the open literature or on the web, and the reference should be complete, so that it is possible for the reader to locate the source without difficulty. The number of cited works should not be excessive – do not give many similar examples.

Responsibility for the accuracy of bibliographic citations lies entirely with the authors. Please use exclusively the Harvard Referencing System. For more information consult the fifth edition of the Guide to Referencing in the Harvard Style, used with consent of Anglia Ruskin University, released by ARU University Library, available at: <https://library.aru.ac.uk/referencing/harvard.htm>

C – Technical requirements for text processing

For technical requirement related to your submission, i.e. page layout, formatting of the text, as well of graphic objects (images, charts, tables etc.) please see detailed instructions at:

<http://iarigai.com/publications/journals/guidelines-for-authors/>

D – Submission of the paper and further procedure

Before sending your paper, check once again that it corresponds to the requirements explicated above, with special regard to the ethical issues, structure of the paper as well as formatting.

Once completed, send your paper as an attachment to: journal@iarigai.org

If necessary, compress the file before sending it. You will be acknowledged on the receipt within 48 hours, along with the code under which your submission will be processed.

The editors will check the manuscript and inform you whether it has to be updated regarding the structure and formatting. The corrected manuscript is expected within 15 days.

Your paper will be forwarded for anonymous evaluation by two experts of international reputation in your specific field. Their comments and remarks will be in due time disclosed to the author(s), with the request for changes, explanations or corrections (if any) as demanded by the referees.

After the updated version is approved by the reviewers, the Editorial Board will decide on the publishing of the paper. However, the Board retains the right to ask for a third independent opinion, or to definitely reject the contribution.

Printing and publishing of papers, once accepted by the Editorial Board, will be carried out at the earliest possible convenience.

4-2023

Journal of Print and Media Technology Research

A PEER-REVIEWED QUARTERLY

The journal is publishing contributions
in the following fields of research

- ⊕ Printing technology and related processes
- ⊕ Premedia technology and processes
- ⊕ Emerging media and future trends
- ⊕ Social impacts

For details see the Mission statement inside

JPMTR is listed in

- ⊕ Emerging Sources Citation Index
- ⊕ Scopus
- ⊕ DOAJ – Directory of Open Access Journals
- ⊕ Index Copernicus International
- ⊕ NSD – Norwegian Register for Scientific Journals, Series and Publishers

Submissions and inquiries

journal@iarigai.org

Subscriptions

office@iarigai.org

More information at

www.iarigai.org/publications/journal



Publisher

The International Association of Research Organizations
for the Information, Media and Graphic Arts Industries
Magdalenenstrasse 2
D-64288 Darmstadt
Germany

